National Aeronautics and Space Administration

CF6 JET ENGINE DIAGNOSTICS PROGRAM

High Pressure Turbine Roundness/Clearance Investigation

by

W.D. Howard and W.A. Fasching

GENERAL ELECTRIC COMPANY

June 1982

Prepared For

National Aeronautics and Space Administration

1. Report No.	2. Government Accession No.	3. Recipient's Catalog No.
NASA CR-165581		

4. Title and Subtitle	5. Report Date
CF6 Jet Engine Diagnostics Program - High Pressure Turbine Roundness/Clearance Investigation	June 1982
	6. Performing Organization Code
7. Author(s)	8. Performing Organization Report No.
W. D. Howard, W. A. Fasching	R82AEB340
9. Performing Organization Name and Address	10. Work Unit No.
General Electric Company Aircraft Engine Group Cincinnati, Ohio	11. Contract or Grant No.
	NAS3-20631
12. Sponsoring Agency Name and Address	13. Type of Report and Period Covered
National Aeronautics and Space Administration Washington, D.C. 20546	Contractor Report
	14. Sponsoring Agency Code

15. Supplementary Notes

Project Manager - J. McAulay, Project Engineer - R. P. Dengler
NASA-Lewis Research Center, Cleveland, Ohio

16. Abstract

A systematic test program was conducted to evaluate the effects of high pressure turbine clearance changes on engine and module performance and to measure CF6-50C high pressure turbine Stage 1 tip clearance and stator out-of-roundness during steady-state and transient operation.

The results indicated a good correlation of the analytical model of round engine clearance response with measured data. The stator out-of-roundness measurements verified that the analytical technique for predicting the distortion effects of mechanical loads is accurate, whereas the technique for calculating the effects of certain circumferential thermal gradients requires some modifications. A potential for improvements in roundness was established in the order of 0.38 mm (0.015 in.), equivalent to 0.86 percent turbine efficiency which translates to a cruise SFC improvement of 0.36 percent.

The HP turbine Stage 1 tip clearance performance derivative was established as 0.44 mm (17 mils) per percent of turbine efficiency at take-off power, somewhat smaller, therefore, more sensitive than predicted from previous investigations.

17. Key Words (Suggested by Author(s))	18. Distribution Statement
Jet Engine High Pressure Turbine Clearance/Roundness Turbofan Engine Performance Deterioration	Unclassified Unlimited

19. Security Classif. (of this report)	20. Security Classif. (of this page)	21. No. of Pages	22. Price*
Unclassified	Unclassified	115	

* For sale by the National Technical Information Service, Springfield, Virginia 22161

FOREWORD

The work was performed by the Evendale Product Engineering Operation of General Electric's Aircraft Engine Group, Aircraft Engine Engineering Division, Evendale, Ohio. The program was conducted for the National Aeronautics and Space Administration, Lewis Research Center, Cleveland, Ohio, under Subtask 5.2 of the CF6 Jet Engine Diagnostics Program, Contract Number NAS3-20631. The CF6 Jet Engine Diagnostics Program is part of the Engine Component Improvement (ECI) Project, which is part of the NASA Aircraft Energy Efficiency (ACEE) Program. The NASA Project Engineer for this program was R. P. Dengler. The program was initiated in January 1980 and completed in May 1981.

The report was prepared by W. A. Fasching, General Electric Program Manager, and W. D. Howard, Project Engineer, with the assistance of M. W. Thomas, M. P. Murphy, and B. D. Beck.

TABLE OF CONTENTS

TABLE OF CONTENTS (CONCLUDED)

LIST OF ILLUSTRATIONS

LIST OF ILLUSTRATIONS (Continued)

LIST OF ILLUSTRATIONS (CONTINUED)

LIST OF ILLUSTRATIONS (Concluded)

1.0 SUMMARY

In the CF6 Jet Engine Diagnostics Program, the causes of performance degradation were determined for each component of revenue service engines. It was found that a significant contribution to performance degradation was caused by increased airfoil tip radial clearances in the high pressure turbine.

Since the influence of these clearances on engine performance and fuel consumption is significant, it is important to establish these relationships, especially considering the high price of fuel. It is equally important to understand the causes of clearance deterioration so that they can be reduced or eliminated.

The objective of this investigation was to conduct a systematic test program to evaluate the effects of high pressure turbine clearance changes on engine and module performance and to measure CF6-50C high pressure turbine Stage 1 tip clearance and stator out-of-roundness during steady-state and transient operation.

An instrumented engine test was conducted with eight clearanceometer probes installed in the Stage 1 high pressure turbine shrouds. Stage 1 tip clearances and stator out-of-roundness were measured during steady-state and transient operating conditions. The turbine static parts were instrumented with pressure and temperature probes to monitor the behavior of these structures and the corresponding clearanceometer data. The effect of clearance on engine and module performance was established from performance calibrations before and after the basic running clearance of the Stage 1 turbine was increased by blade-tip-on-shroud rubs.

The data from the program were analyzed to determine (1) the effect of high pressure turbine clearance changes on engine and module performance, (2) the Stage 1 high pressure turbine clearance map, (3) the high pressure turbine stator out-of-roundness map, (4) a correlation between measured and predicted clearances, and (5) a quantitative baseline to which clearance control improvements can be compared.

The results indicated a good correlation of the analytical model of round engine clearance response with measured data. The stator out-of-roundness measurements verified that the analytical technique for predicting the distorting effects of mechanical loads is accurate, whereas the technique for calculating the effects of certain circumferential thermal gradients requires some modifications. A potential for improvements in roundness was established in the order of 0.38 mm (0.015 in.), equivalent to 0.86 percent in turbine efficiency which translates to a cruise SFC improvement of 0.36 percent.

The HP turbine Stage 1 tip clearance performance derivative was established as 0.44 mm (17 mils) per percent of turbine efficiency at take-off power, somewhat smaller, therefore, more sensitive than predicted from previous investigations.

2.0 INTRODUCTION

The recent energy demand has outpaced domestic fuel supplies creating an increased United States dependence on foreign oil. This increased dependence was accentuated by the OPEC embargo in the winter of 1973-74 which triggered a rapid rise in the price of fuel. This price rise, along with subsequent increases, brought about a set of changing economic circumstances with regard to the use of energy. These events were felt in all sectors of the transportation industry. As a result, the Government, with the support of the aviation industry, initiated programs aimed at both the supply and demand aspects of the problem. The supply aspect is being investigated by determining the fuel availability from new sources such as coal and oil shale, with concurrent programs in progress to develop engine combustors and fuel systems to accept these broader based fuels.

Reduced fuel consumption is the approach being employed to deal with the demand aspect of the problem. Accordingly, NASA is sponsoring the Aircraft Energy Efficiency (ACEE) program which is directed toward reducing fuel consumption for commercial air transports. The long-range effort to reduce fuel consumption is expected to evolve new technology which will permit development of a more energy efficient turbofan, or an improved propulsion cycle such as that for turboprops. Studies have indicated large reductions in fuel usage are possible (e.g., 15 to 40 percent) from this approach, however, significant impact in fuel usage is considered to be 10 or more years away. In the near term, the only practical propulsion approach is to improve the fuel efficiency of current engines since these engines will continue to be the significant fuel users for the next 15 to 20 years.

The Engine Component Improvement (ECI) program is the element of the ACEE program directed at improving the fuel efficiency of current engines. The ECI program consists of two parts: (1) Performance Improvement and (2) Engine Diagnostics. The Performance Improvement program is directed at developing engine performance improvement and retention concepts for new production and retrofit engines. The Engine Diagnostics effort is to provide information related to determining the sources and magnitudes of performance deterioration for the high bypass ratio turbofan engines utilized on widebody aircraft.

As part of the Engine Diagnostics effort, NASA-Lewis initiated a program with the General Electric Company to conduct high pressure turbine clearance investigations.

The modern aircraft gas turbine engine typically uses highly loaded compressor and turbine stages. Although this design approach tends to reduce weight and improve overall efficiency, the high pressure ratio turbine blading is more sensitive to blade tip-to-shroud clearance. Since clearance is directly related to gas leakage, aerodynamic losses result.

As a jet engine accumulates operating time in revenue service, its performance deteriorates as a function of time and operating cycles. A large part of the CF6-50 engine performance deterioration has been determined to be chargeable to the high pressure turbine (Ref. 1). This deterioration is primarily due to an increase in blade tip-to-shroud clearance which results from loss of tip or shroud materials by rubbing of blade tips on the shrouds. The major cause of CF6-50 rubs is stator out-of-roundness brought about by thermal gradients and transient thermal responses of adjacent structures, such as the compressor rear frame, turbine midframe and low pressure turbine case.

It is very important to the engine designer to determine the effect of clearance on turbine performance and to understand the relationship of the radial growth of the rotor and stator for both transient and steady-state operating conditions. Achieving and maintaining small tip clearances requires that rubs be avoided, or at least closely controlled.

Studies have shown that significant improvements in engine performance (reduced fuel consumption) and engine life extension (cost savings) can result if proper tip clearance techniques are implemented. It is very important, therefore, to obtain running clearance measurements during engine operation, quantitatively evaluate the effect of clearance on performance and to understand the nature of shroud out-of-roundness.

In order to clearly identify causes and effects of turbine clearance changes, measurements of these clearances in the turbine temperature environment of an engine to an accuracy of $\pm$ 0.05 mm (0.002 in.) are required. Various measuring devices have been used in the past, but most of them have serious limitations. Rub pins have been used which show only the minimum clearance requirements, but with no reference as to when the event occurred in time. High energy X-ray has been used, but is difficult to determine roundness and requires specially equipped test sites. The touch probe device is widely used, however, it cannot measure individual blade clearances or clearance during transients. The capacitance sensor is also being used increasingly, but has shown limitations precluding use in the hot turbine environment.

A clearance measuring device which overcomes all of the above problems and provides accurate clearance measurements is an optical, non-contacting sensor called a clearanceometer probe. Such a device has been designed, built, and demonstrated by the General Electric Company. A bench model was fabricated and tested in a controlled laboratory environment to assess accuracy and toughness in a simulated turbine environment. This initial evaluation was followed by a factory engine test on a J79 engine in August 1979. The success of both demonstrations provided the necessary tool to attain accurate measurements of high pressure turbine blade tip clearances, stator roundness and rotor/stator concentricity on the CF6-50 engine.

An instrumented engine test was conducted at the General Electric, Evendale, Ohio, test facility. This test was concluded in September, 1980. The objectives of this effort were to measure CF6-50 high pressure turbine Stage 1 tip clearance and stator out-of-roundness, and to evaluate the effects of high pressure turbine clearance changes on engine and module performances. The testing included both steady-state and transient engine operating conditions.

The data obtained from this test program have been analyzed to determine: (1) the effect of high pressure turbine clearance changes on engine and module performance, (2) the high pressure turbine Stage 1 clearance map, (3) the high pressure turbine stator out-of-roundness map, (4) a correlation between experimentally measured and analytically predicted average clearances and roundness, and (5) a quantitative baseline to which clearance control improvements can be compared.

3.0 BACKGROUND

It had previously been determined that turbine blade-to-shroud clearance increases are one of the leading causes of engine performance deterioration (Ref. 1). The most needed information pertaining to the clearance/performance relationship was a quantitative measurement of the effect of clearance changes upon engine performance. Once this relationship is established, the round engine clearance-response with respect to different engine operating parameters, such as core speed (N_2) and compressor discharge pressure (P_3), is required to determine when clearance increasing rubs could occur. Finally, shroud surface roundness must be addressed because the combined effects of out-of-roundness and round engine response determine when rubs occur.

Rotor eccentricity is a topic often discussed with respect to blade-to-shroud clearance and performance deterioration. Because the CF6-50 high pressure turbine rotor (Figure 1) is supported by bearings at each end, the eccentricity is a function only of the bearing clearances, runout of bearing centers and relative structural stiffnesses. This eccentricity has been shown to be a small, repeatable, and known effect in the CF6-50 engine and is not addressed in this report.

3.1 High Pressure Turbine Clearance Response

Clearance response may be determined analytically through deflection analyses of both the rotating and static engine structures. Heat transfer and aerodynamic models of the components are required to provide appropriate and consistent temperature and pressure boundary conditions as inputs to the structural models.

Typical portions of the structural model of the CF6-50 high pressure turbine stator are shown in Figures 2 and 3. These high pressure turbine components have been analyzed primarily with a General Electric computer program called CLASS/MASS, employing an axisymmetric analysis.

Engine throttle movements, such as accels, decels, and rebursts have been analyzed using this model. The steady-state operating points of ground idle, takeoff power, and cruise power have also been analyzed.

Experience has shown that steady-state engine operating clearances are usually determined as a result of engine transient operating conditions. A calculated or observed minimum which occurs during transient maneuvers will dictate the clearance which must be set initially in order to avoid rubs. The worst case, i.e., minimum clearance or rub condition for the CF6-50 engine, has been predicted to occur during a hot rotor reburst. A reburst is defined as an engine decel from high power to idle, holding at idle for a period of time (generally less than five minutes) and then accelerating the engine back to high power. The turbine shroud support member is considerably less massive than the turbine disk and, consequently, it cools more quickly than the disk during the time at idle. A reacceleration of the engine adds rotational stress growth and blade thermal growth to the already existent disk thermal stress growth. The result is a hot blade tip radius greater than that of the shroud surface which thereby produces blade tip rubbing. The typical growth characteristics for both the rotor and the stator during a reburst maneuver are presented in Figure 4 as a function of time.

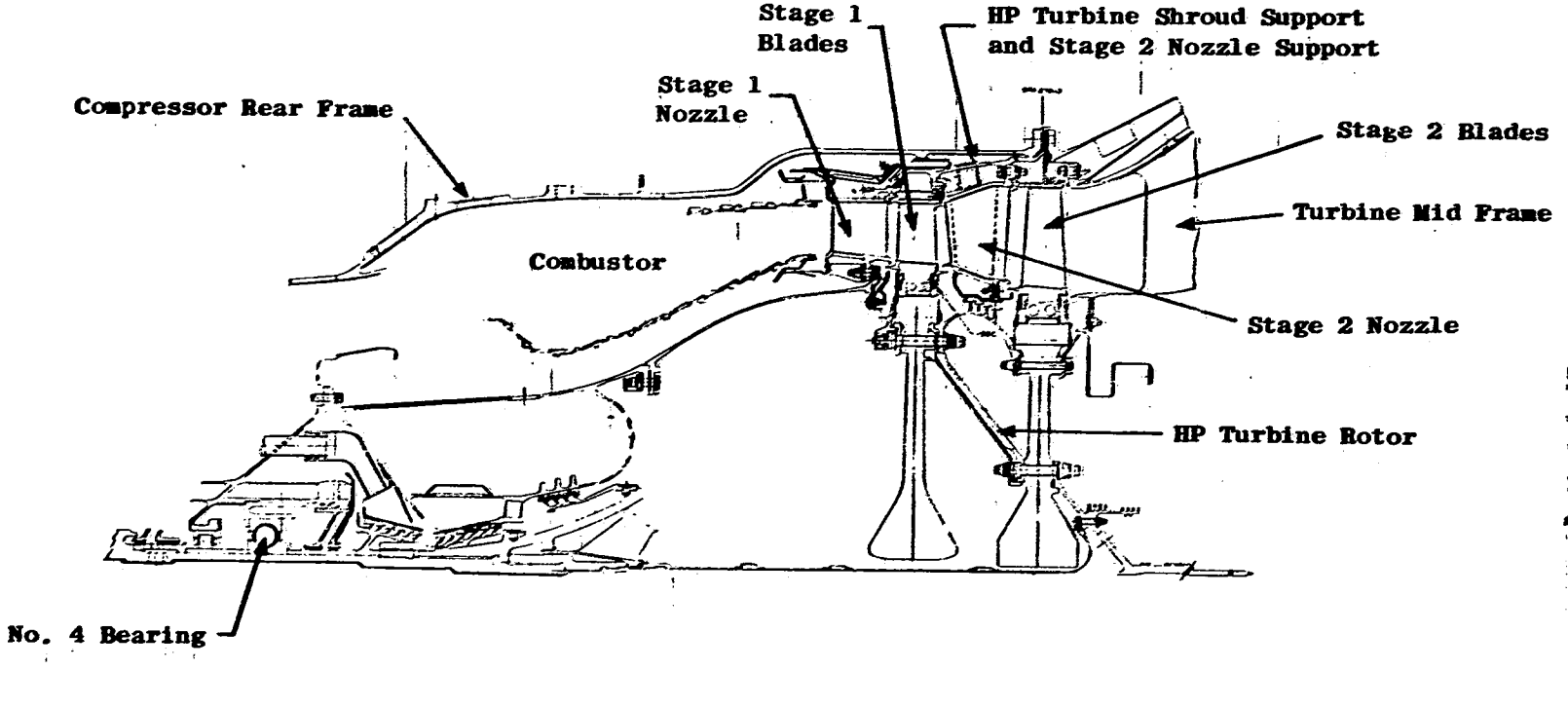

Figure 1. CF6-50 HP Turbine Cross Section.

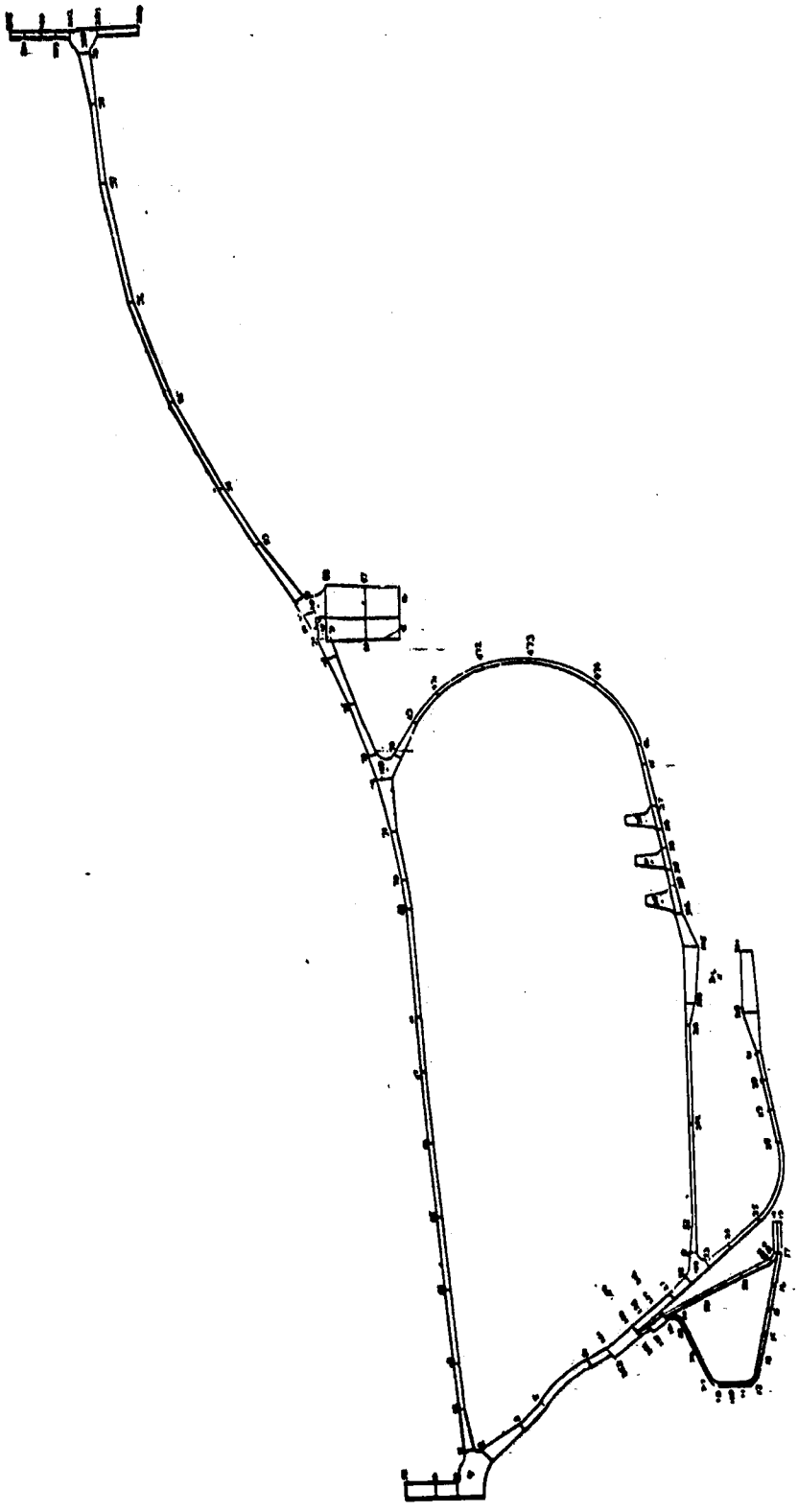

Figure 2. Typical CLASS MASS Model of HPT Stage 1 Nozzle Support.

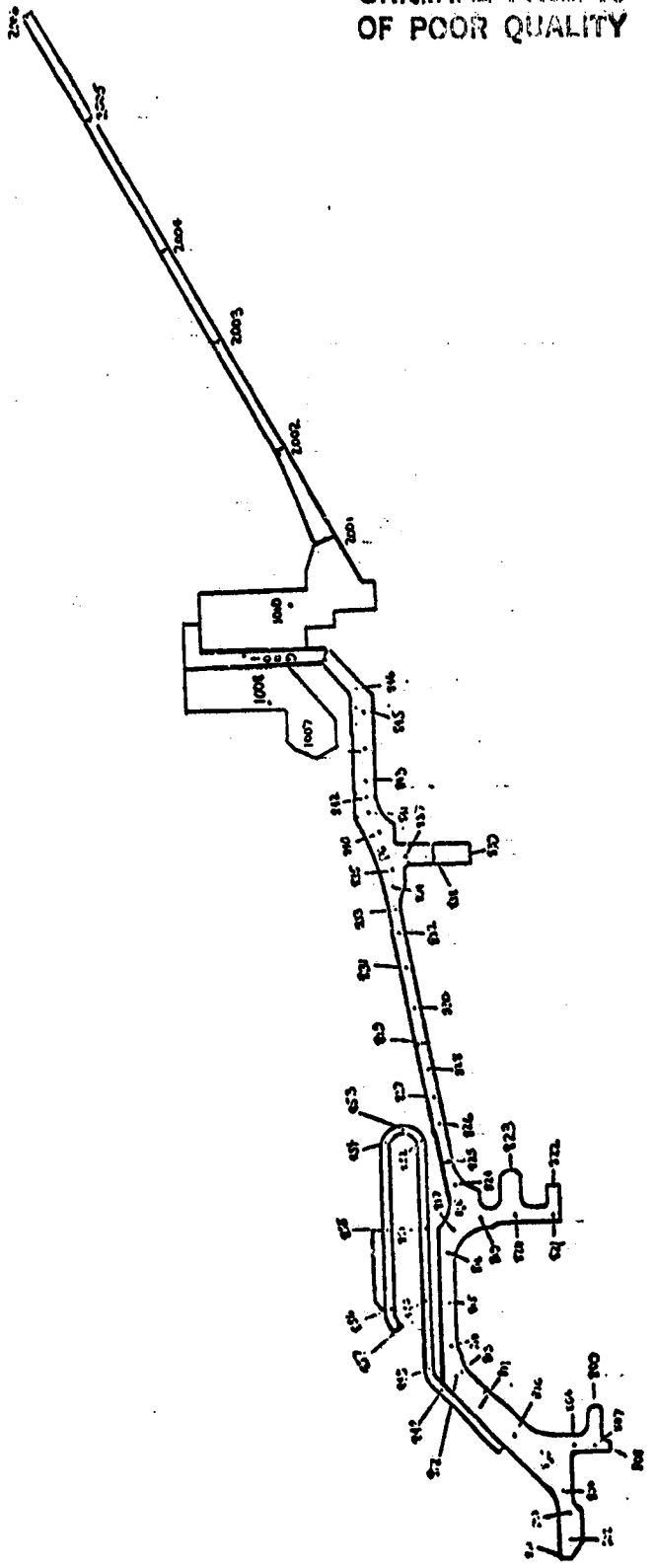

Figure 3. Typical CLASS MASS Model of HPT Shroud Support, Stage 2 Nozzle Support and Turbine Midframe.

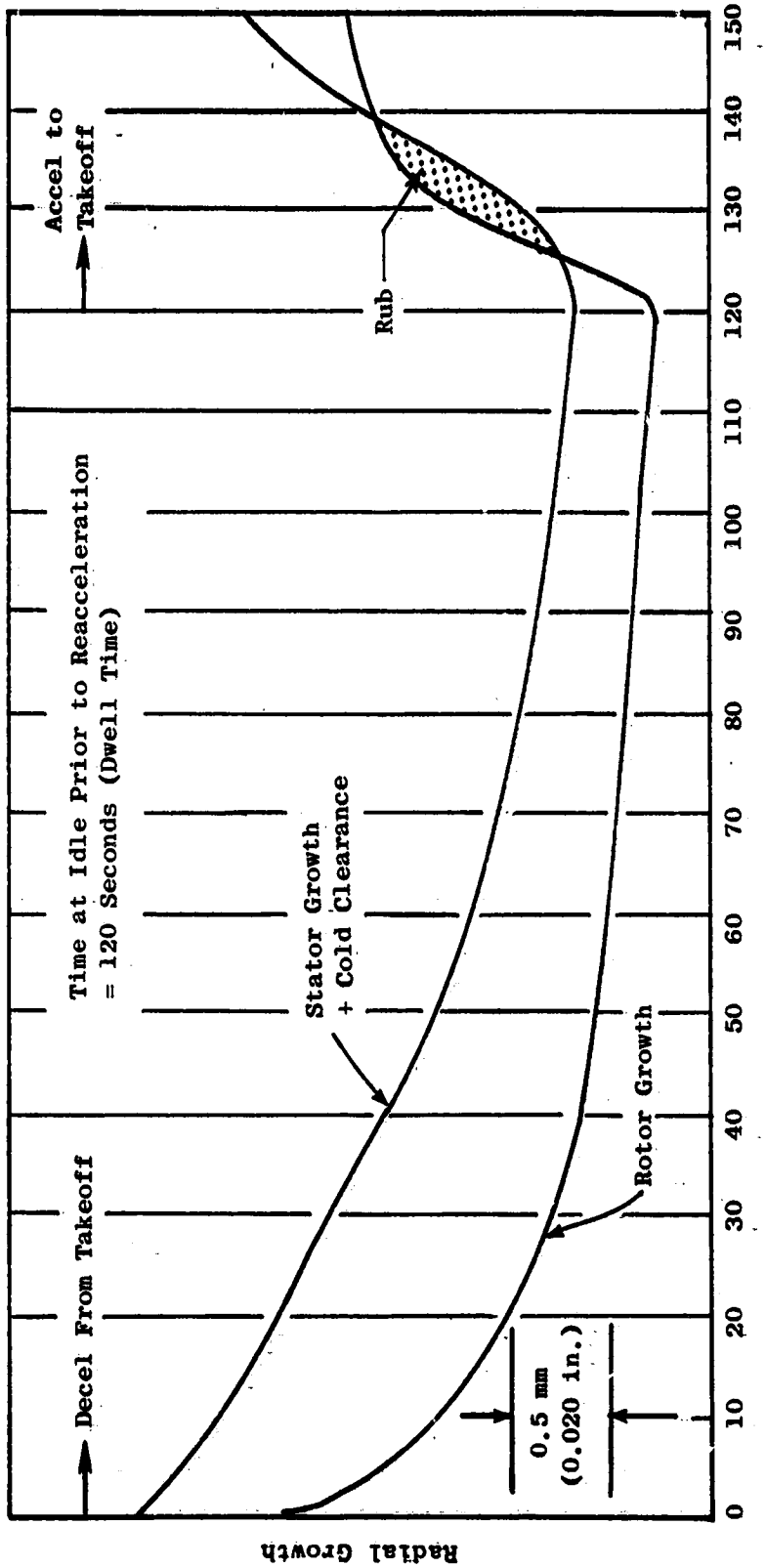

Figure 4. Typical Hot Rotor Reburst.

A significant part of engine deterioration may be caused by warm rotor reburstss (time at ground idle more than five minutes) for which little data are available. This test included warm rotor reburstss to provide data relative to this type of engine operation.

3.2 High Pressure Turbine Roundness

The control of the roundness of a gas turbine engine structure requires an evaluation of the material properties and characteristics as well as environmental influences for all the primary engine structural members. Figure 5 highlights and defines the critical structural members of this engine. These components include the fan casing, the compressor casing, the compressor rear frame (CRF), high pressure turbine (HPT) Stage 1 and 2 nozzle supports, the turbine midframe (TMF), the low pressure turbine (LPT) casing and the turbine rear frame (TRF).

Each of these components is subjected to varying levels of both non-axisymmetric loading and circumferentially nonuniform radial thermal gradients. These effects tend to induce out-of-roundness distortions in these components which can propagate throughout the entire length of the engine. The result is that the study of the roundness of an engine structure must include not only its inherent ability to remain round but also must include the distorting influence of neighboring structures.

The roundness study utilized General Electric Structural Analysis programs "CLASS/MASS" and "MASS", of the entire CF6-50 structural system. These models were used to evaluate the magnitudes of out-of-roundness of each component and the effects that distortions of the various components have on Stage 1 HPT shroud roundness.

Non-axisymmetric frame structures must first be modeled with the "MASS" program and the calculated deformations applied to the "CLASS/MASS" program as boundary conditions. The "MASS" program employs three-dimensional analysis and has the capability of handling non-axisymmetric structures consisting of plate, brick, shell and beam elements. Transient engine conditions were included in these analyses since the most severe thermal effects do not necessarily coincide, timewise, with the most severe mechanical loading effects.

The contributions of each engine component to both high pressure turbine roundness and transient clearances were then determined using Fourier Series approximations. These contributions were superimposed to obtain the roundness and clearance response maps of the high pressure turbine.

The analytical studies indicated that the compressor rear frame has a negligible effect on HPT out-of-roundness.

3.2.1 Turbine Midframe Effects

The blade tip clearance is influenced by the amount of distortion and out-of-roundness in the shrouds. The high pressure turbine shrouds in the CF6-50 engine are supported from the midframe forward flange. This flange is

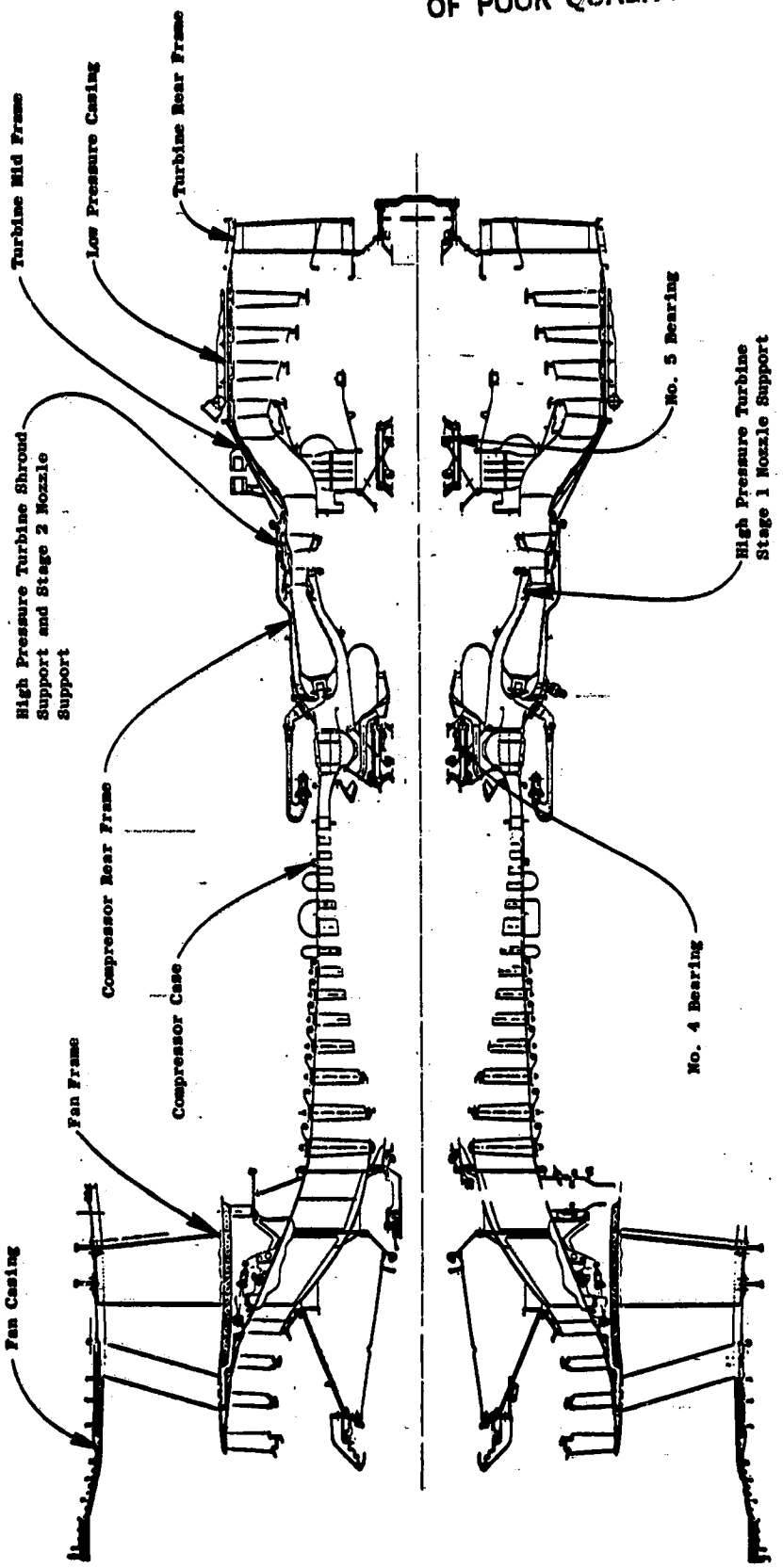

Figure 5. CF6-50 Major Cases and Frames.

connected to the structural hat sections of the turbine midframe by a sheet metal cone. The turbine midframe is shown schematically in Figure 6.

Turbine Midframe Temperature and Pressure Effects

Distortions of the turbine midframe structural hat sections are transmitted through the supporting structure to the high pressure turbine shrouds. Figures 7 and 8 show typically the kind of turbine midframe forward hat section and resultant high pressure turbine shroud distortions which result from the transients following the engine acceleration from idle to maximum power. These distortions primarily occur due to (a) mechanical loading on the turbine midframe, (b) pressure loadings transmitted to the turbine midframe, and (c) temperature differences in the engine structure. Structural temperature gradients are caused by different thermal response rates, gas stream circumferential temperature variations and strut internal air temperature variations. Three of the struts operate approximately 110°C (200°F) hotter than the other five struts. The varying strut temperatures result in different amounts of thermal expansion in the struts. This causes a nonuniform distortion of the turbine midframe hat sections and an out-of-roundness distortion of the high pressure turbine shrouds.

Turbine Midframe Deformation Due to Engine Mounting Loads

The turbine midframe is also deformed by loads from the mounting of the engine. The aft engine mount is an integral part of the structural hat section. These effects are included in the overall structural model.

Correlation of Analysis Techniques of High Pressure Turbine Stator Distortion Resulting from Turbine Midframe Distortion

An analysis of HPT stator distortion resulting from TMF distortion was performed using the General Electric Structural Analysis computer programs. The analysis method had been correlated by means of static testing (independent of and prior to this contract) of the full engine structure during which both TMF hat section and HPT stator out-of-roundnesses were measured. Three tests were conducted for the following loadings:

a. Vertical load reaction at engine aft mount points
b. Torque load reaction at engine aft mount point
c. Thermal loading where three of the eight TMF struts were heated 90°C (162°F) above the rest of the structure

The correlation between measured and calculated out-of-roundness is shown in Figures 9 through 11.

3.2.2 HPT Shroud Support Temperature Effects

Since roundness must be assured before any significant work can be directed toward blade tip clearance reduction, the turbine shroud structure itself must stay round. In addition to being influenced by other engine structures, turbine structures may lose their roundness due to recirculation of hot flowpath gases into the cabities between the turbine flowpath hardware. This recirculation of hot gases can induce local overheating of the turbine structural members, causing them to elastically distort.

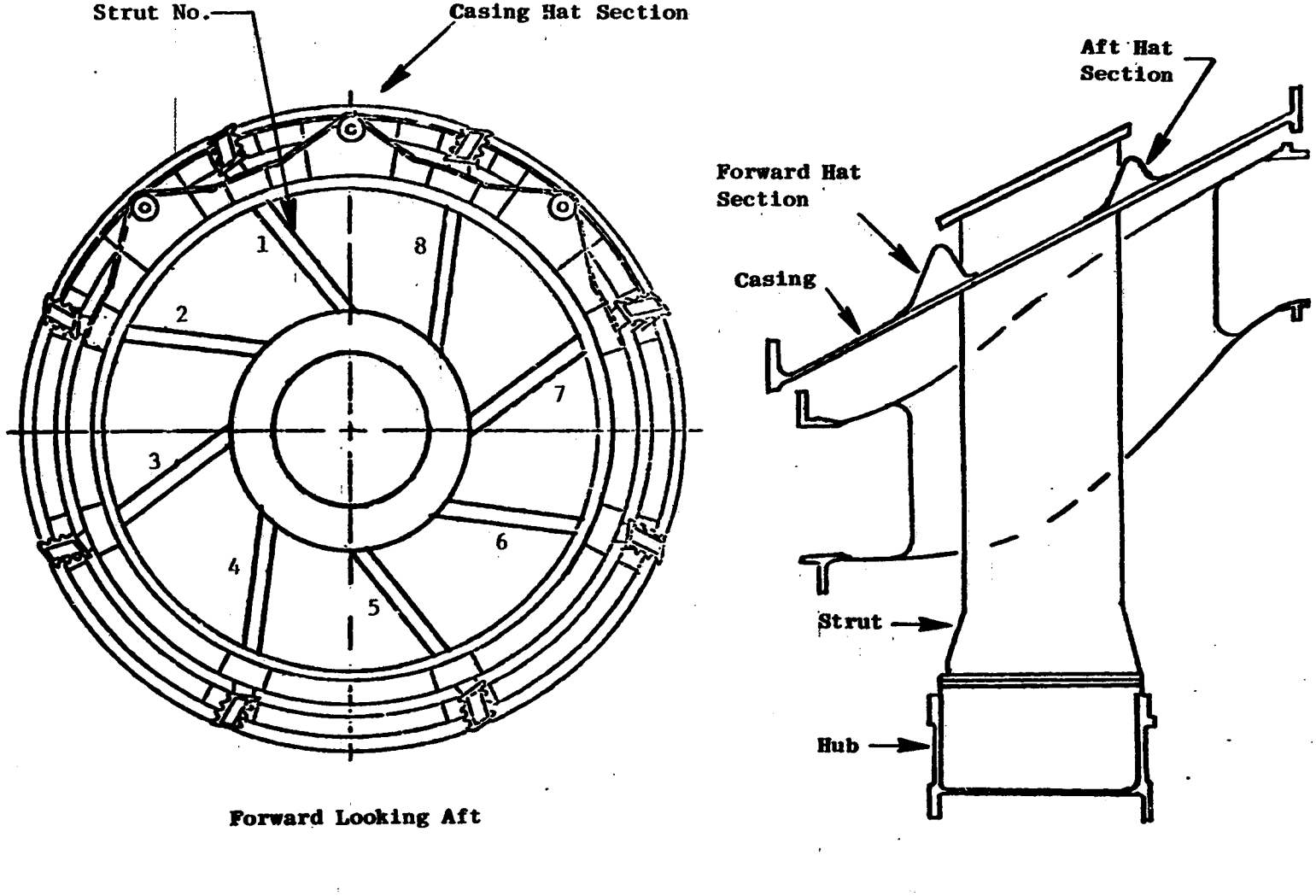

Figure 6. Turbine Midframe.

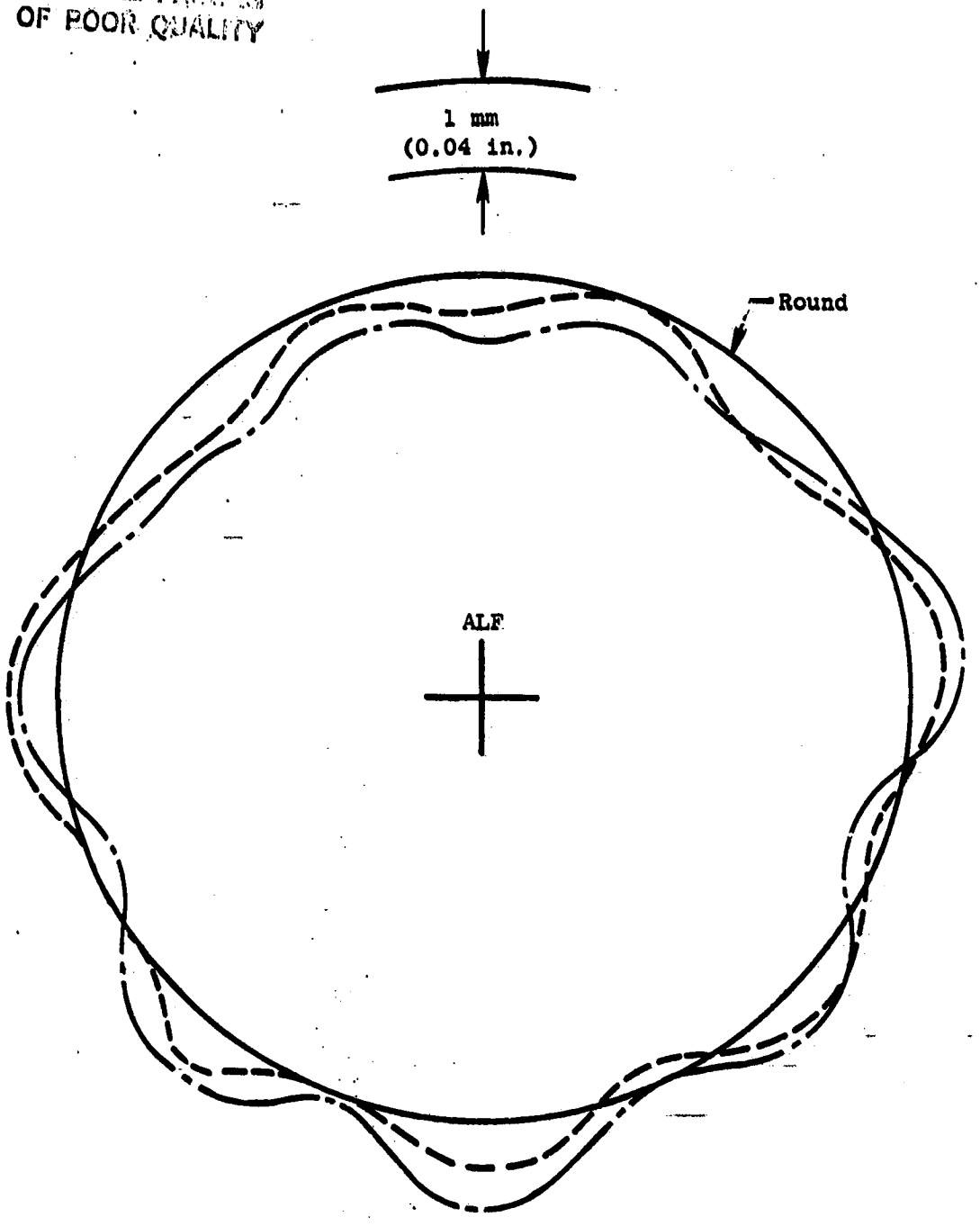

Figure 7. Typical Turbine Midframe Forward Hat Section Deflection Relative to Hub $\mathrm{C_L}$ Resulting from Takeoff Transient Operation.

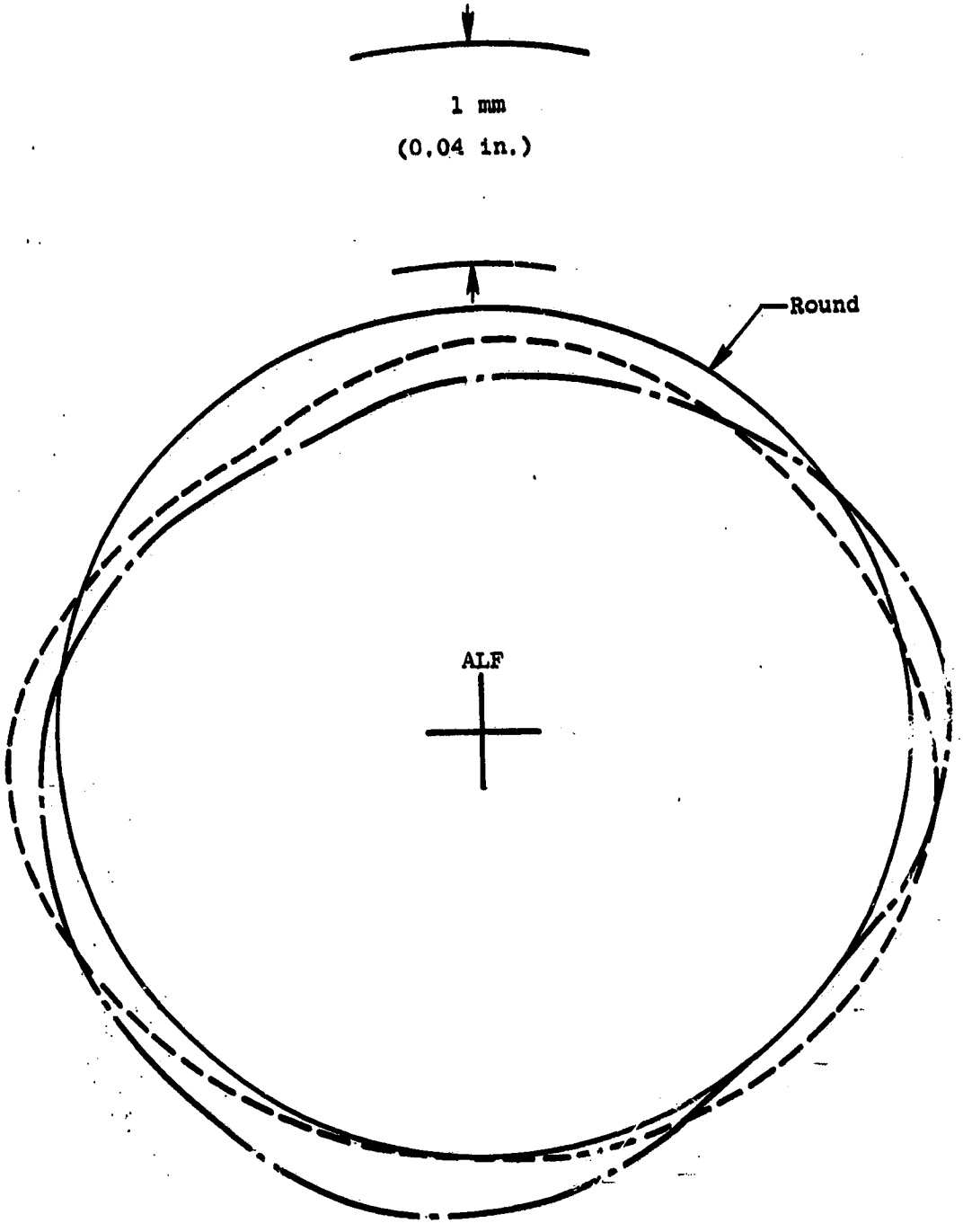

Figure 8. Typical HPT Shroud Support Deflection Relative to TMF Hub $\mathcal{L}$ (Caused by TMF Hat Section Distortion) Resulting from Takeoff Transient Operation.

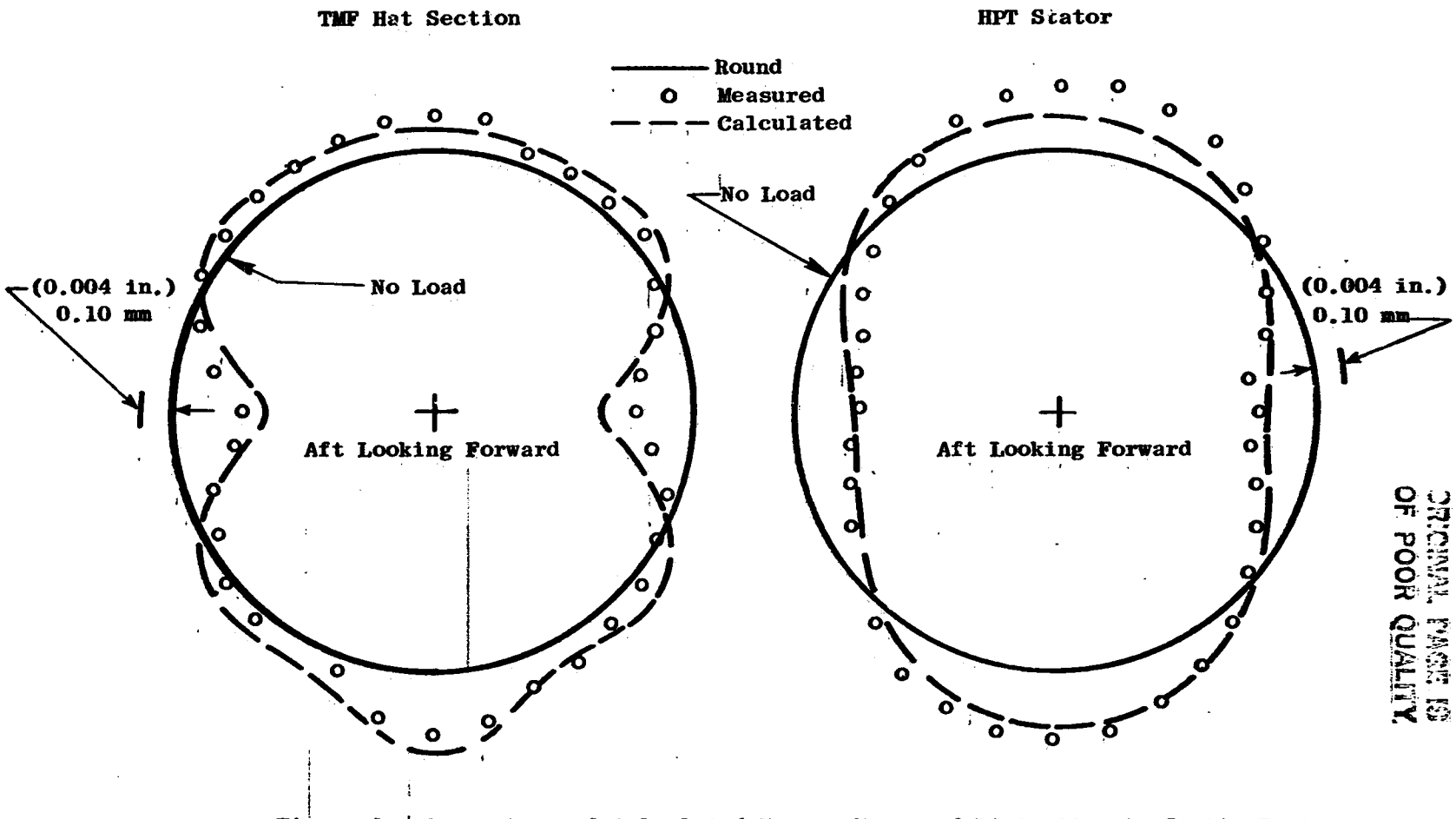

ORIGINAL PAGE IS
OF POOR QUALITY

Figure 9. Comparison of Calculated Versus Measured Distortion in Static Test, Vertical Mount Reaction Loading.

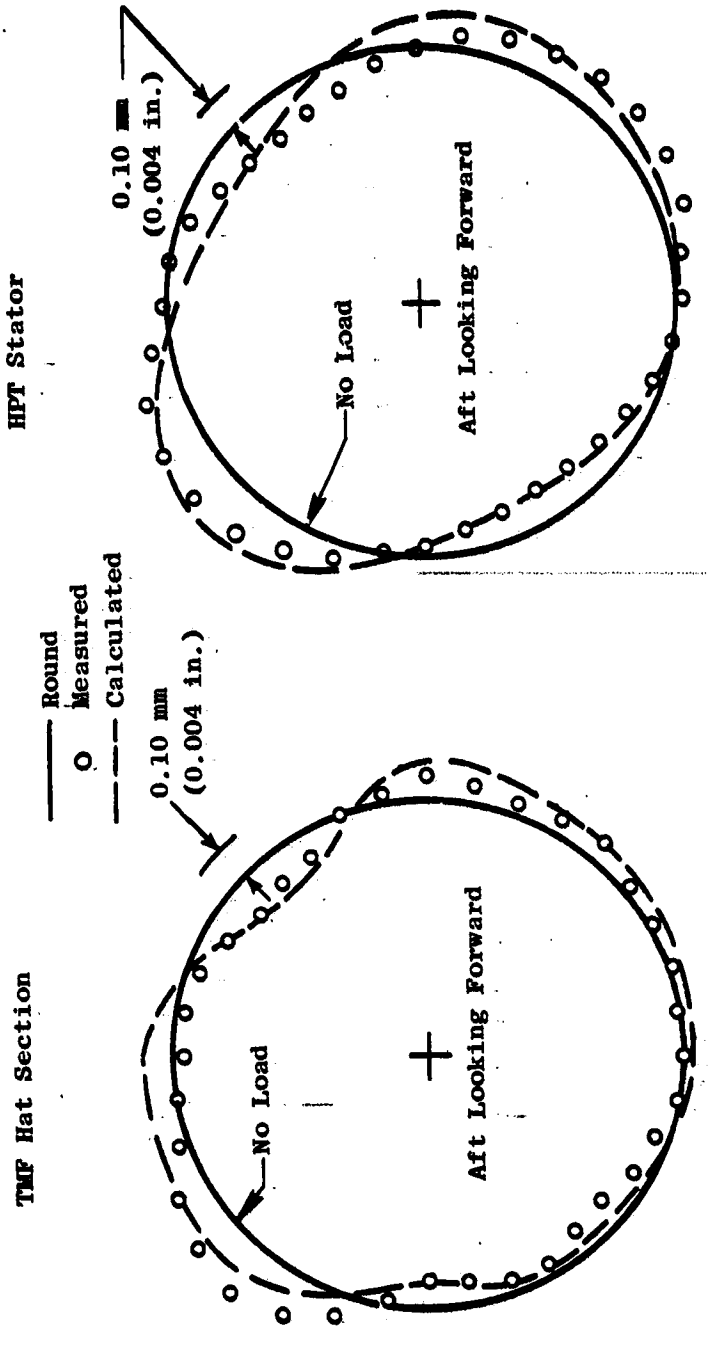

Figure 10. Comparison of Calculated Versus Measured Distortion in Static Test, Torque Reaction Mount Loading.

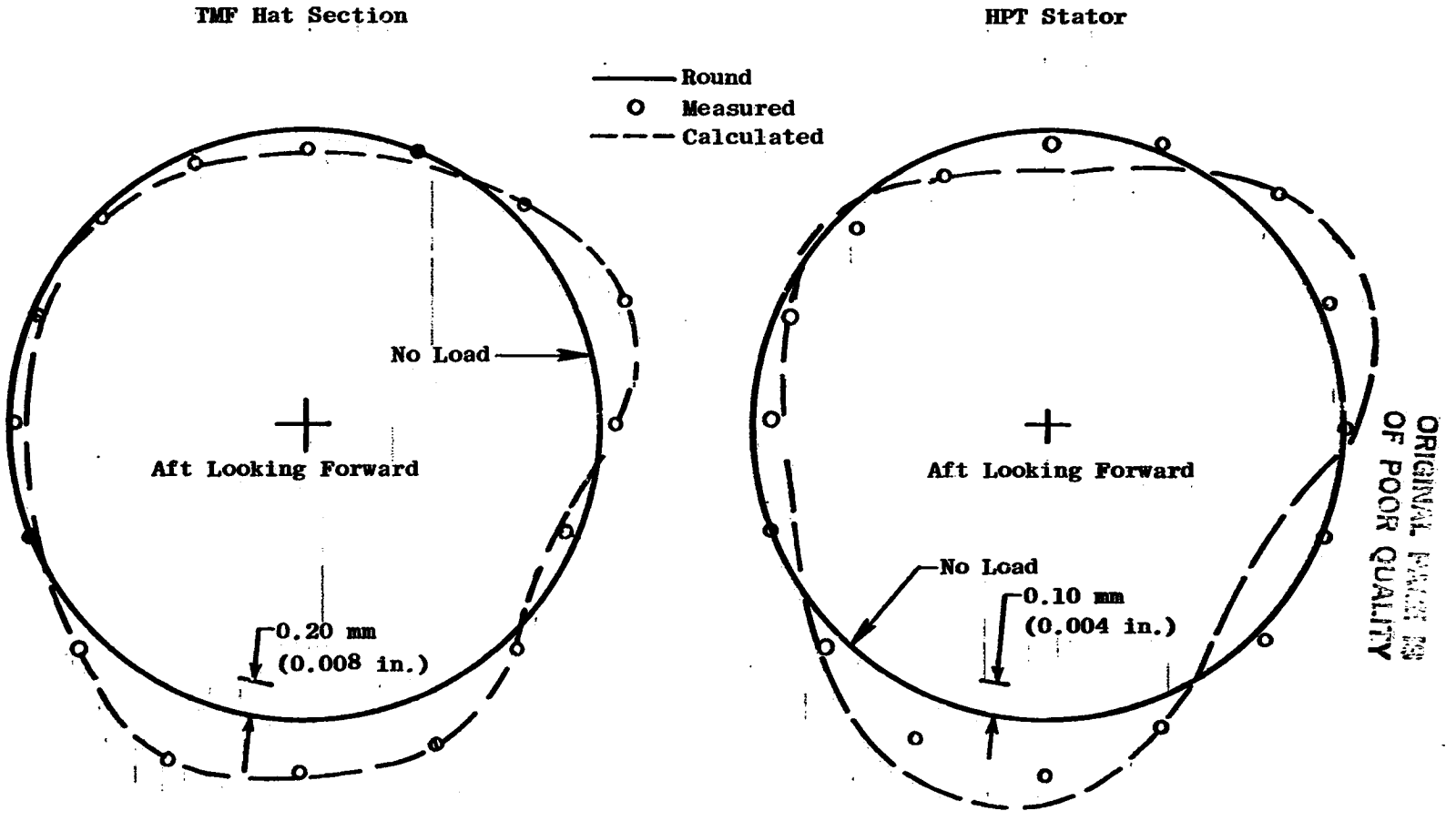

Figure 11. Comparison of Calculated Versus Measured Distortion in Static Test, TMF Struts Number 2,4,5 Heated Above Rest of Structure.

3.2.3 Low Pressure Turbine Casing Distortion Effects

The low pressure turbine casing, like the turbine midframe, is subjected to both axially and circumferentially varying temperatures and loads. Two mechanisms were judged to be possible contributors to HPT out-of-roundness. These mechanisms are:

1. Temperature differentials between the LPT stator case horizontal flanges and skin cause the horizontal flanges to grow relative to the skin, thereby distorting the LPT forward flange. These distortions are transmitted forward to the HPT stator.

2. Circumferential temperature gradients in the LPT stator case skin force the LPT stator case into an out-of-round shape and propagate forward to induce HPT stator out-of-roundness.

The HPT out-of-roundness caused by the horizontal flange/skin temperature gradients and circumferential thermal gradients was evaluated by using both computer and empirical models. The method of determining out-of-roundness had been verified by tests in which the flanges and skin of the LPT casing were heated and the resulting HPT deflections measured.

4.0 TEST VEHICLE AND INSTRUMENTATION

The test vehicle used in this investigation was a CF6-50C engine which had been assembled using standard turbine components representative of production engines currently operating in revenue service. Several components were modified for the installation of the clearanceometer probes and other required instrumentation leadouts.

The engine was assembled with large rotor-to-stator clearances except for the Stage 1 high pressure turbine (HPT). By building only the Stage 1 HPT with tight clearances, the intent was to isolate the effect upon performance of Stage 1 blade-to-shroud clearance by sustaining a blade-on shroud rub. Provided that no other components deteriorated during the time the rub was sustained, or that any deterioration which did occur could be identified and quantitatively assessed, the clearanceometer readings before and after the rub could be correlated with engine performance monitored before and after the rub to determine a relationship between changes in tip clearances and changes in engine health parameters (Exit Gas Temperature (EGT), Turbine Efficiency (η_T), Specific Fuel Consumption (sfc), Thrust (F), etc.). In particular, the relationship of clearance and efficiency determined through this test could be compared with those established in other tests to determine whether or not the relative significance of HPT tip clearance deterioration was weaker, stronger or about the same as had been assessed previously.

4.1 ENGINE CONFIGURATION

A description of the test vehicle and its associated component configuration is given as follows:

- Fan Frame — A standard CF6-50C front frame with rake pad capability to record compressor inlet characteristics, if needed.
- Compressor Stator — Standard CF6-50C compressor stator.
- Compressor Rotor — Standard CF6-50C rotor.
- Compressor Rear Frame — A CF6-50C frame modified to receive clearanceometer probes.
- Combustor — Standard CF6-50C combustor
- Fuel Nozzle — CF6-50C fuel nozzles.
- Stage 1 High Pressure Turbine Nozzle Assembly (including mini-nozzle) — CF6-50C assembly.

• Stage 2 High Pressure Turbine Nozzle Assembly	CF6-50C configuration modified to receive clearanceometer probes
• High Pressure Turbine Rotor	CF6-50C
• Turbine Midframe	CF6-50C
• Low Pressure Turbine	CF6-50
• Exhaust Nozzle	CF6-50C configuration

4.2 INSTRUMENTATION

Engine station (plane) designations used for the testing were in accordance with ARP755A. Figure 12 illustrates the plane locations on a CF6-50 engine cross section and identifies the instrumentation used. The instrumentation is broken down into four groups: general instrumentation, aerodynamic instrumentation, turbine structural instrumentation, and clearanceometer probe instrumentation.

4.2.1 General Instrumentation

- Barometric Pressure - The local barometric pressure measured using a recording microbarograph.
- Humidity - The absolute humidity measured in grains of moisture per pound of dry air using a humidity indicator.
- Cell Static Pressure (P_o) - Test cell static pressure measured at four locations in the cell.
- Fan Speed (XNL) - Low pressure rotor speed measured using two fan case mounted, fan speed sensors.
- Core Speed (XNH) - High pressure rotor speed measured using engine core-speed sensor driven off the end of the lube and scavenge pump.
- Main Fuel Flow (WFM) - Volumetric flowmeter, facility mounted.
- Verification Fuel Flow (WFV) - Second fuel flowmeter mounted in series with WFM.

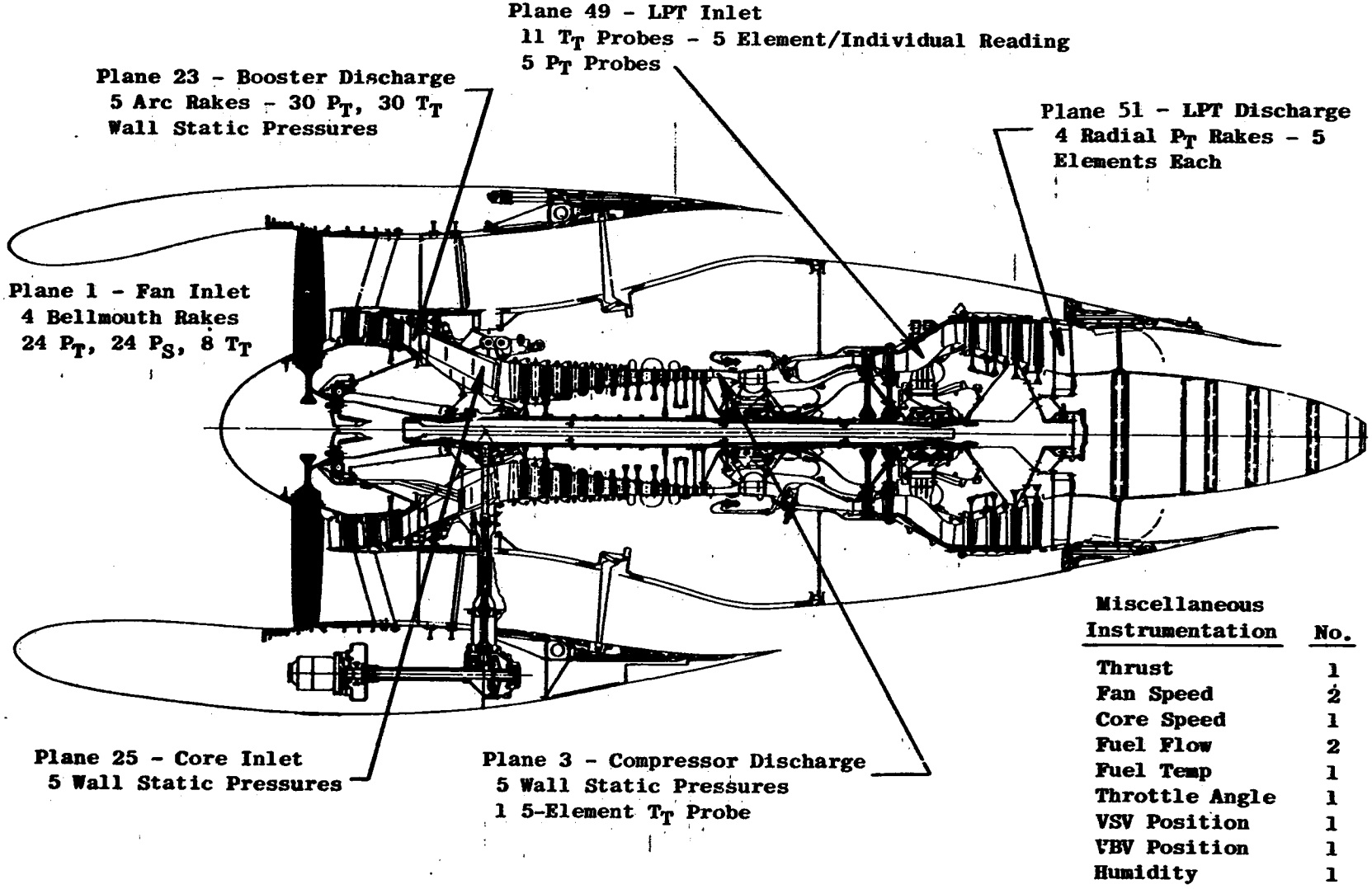

Miscellaneous Instrumentation	No.
Thrust	1
Fan Speed	2
Core Speed	1
Fuel Flow	2
Fuel Temp	1
Throttle Angle	1
VSV Position	1
VBV Position	1
Humidity	1
Barometer	1

Figure 12. Engine Instrumentation.

- Fuel Temperature - Temperature of fuel measured at the facility flowmeter using a single chromel/alumel probe in the fuel line.
- Fuel Sample Specific Gravity (SGSAMP) - Specific gravity of the fuel sample measured using a hydrometer.
- Fuel Sample Temperature (TSAMP) - Fuel sample temperature measured during the specific gravity measurement.
- Fuel Lower Heating Value (LHV) - Lower heating value of the fuel sample as determined by a bomb calorimeter.
- Thrust (FG) - Thrust-frame, axial force measuring using three strain-gage type load cells for redundant measurement.
- Variable Stator Vane Position (VSV) - Readout of the LVDT attached to the high pressure compressor variable stator pump handle.
- Variable Bleed Valve Position (VBV) - Readout of the LVDT attached to the variable bleed valve actuation mechanism.

4.2.2 Aerodynamic Instrumentation

The following rakes, probes, and static pressure taps were installed to measure airflow, temperature, and pressure as required to define component performance. (See Figure 12.)

Fan Inlet (Plane 1)

Bellmouth rakes were installed to measure static pressure, total pressure, and total temperature at the fan inlet. Four rakes, each having six total pressure probes, six static pressure probes, and two total temperature probes were used.

Booster Discharge (Plane 23)

Five arc rakes, each having six temperature and six pressure probes were installed to measure booster discharge total temperature and total pressure. Ten taps were installed to measure booster discharge static pressure.

Compressor Inlet (Plane 25)

Five flowpath-wall static pressure taps were installed.

Compressor Discharge (Plane 3)

Five of the borescope port plugs in the compressor rear frame were modified to permit compressor discharge static pressure measurement. A single 5-element thermocouple probe was used to measure compressor discharge temperature.

Low Pressure Turbine Inlet (Plane 49)

Temperature in this plane is measured by eleven 5-element rakes with individual probe readout to permit monitoring of temperature profiles. Pressure is measured using five probes, each having five elements all feeding a single fitting.

Low Pressure Turbine Discharge (Plane 5)

Low pressure turbine discharge pressure is measured using four rakes, having five elements each.

4.2.3 Turbine Structural Instrumentation

- HPT Stator Thermocouples: 24 imbedded in structure and 2 air thermocouples
- HPT Stator Pressure Probes: 4 basket-type pressure probes in the Stage 1 shroud cooling air supply cavity
- Engine Structure Thermocouples: 156 metal and 14 air thermocouples
- Engine Structure Cooling Air Temperatures and Pressures: 14 air thermocouples and 10 pressure probes
- LPT Case Thermocouples: 48 metal thermocouples
- LPT Case Cooling Manifold and Under Cowl Instrumentation: 17 pressure probes under cowl and in supply tubes

4.2.4 Clearanceometer Probe Instrumentation

Eight clearanceometer probes were installed in the test vehicle above the Stg. 1 blade tips as shown in Figure 13. These probes were used to obtain real-time, individual high pressure turbine blade tip-to-shroud clearance measurements to an accuracy of $\pm$0.05 mm (0.002 in.). The high pressure turbine stator on the test vehicle was modified to receive the probes. The reworked stator components included: Stage 1 shrouds, Stage 2 nozzle support, filter screen and 10th stage air seal. The clearanceometer probes were located at eight circumferential positions, as nearly equally spaced as was practical (Figure 13).

Each clearanceometer probe was individually calibrated and checked during assembly on the HPT stator. A final reference calibration was obtained during initial cold rotation and motoring of the engine.

A proven light-beam triangulation technique was utilized for the clearance measuring sensors. Data were collected for fixed-time intervals and individual blade clearances were obtained from each probe. Individual probe processors were used to store clearance data and the processor calculated blade minimum, maximum and average clearances from all the data collected. A high speed data tape recorder was used to independently record individual blade clearances.

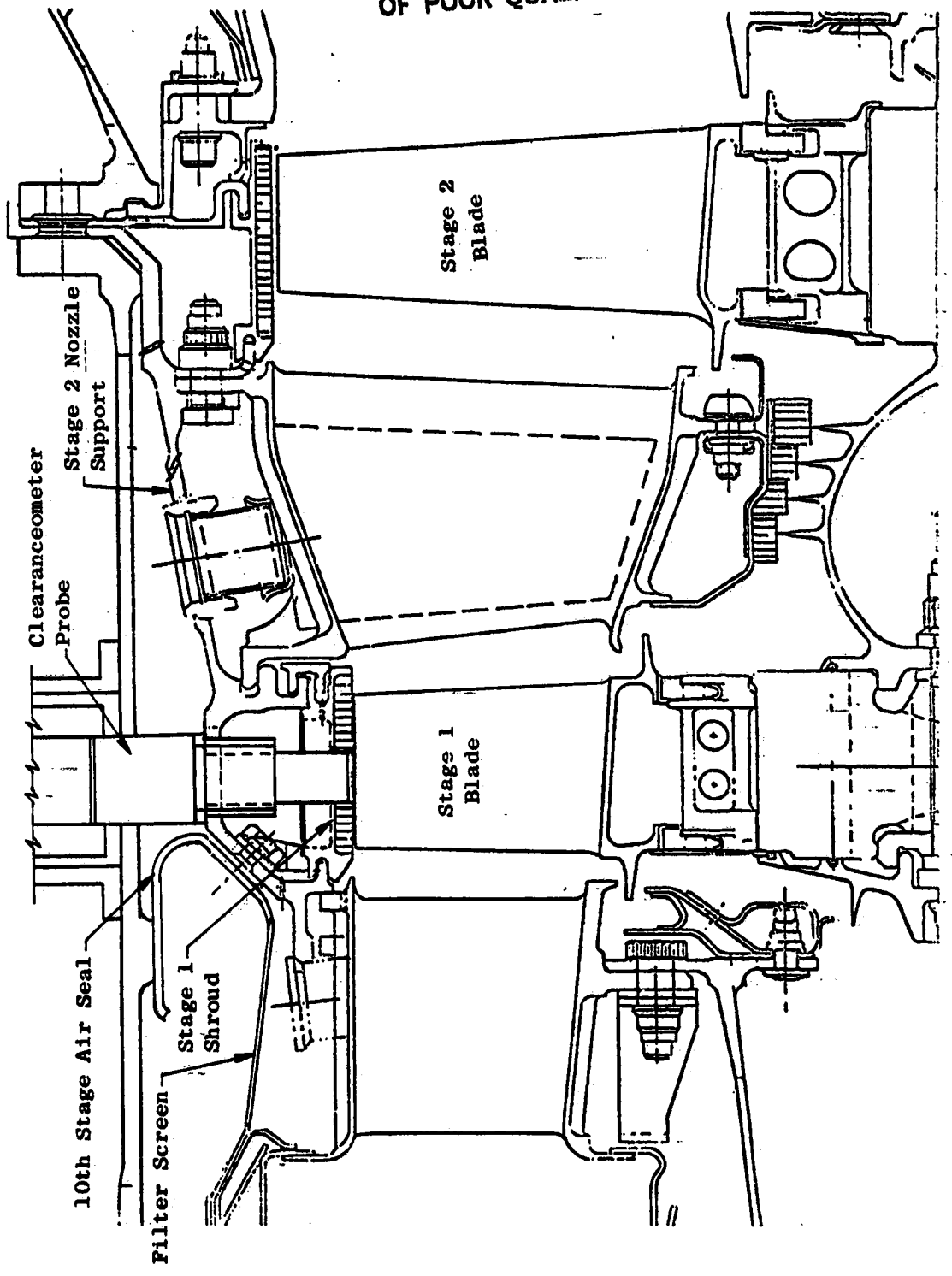

Figure 13. HP Turbine Probe Location/Reworked Components.

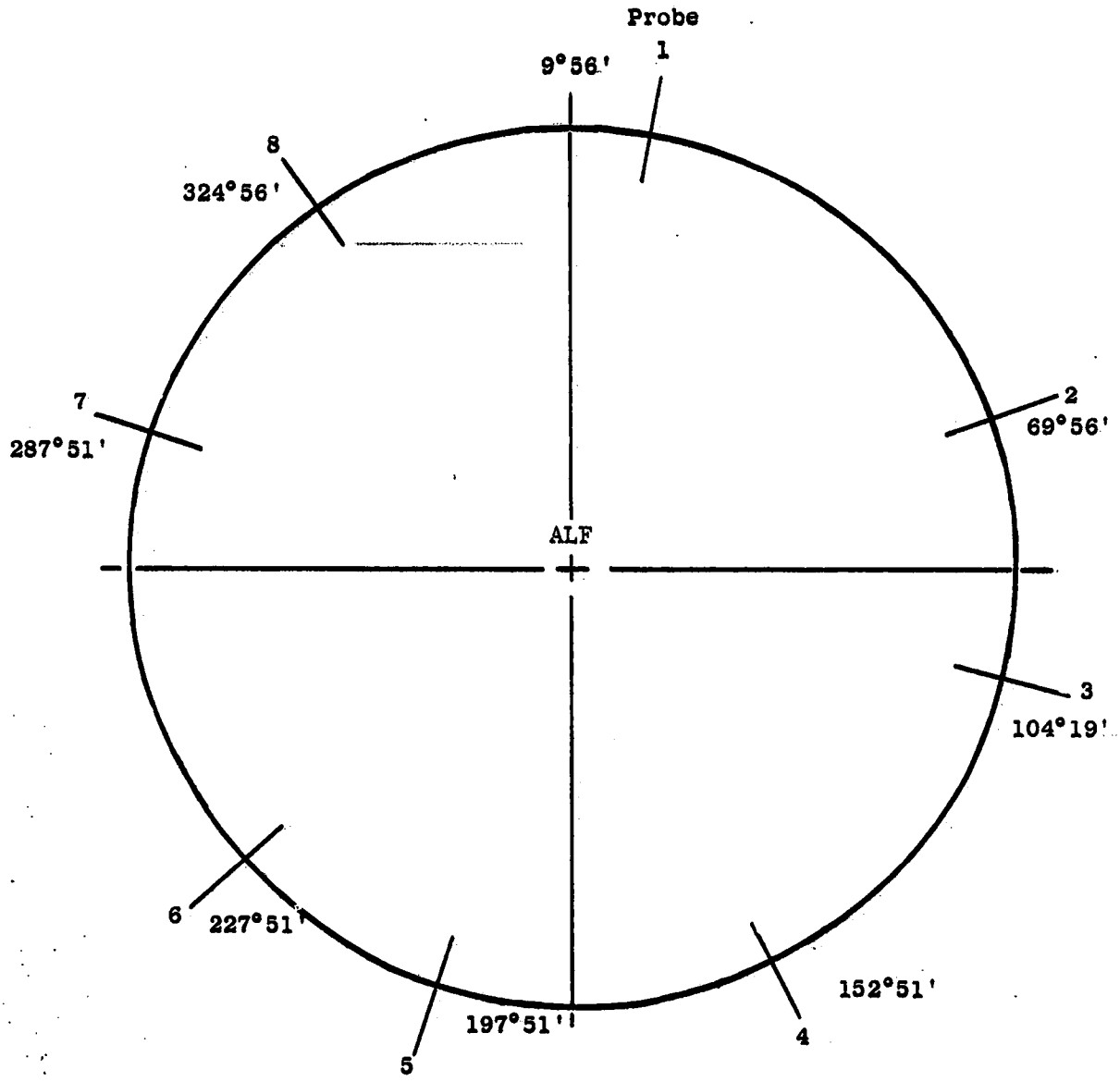

Figure 14. Probe Angular Position Aft Looking Forward.

5.0 TEST FACILITY

All testing was conducted in Test Cell 2, Building 500, at the General Electric Company plant in Evendale, Ohio. A photograph of an engine installed in the test cell is shown in Figure 15.

Cell 2 has access to the data recording systems in the Instrumentation Data Room. In addition to the standard test cell equipment, a clearanceometer probe cooling system was provided which utilized engine compressor bleed air. A microcomputer and high speed signal processor were used to collect and record the clearanceometer data.

The data acquisition and processing system in use in Evendale consist of a Cell System and a Site System. The Cell System performs steady-state and transient data acquisition, conversion to engineering units, quick-look performance calculations, and short-term storage. Converted data is automatically transmitted to the Site System for further on-line processing and hard-copy output. The Site System utilizes a data-base concept for efficient storage, retrieval, and reprocessing of current and historical data. In addition, data may be transmitted to the General Electric Evendale Time Sharing Computer Center for further processing, such as cycle deck analysis and comparison.

Data acquisition capability consists of 400 pressure channels, 400 temperature channels, 10 frequency channels, and 28 d.c. voltages, such as: load cells, individual pressure transducers, position potentiometers, etc. The pressure system consists of ten 40-port scannivalves with available pressure ranges from $\pm$ 6.9 N/cm^2 (10 psig) through $\pm$ 345 N/cm^2 (500 psig). The system incorporates auto-ranging and multiple sampling capability for all data channels to assure optimal resolution and precision in addition to variable averaging time for frequency measurements. Data may be achieved and processed in either a steady-state or transient mode. Typical acquisition time for all data to be recorded for a steady state test point (condition) is 30 seconds and each measurement (parameter) is sampled 40 times over that time period. Transient acquisition rates are variable from one sample per second per channel to 250 samples per second per channel. Redundant measurements are made of key parameters such as fuel flow, fan speed, and thrust. Automatic data rejection techniques, ratio of redundant measurements, and on-line system-verification analysis further enhance overall data quality.

All data is converted to engineering units on the Cell System and automatically transferred to the Site System. These are then used in various data-analysis computer programs. Quick-look programs are available on the Cell System to provide on-line and hard copy of overall engine performance and health calculations. Simultaneously, these data are available at the Site System for hard copy and plotting of corrected overall and interstage performance characteristics. Engineering units and/or calculated data may be transmitted to the General Electric Evendale Time-Sharing Computer Center for archival storage and additional analysis such as cycle deck comparison.

Figure 15. CF6 Engine in Test Cell.

6.0 TEST PROCEDURE

The test objectives were to secure round engine clearance maps, i.e., blade tip clearances as a function of core speed, compressor exit temperature, compressor exit pressure, and time; and both steady-state and transient out-of-roundness maps. The effect of varying clearance upon engine performance was also to be evaluated. The clearance and out-of-roundness maps were to be determined from the data generated by clearanceometer probes.

In order to achieve these objectives, a test plan was developed which consisted of operating the engine at the following test conditions:

- Cold motoring
- Ground idle
- Slow accels to, and decels from takeoff power
- Steady-state operation at takeoff power
- Several bursts to and chops from, takeoff power with specified time intervals at takeoff
- Several rebursts to takeoff power after specified time intervals at ground idle (dwell time)
- Sufficient engine speed settings to establish the performance power calibration
- Stopcock

A schematic presentation of the test sequence, showing power level conditions or settings for specified times, is given in Figures 16 and 17. There were actually two types of test operations. One was performed to provide accurate transient response; the other was used to evaluate the relationship of clearance to performance. The stopcock, or engine shutdown from cruise power by turning the fuel flow off, concluded the second test sequence. The intent of this investigation was to obtain data on the effect of this operation, which is performed in aircraft acceptance testing, on short term performance deterioration.

6.1 PERFORMANCE TEST

The performance test program was designed to evaluate the performance and Stage 1 rotor tip clearance over a range of power settings after the engine reached steady-state conditions. Each power calibration consisted of back-to-back sets of power levels in descending order of fan speed with a short shutdown in-between. The engine shutdown was included to assure testing repeatability.

A list of the speed settings and stabilization times for the power calibration checks (both "A" and "B") is presented in the following table:

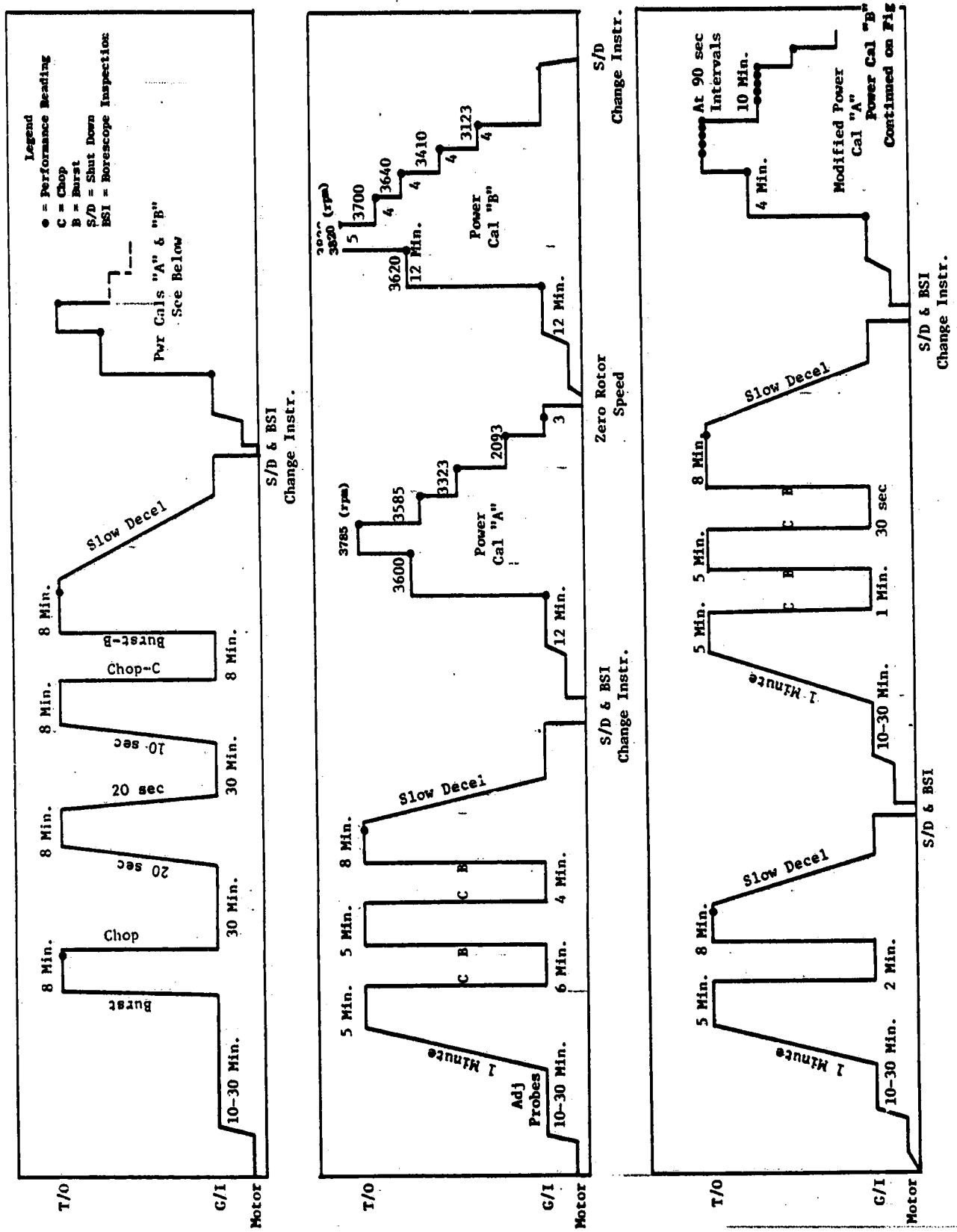

Figure 16. Test Sequence (Continued on Figure 17).

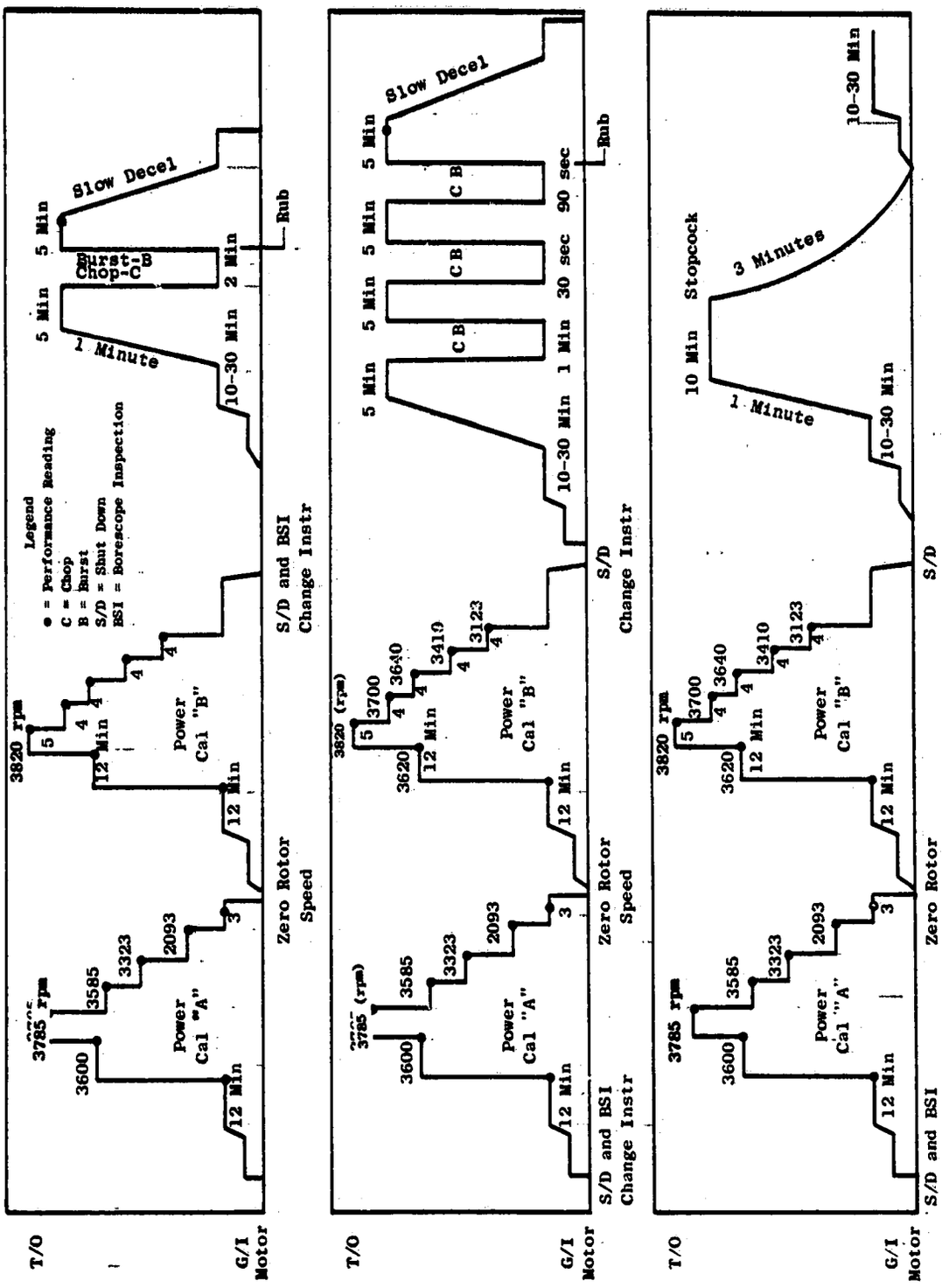

Figure 17. Test Sequence.

POWER CALIBRATION TEST RUNS

Corrected Fan Speed (rpm)	Stabilization Time (Min)
Power Calibration "A"	
Ground Idle	12
3600	12
3785	5
3585	4
3323	4
2093	4
Ground Idle	3

Shut down, obtain new thrust balance measurement (or reading) and restart engine

Power Calibration "B"	
Ground Idle	12
3600	12
3820	5
3700	4
3640	4
3410	4
3123	4
Ground Idle	3
Shut Down	-

Data Analysis Technique

The data were analyzed using the General Electric Phase II computer program. This program has for its basis a status cycle deck representative of the particular engine model being tested. Some of the key features of this data analysis program are:

a. For each test reading, a pretest prediction point is run on the cycle deck at the tested conditions (ambient temperature, pressure, humidity, etc.), and this pretest point is used to check raw data quality.

b. Several alternate analysis paths are built in for determination of core flow, low pressure system work, etc. In addition, it is possible for the user to select his own analysis setup. All of these analysis paths guarantee a balanced cycle; that is, the solution is self-consistent and satisfies the continuity, momentum, and energy equations.

c. The built-in analysis options feature mission data protection. When a measurement is missing, a suitable assumption is made to replace the measurement in the analysis; for example, when compressor discharge temperature is unavailable, compressor efficiency is held at the predicted level to effectively take its place. For a few key measurements, the analysis is terminated when they are unavailable, but for the majority of the measurements, an alternate analysis is performed instead.

d. At the conclusion of the analysis, the cycle deck is matched to the test data; that is, the cycle deck maps, etc., have been rescaled to be consistent with the measurements.

e. The data is adjusted to dry, sea level, static, standard-day condition by running the rescaled cycle deck at the standard condition. This method for correcting the data eliminates the problem, encountered in the past, of trying to select a single number to represent, for example, the temperature effect on fuel flow independent of power setting or type of day. This is particularly significant in modern engines because they employ more variable geometry.

6.2 POSTTEST TEARDOWN AND HARDWARE ANALYSES

After the conclusion of the engine testing, the turbine section of the engine, including the high pressure turbine rotor, Stage 2 nozzle assembly (with Stage 1 and 2 shrouds) and turbine midframe, was disassembled and visually and dimensionally inspected. These measurements were then correlated with the clearanceometer data, especially the data obtained during cold motoring.

7.0 TEST RESULTS

7.1 ENGINE PERFORMANCE

During the clearance phase of the testing, performance was measured several times throughout the test to ascertain any resulting effects on engine parameters.

Analytical studies predicted a stage one blade-on-shroud rub to occur during both a two-minute and a ninety-second reburst. Performance was monitored initially prior to any of the reburst and again prior to the two-minute reburst, after the two-minute reburst, prior to the ninety-second reburst, and after the ninety second reburst.

The clearance probe measurements showed that a rub of 0.305 mm (0.012 in) was sustained during the reburst testing. The performance instrumentation provided data for the G.E. Phase II computer analysis of engine performance. Assumptions and data adjustments made in this performance study were:

a. All data were adjusted within the program to sea level, dry, standard day conditions.

b. Core flow was based on high pressure turbine flow function.

c. Compressor discharge temperature was based on the initial build status deck compressor map and compressor efficiency characteristics were assumed to remain constant throughout this testing. This assumption or correlation use was necessitated by difficulties encountered with compressor discharge instrumentation. This is considered a valid deviation, however, since the compressor stages were intentionally assembled with large tip clearances to avoid rubbing, which could very well result in lower efficiencies.

d. The High Pressure Turbine efficiency was calculated from the turbine pressure ratio, inlet temperature and work extraction. The turbine inlet temperature (not measured) was determined from the compressor discharge temperature and the combustor temperature rise associated with the measured fuel flow. The turbine work was determined from an energy balance with the measured compressor system. This is an accepted procedure.

e. The low pressure turbine for this test was built with new stationary seals. Thus, some LP turbine deterioration was experienced during the test program and is accounted for in the measured overall performance results. The Phase II data analysis indicated the amount of LP turbine deterioration was on the order of 0.1% ΔSFC and 0.6° C (1° F) increase in exhaust gas temperature. The performance data reported herein have been adjusted to account for the LPT deterioration so that the data could be compared with respect to performance effects due to the HPT only.

7.1.1 Discussion of Results

The results shown in Figures 18, 19 and 20 represent the changes in high pressure turbine efficiency, exhaust gas temperature and overall engine specific fuel consumption associated with a clearance change of 0.305 mm (0.012 in) from the baseline performance power calibration.

A prediction of changes in turbine efficiency, exhaust gas temperature and specific fuel consumption was made for an 0.305 mm (0.012 in) change in Stage 1 rotor tip clearance. This prediction was based upon the analysis of test results obtained in several air turbine component tests and the attendant engine performance models developed as a result of these and others designed to isolate the performance related characteristic. A comparison of the test data and predictions is shown in the following table:

Effect of 0.305 mm (12 mils) Stage 1 Tip Clearance Increase at Takeoff

(F = 222kN/50,000 Lb)

	Test Results	Pre-Test Prediction
$\Delta\eta$ %	-0.7	-0.57
Δ EGT ^{o}C	9	7
Δ SFC %	0.37	0.55
$\frac{\Delta \text{ Clearance (mm)}}{\Delta\eta \text{ T (\%)}}$	-0.44	-0.53
$\frac{\Delta \text{ Clearance (mils)}}{\Delta\eta \text{ T (\%)}}$	-17	-21

If all of the calculated deterioration in engine performance is assignable to the measured change in HPT Stage 1 blade tip clearance, the results of this test show a stronger effect of Stage 1 clearance on performance than determined by previous tests. Therefore, explanations for this difference were sought.

Mentioned previously was the assumption during performance data reduction that the compressor had not deteriorated during this test. There is no evidence, based on tip clearance, that the compressor changed.

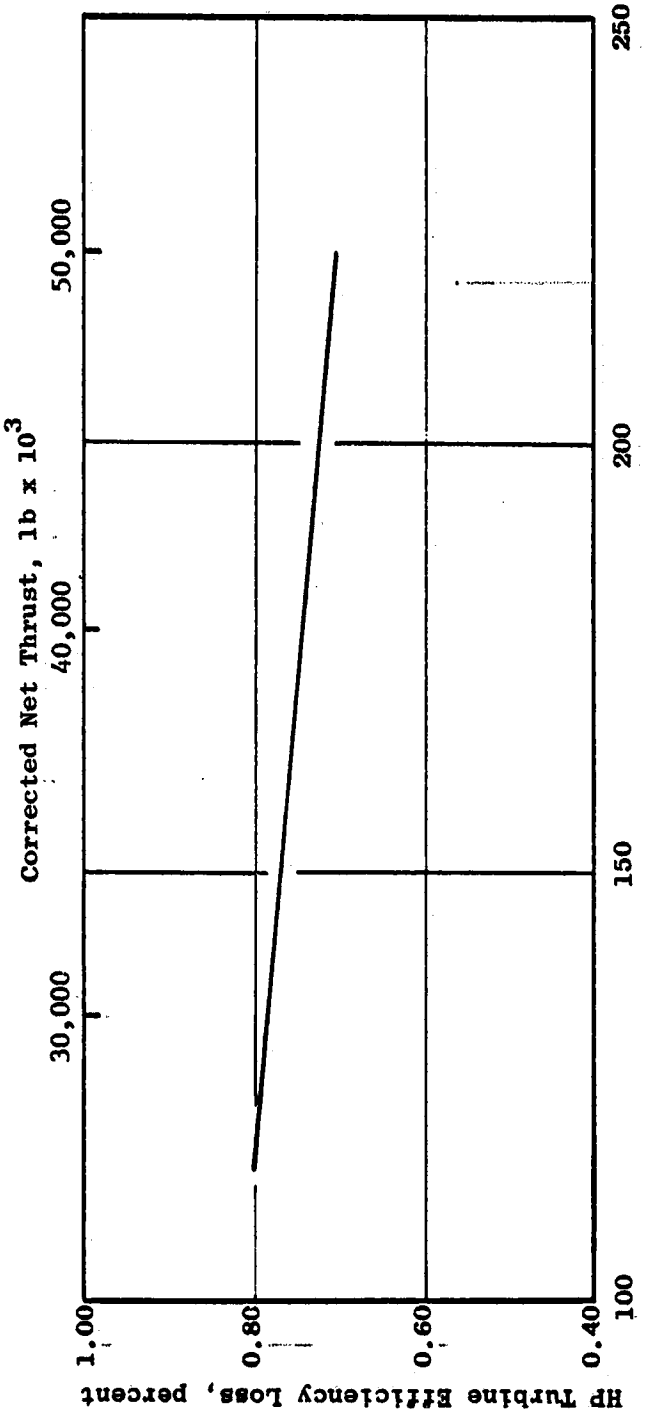

Figure 18. HP Turbine Efficiency Loss Associated with Tip Clearance Change of 0.305 mm (0.012 inch).

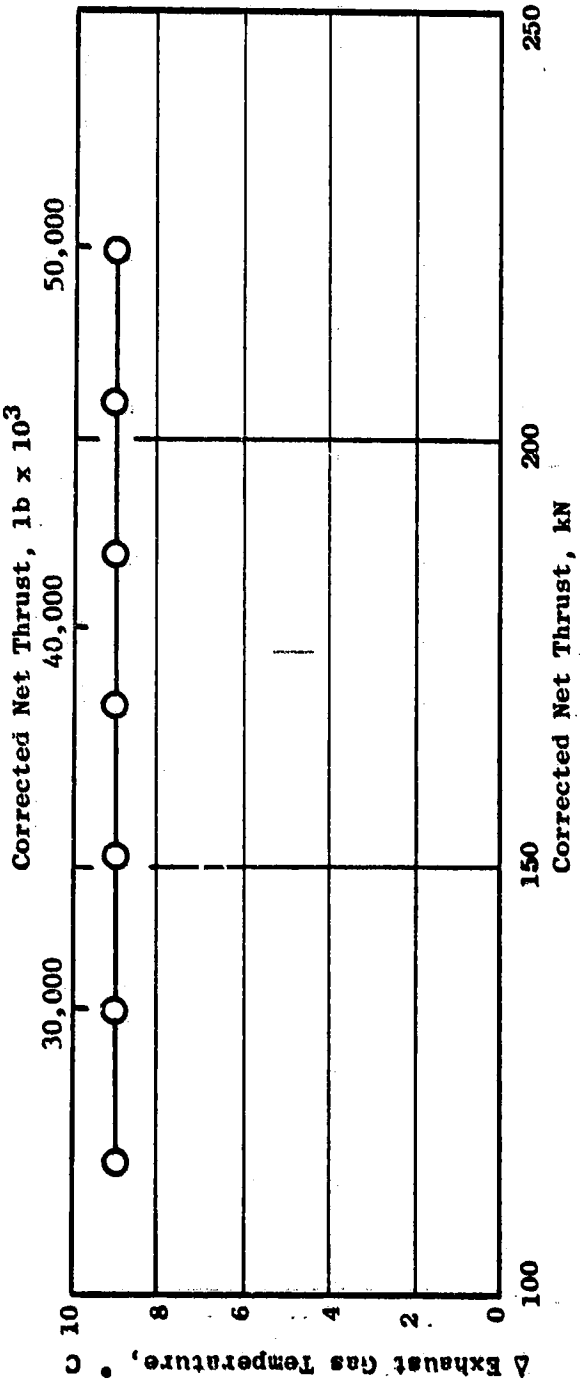

Figure 19. Exhaust Gas Temperature Increase Associated with 0.305 mm (0.012 inch) Increase in HP Turbine Tip Clearance.

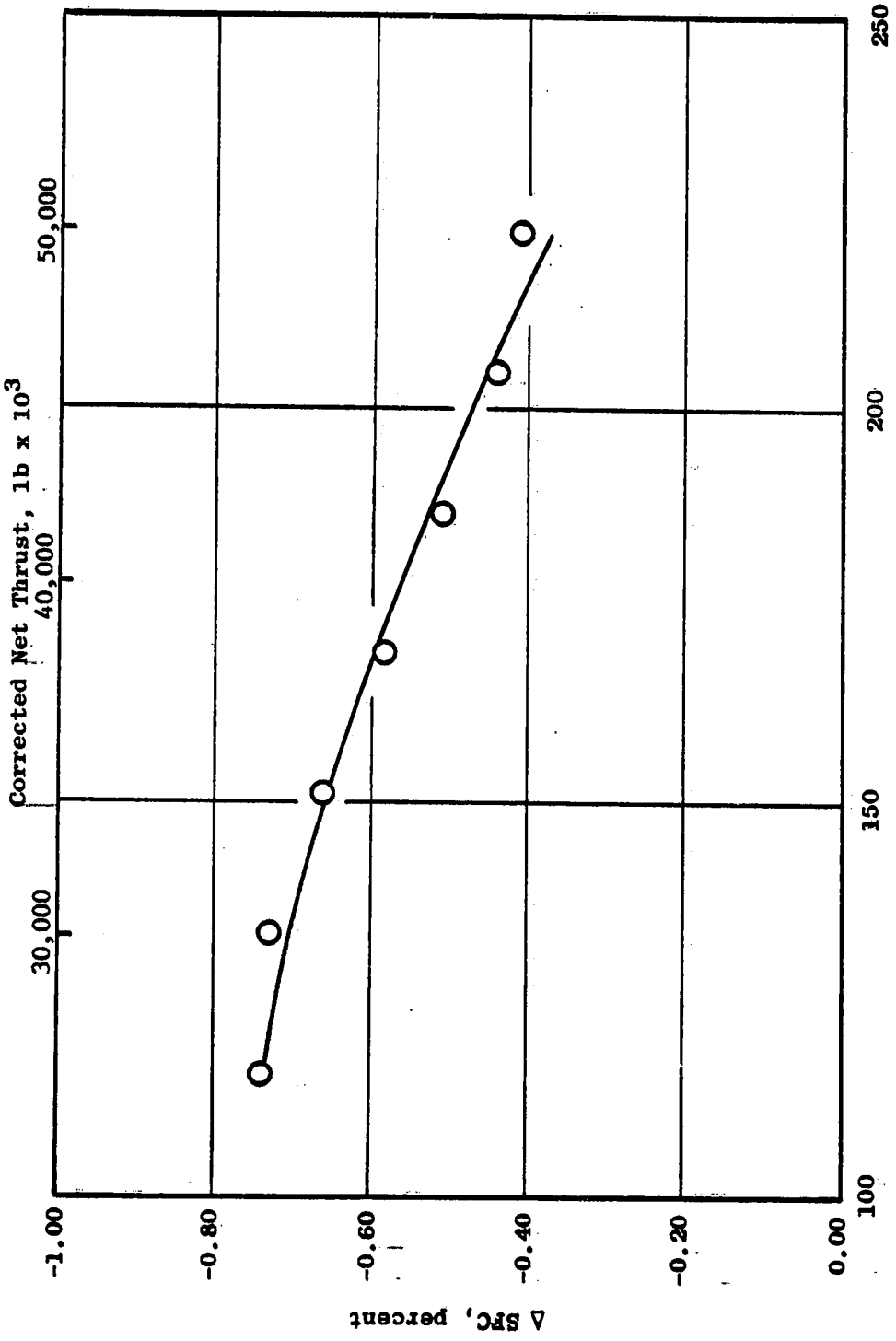

Figure 20. Loss Overall Engine Performance Associated with HP Turbine Tip Clearance Change of 0.305 mm (0.012 inch).

The deterioration of the Low Pressure Turbine was assessed at 0.1% in SFC. If this number were in error, the results for HPT Stage 1 clearance derivative would change.

Throughout the CF6 diagnostic program, a cause of deterioration, which has been consistently identified as significant, is increased airfoil surface roughness on fan, HP compressor, HP Turbine and LP Turbine airfoils. Although it would not be anticipated that significant roughness increases occur over the relatively short time encompassed by this test, the tip clearance derivative was established on the basis of small changes in performance for small changes in measured clearance. This means then that variables, such as small increases in roughness, may have some effect on these test results that is not readily recognizable. Any unassessed deterioration which did occur would be in the direction of improving the agreement between the derivative measured in this test and the previously accepted derivative.

One thing is clear. The Stage 1 HPT blade tip clearance has a significant effect on engine performance and the derivative of Stage 1 clearance on performance was assessed to be at least as influential as that which has been previously accepted.

7.2 HP TURBINE STAGE 1 CLEARANCE MAP

The results of the clearanceometer test are presented for several operational conditions. Tip clearance is presented as a function of time for the following throttle movements; an accel from ground idle to steady-state takeoff power in which takeoff power is attained within 10 seconds; a decel from steady-state takeoff conditions to ground idle; and varying times at ground idle followed by a burst to takeoff power. In addition, clearance is presented as a function of rotational speed, as a function of compressor exit temperature (T_3), and as a function of compressor exit pressure (P_3). The clearances presented are the average of the readings of the eight probes and data have been corrected where necessary to reflect a consistent set of ambient conditions.

7.2.1 Clearance As a Function of Time for a 10-Second Accel from Ground Idle to Takeoff Power

The measured Stage 1 blade-to-shroud clearance as a function of time for a 10-second accel is shown in Figure 21. The predicted clearance is also plotted. There is approximately an 0.25 mm (0.010 in) difference between measured and predicted clearance with the measured clearance being larger than the predicted clearance. The major difference between the predicted and measured clearance appears to occur at the steady-state takeoff and idle conditions. The shape of the curves, however, are very similar.

Three distinct areas of clearance behavior may be observed. First, as rotor speed increases from 0-10 sec., the clearance decreases due to mechanical (primarily speed) effects. From 10-35 sec. the static structures become warmer than the rotating structures, resulting in a clearance increase. From 35-1000 sec., the more massive rotating structures warm up causing clearance to decrease and eventually reach a steady-state value.

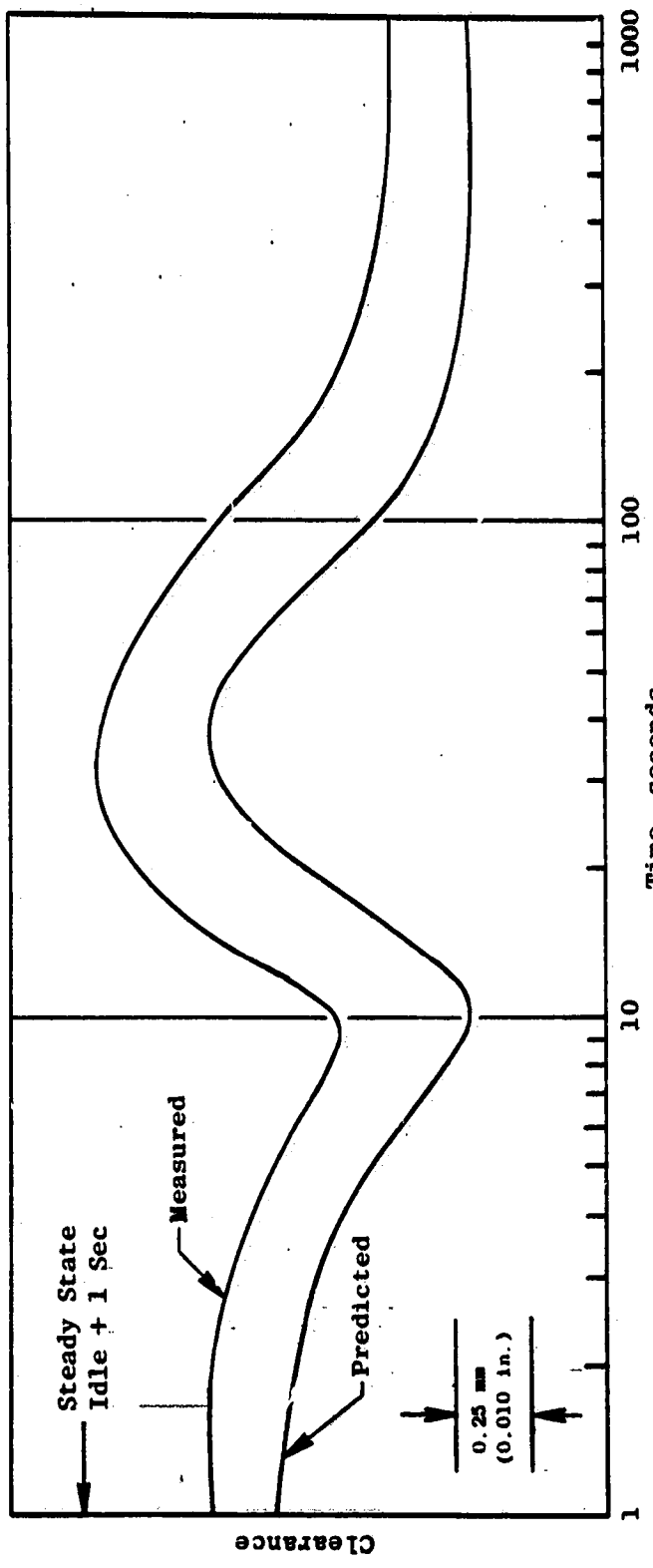

Figure 21. Stage 1 Blade Clearance as a Function of Time During an Acceleration from Ground Idle to Takeoff Power.

7.2.2 Clearance As a Function of Time for a Decel from Steady-State Takeoff Power to Ground Idle

The measured Stage 1 blade-to-shroud clearance as a function of time for a decel from steady-state takeoff power to ground idle is presented in Figure 22. The predicted clearances are also plotted. As is evident from this figure, the measured clearance compares very well with the analytical prediction.

Again, clearance as a function of time for a decel is characterized by three regions. As RPM decreases, clearance initially increases (up to 10 seconds). Then the stator cools down, closing around the rotor (10 to 100 seconds); finally the rotor cools, causing a clearance increase (100 to 1000 seconds).

7.2.3 Reburst

Previous to this investigation, throttle rebursts were thought to be the significant cause of resultant clearance increases and consequent performance losses. One of the objectives of this test was to obtain clearance and temperature data for various reburst operational conditions to verify this.

Reburst-type data were obtained for engine idle times of 8, 6, 4, 2, 1, and ½ minutes. Figure 23 presents the round engine clearance data resulting from these tests. The starting point for each of the plotted curves is the beginning of the reaccel from ground idle after the labeled dwell time. A reburst from stabilized ground idle (i.e., 30 minutes) is also shown for reference. This represents a "cold" rotor reburst or a accel from stabilized ground idle.

It is evident from Figure 23 that a minimum clearance exists for rebursts following a one to two minute dwell time at ground idle. This is also supported by data presented in Figure 22 which shows that the minimum clearance during a decel occurs at approximately 100 seconds.

Clearance as a function of time from the steady-state takeoff power point through the accel minimum clearance point for a reburst after a two-minute dwell time at ground idle is shown in Figures 24 and 25. Figure 24 shows the effect of reburst on clearance. Figure 25 shows HP turbine rotor RPM as a function of time during this throttle sequence. The additional closure from steady-state takeoff resulting from a two-minute reburst is 0.74 mm (0.029 in.). This agrees extremely well with the predicted closure of 0.79 mm (0.031 in.).

This reburst data shows that warm and hot rotor (dependent upon ground idle dwell time) rebursts are engine operating conditions which potentially cause rubs and consequent performance deterioration. The time correlated clearance and temperature data obtained from this test has significantly enhanced the understanding of rebursts and verified that the closure (and subsequent rub) predictions are correct.

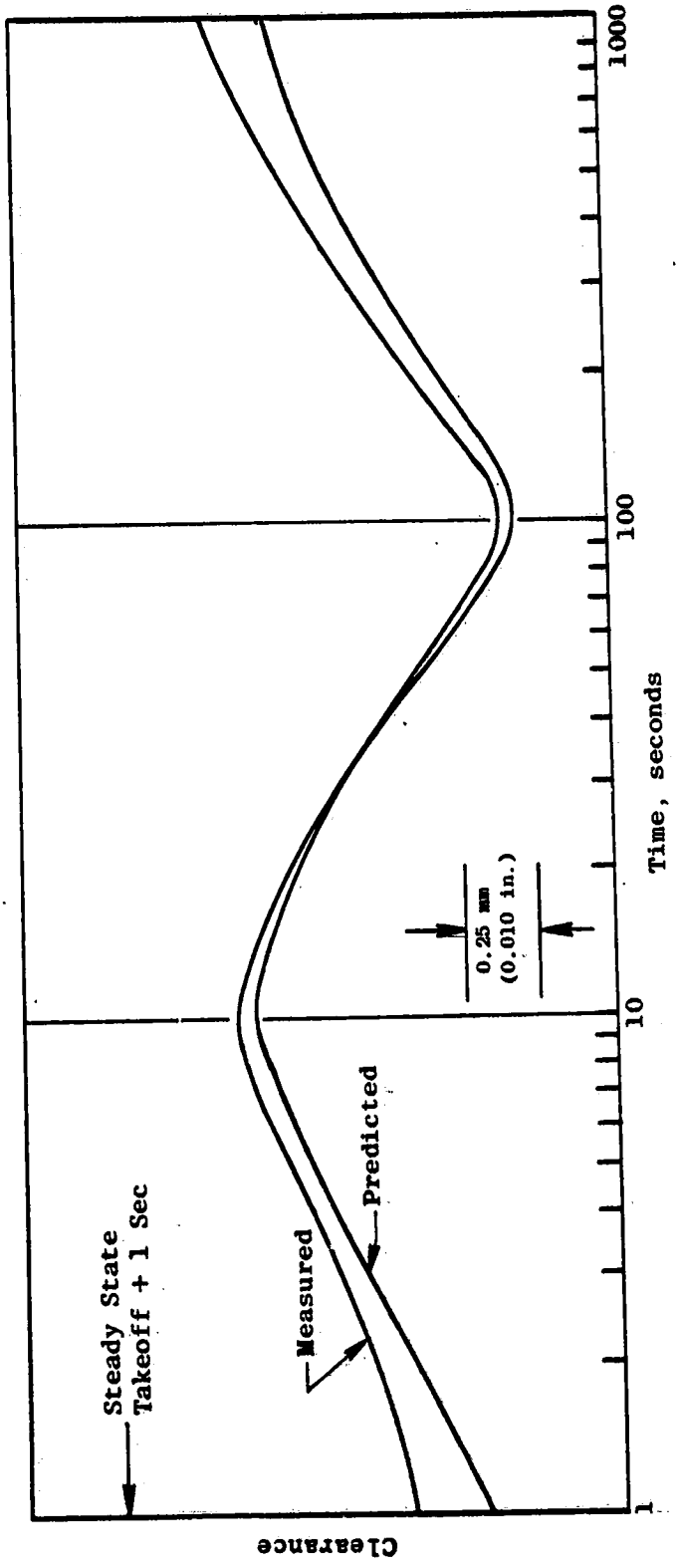

Figure 22. Stage 1 Blade Clearance as a Function of Time During a Deceleration from Takeoff Power to Ground Idle.

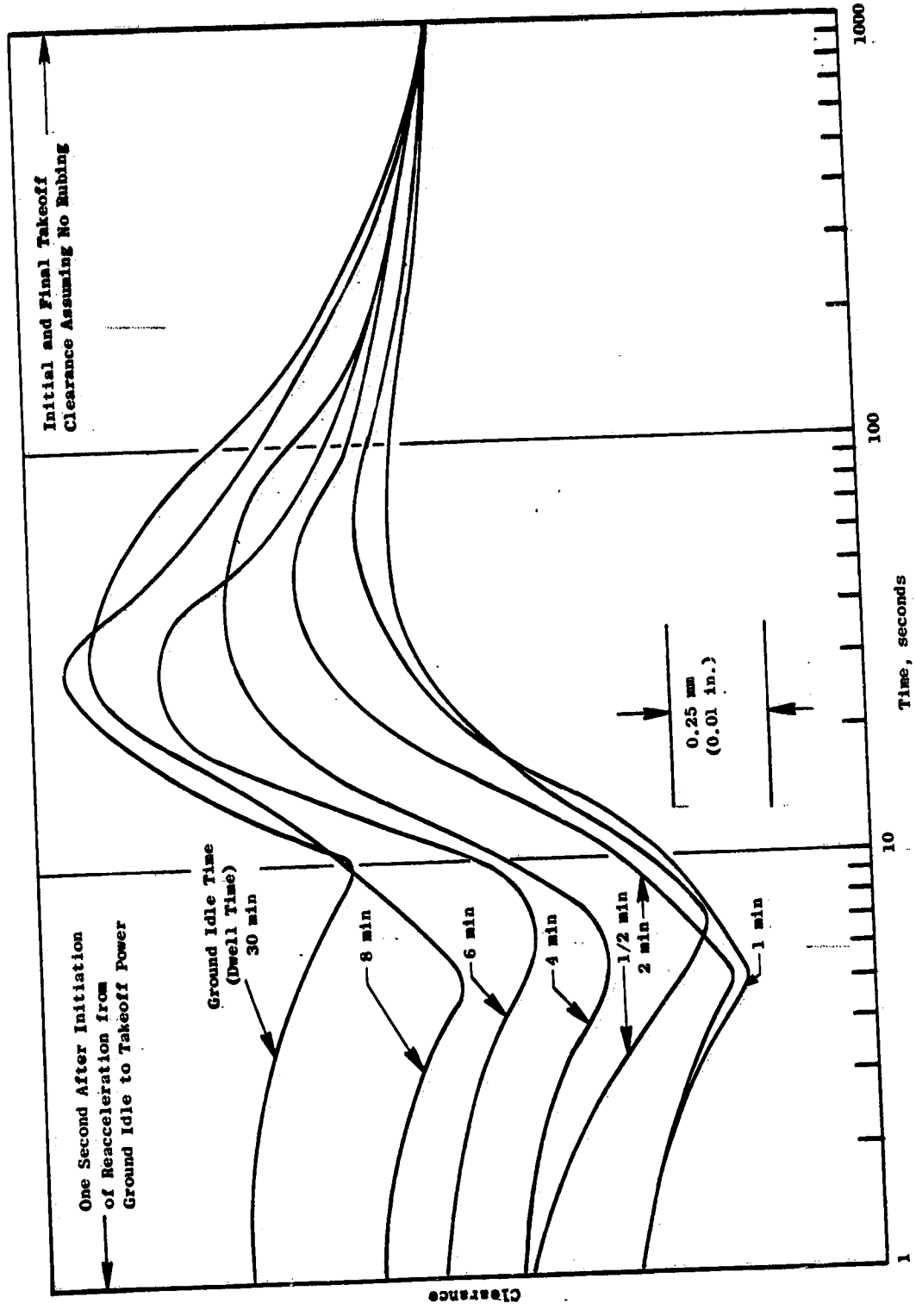

Figure 23. Clearance Versus Time After Reburst for Various Ground Idle Dwell Intervals.

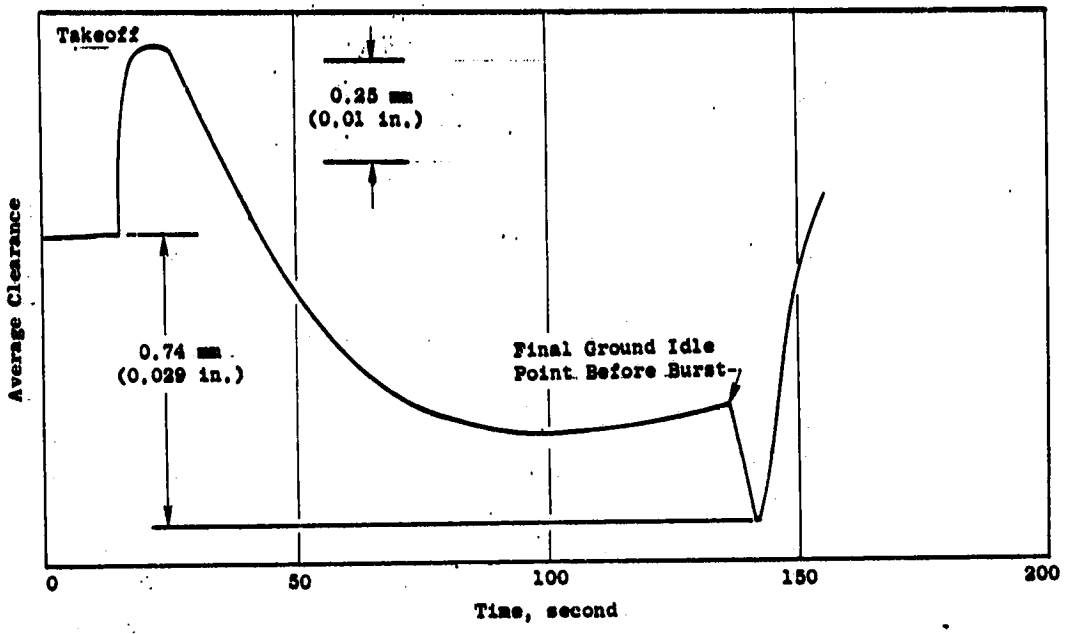

Figure 24. Clearance Effects from Engine Reburst After Two Minute Dwell Time.

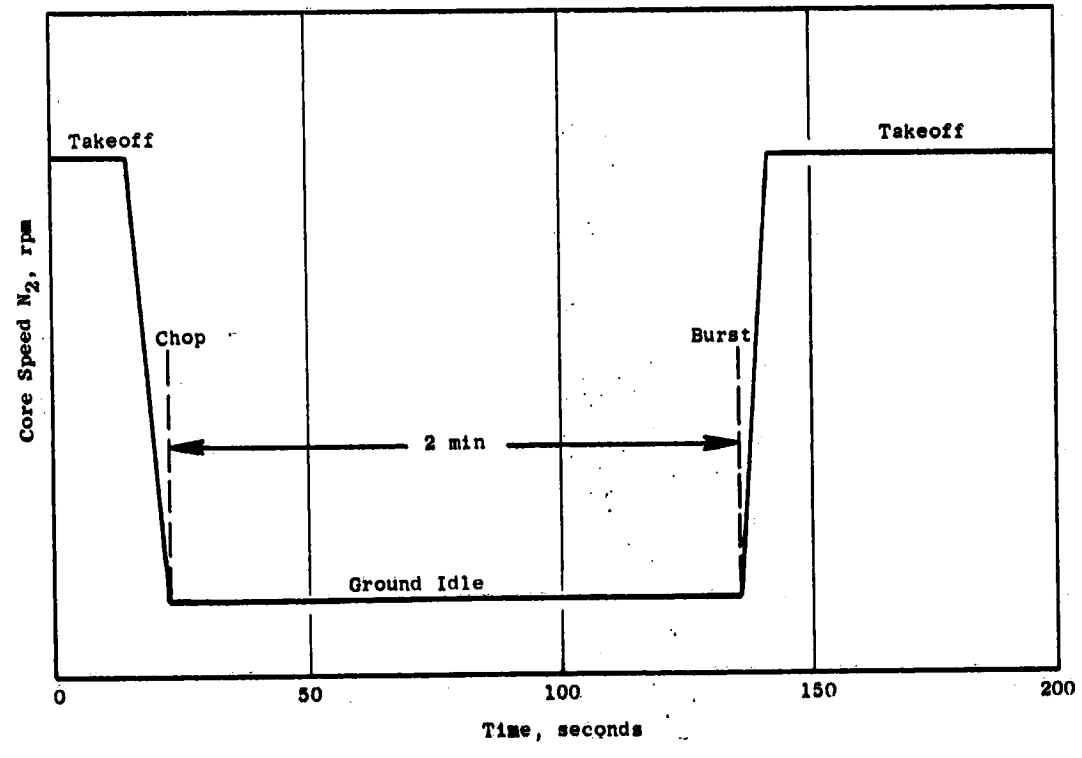

Figure 25. Core Speed As a Function of Time Exhibiting a 2 Minute Dwell Prior to Reburst.

7.2.4 Clearance As a Function of Core Speed, N_2; Compressor Exit Temperature, T_3; and Compressor Exit Pressure, P_3

The relationships of clearance as a function of core speed, compressor exit temperature and compressor exit pressure are presented in Figures 26, 27 and 28. The data used to construct these curves were obtained from steady-state conditions achieved during the power calibration work. Steady-state is defined as that time when all engine parameters have ceased to appreciably change. Most of these steady-state data are "off-design" conditions, i.e., other than ground idle, take-off, and cruise.

The data were used as the baseline relationships to establish an empirical model to predict clearance for any steady-state operating condition. This is a very useful tool because, to obtain approximate clearances for a given operating condition, it eliminates the need for heat transfer and aero modeling using the resulting heat transfer and aero model temperatures and pressures. This empirical model is only an approximation and certainly not a totally valid analytical picture. It is extremely useful, however, in translating from a new engine to a deteriorated one, from a hot day, high altitude takeoff to a sea level standard condition takeoff, etc.

These functional relationships are also quite useful in assessing the accuracy of steady-state calculations, especially the heat transfer portion of such analyses.

7.3 ENGINE SHUTDOWN (STOPCOCK) TEST

An engine shutdown from cruise, or higher, power is termed a stopcock. The testing for this investigation included a stopcock from cruise in order to establish the transient clearance response during this type of maneuver. It is common in aircraft acceptance testing to perform stopcocks. The intent of this investigation was to gather data which would be of value in assessing the effect that aircraft acceptance test stopcocks might have on short term performance deterioration.

The stopcock test sequence was initiated from a core speed of 9500 RPM after having stabilized at this speed for approximately 10 minutes. The fuel flow to the engine was cut. The engine coasted down and was restarted after 200 seconds. This restart was done to eliminate the possibility of both high and low speed rotor seizure and of sump and bearing as a result of losing oil cooling.

The average Stage 1 blade-to-shroud clearance versus time during stopcock is presented in Figure 29. The core speed, N_2, versus time is presented in Figure 30 as a reference.

The clearance curve may be divided into three regions of interest. The first region is where clearance is increasing (up to 60 seconds). This clearance increase is caused by the loss of mechanical effects (centrifugal forces and pressure loads). The second region is that clearance decrease caused by the stator cooling down (60 to 240 seconds). This stator cool-down period was interrupted by the engine being restarted. During the restart, the clearance reduction occurs because mechanical effects are somewhat restored by returning to idle. The third region of interest is where clearance increased because the rotor was cooling (240 to 400 seconds).

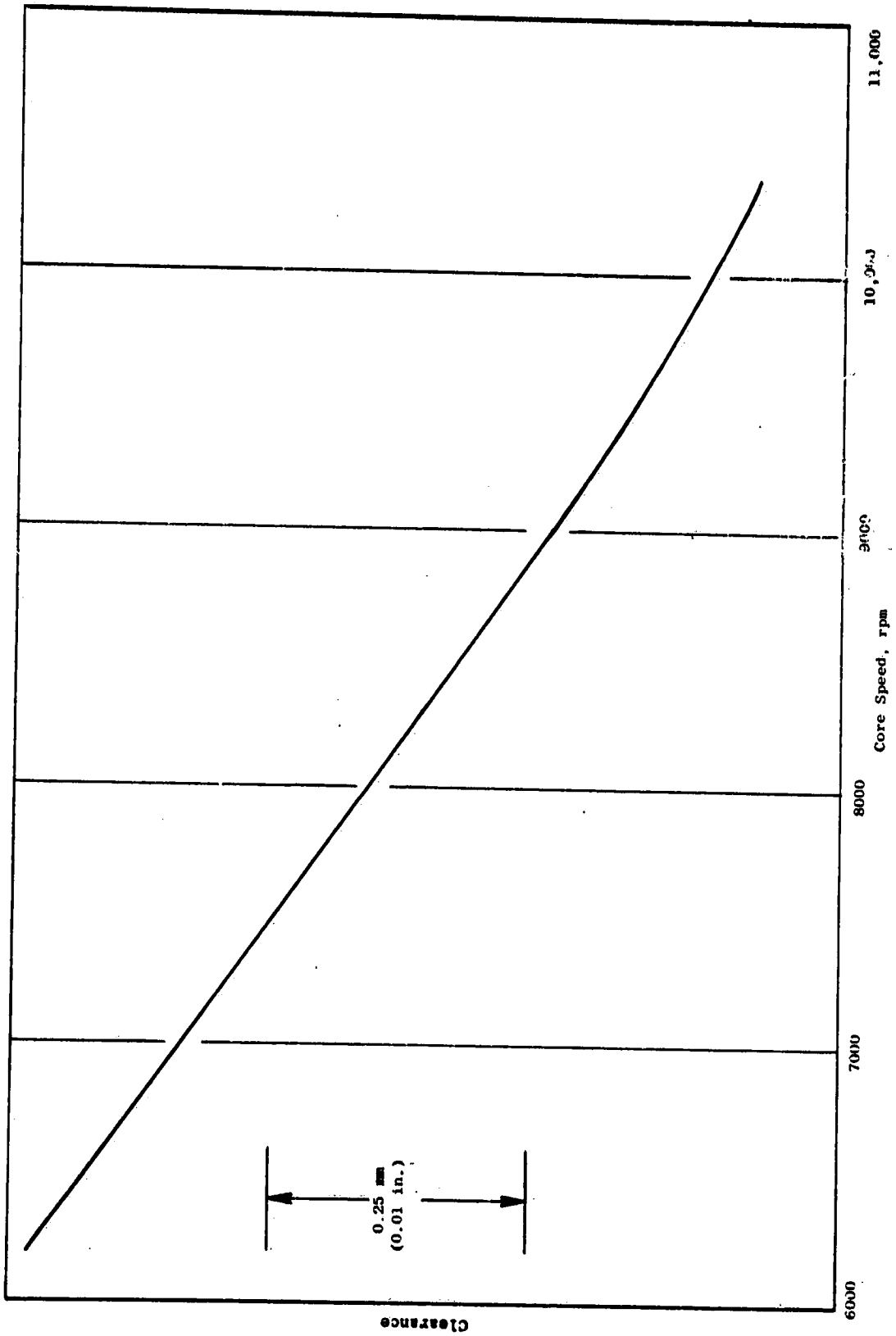

Figure 26. Clearance As a Function of Core Speed.

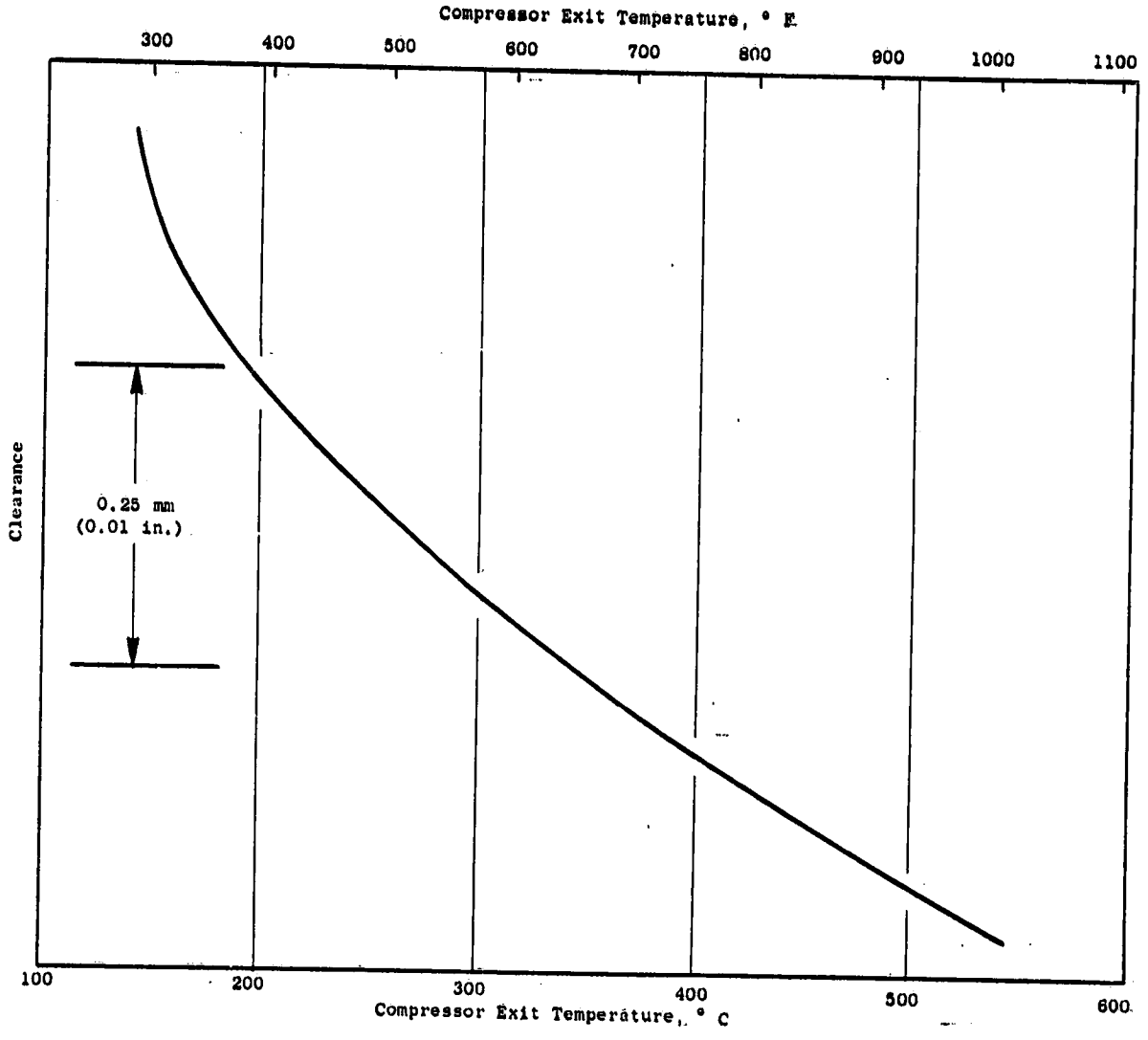

Figure 27. Clearance As a Function of Compressor Exit Temperature.

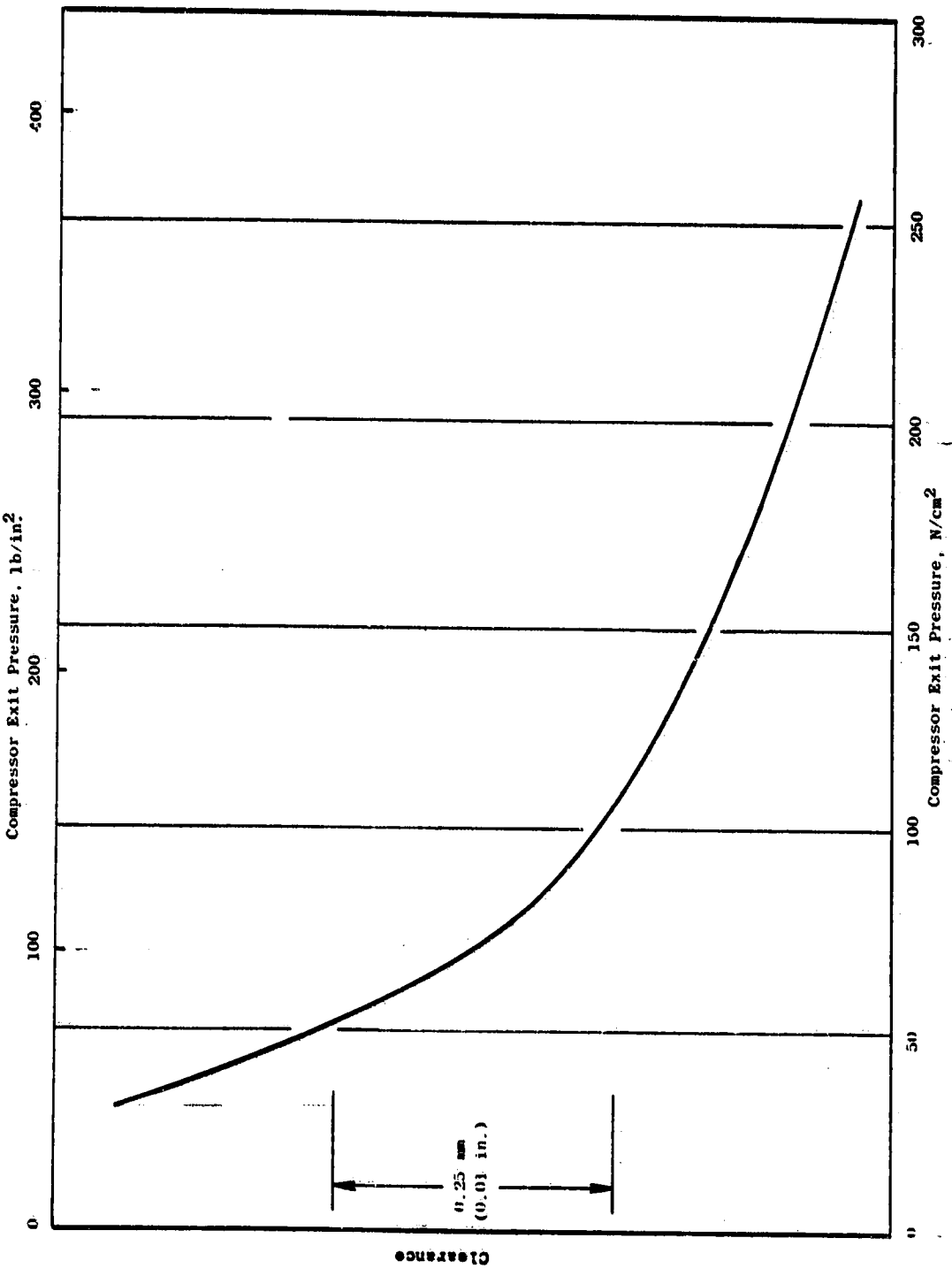

Figure 28. Clearance As a Function of Compressor Exit Pressure.

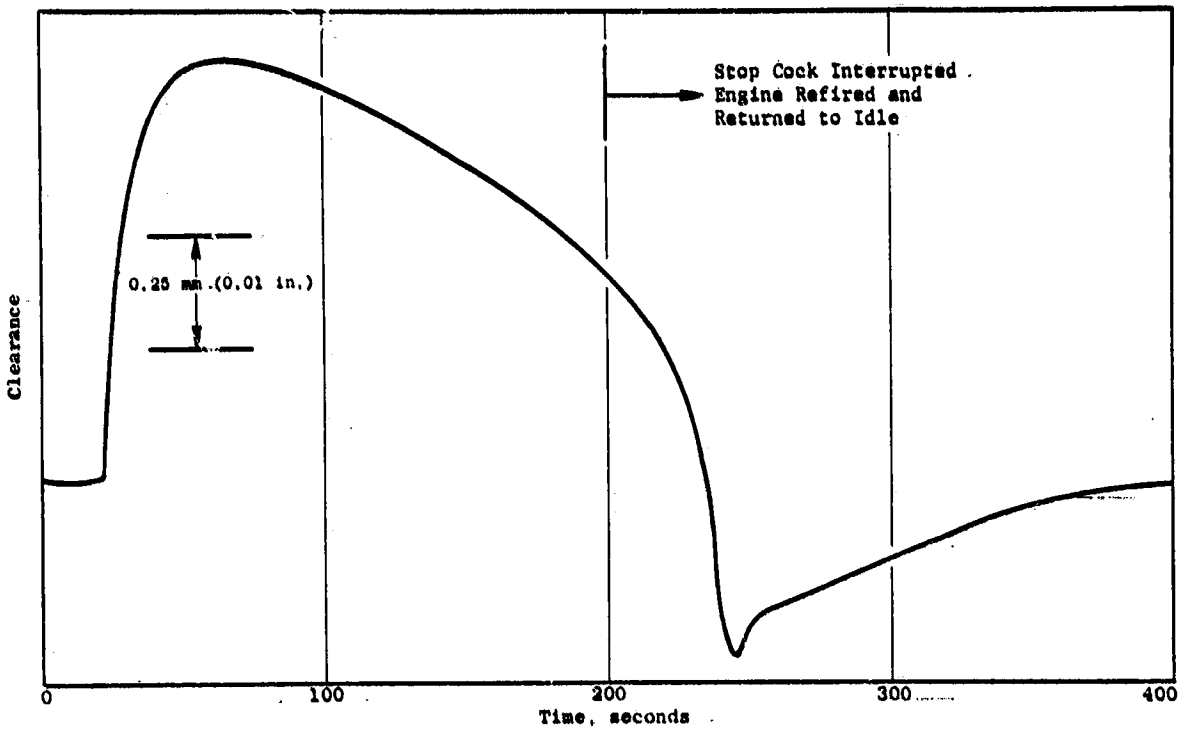

Figure 29. Clearance Versus Time After Stopcock.

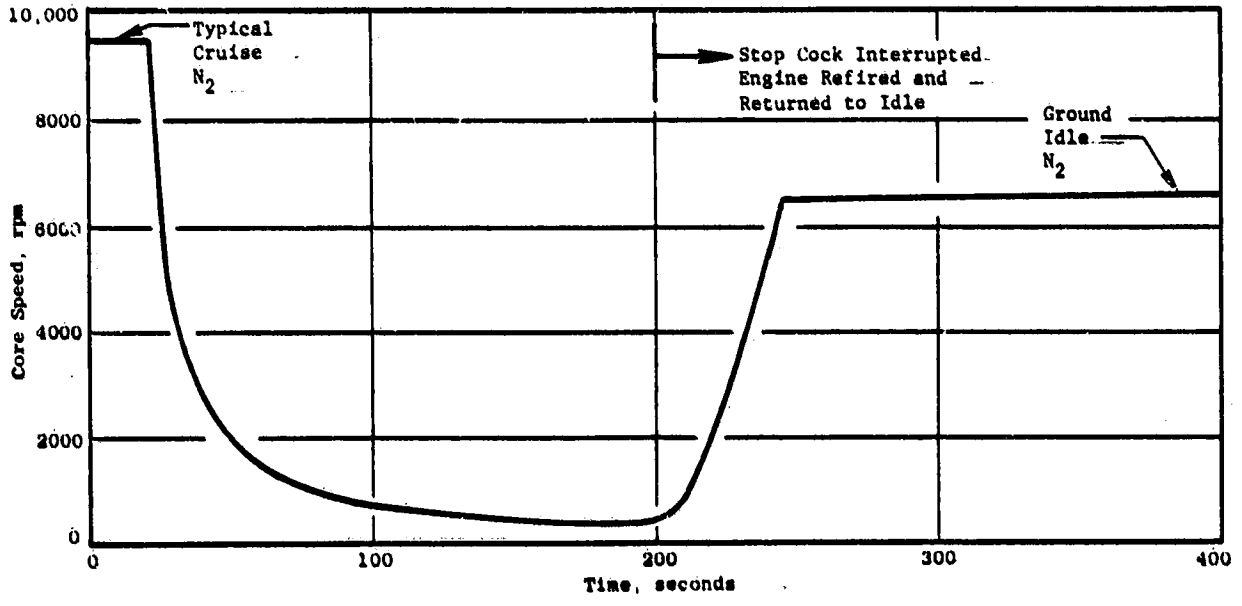

Figure 30. Core Speed Versus Time After Stopcock.

A theoretical approximation of a stopcock from steady-state takeoff power, based on the cruise stopcock measured result, is shown in Figure 31. This curve modifies the information gathered in the stopcock test to reflect the higher power level and removes the interruption in the transient which resulted when the engine was refired. It can be seen that no round engine rub is predicted for an uninterrupted stopcock in which no engine restart was made.

7.4 COLD MOTORING DATA

Cold motoring data were obtained while turning the rotor with an air starter motor. There was no combustion occurring within the engine and prior to this test the engine had not been running for at least 8 hours. Clearanceometer data were taken during this phase of testing. These data are presented in Figure 32. The cold motor roundness is plotted as deviation from the average.

These data are required for accurate analyses of both clearance response and out-of-roundness. The cold motoring data represent the cold clearances and the shape of the HP stator as assembled. These data, therefore, are the basis for both cold clearance and out-of-roundness. It is the composite picture of manufacturing-and assembly caused out-of-roundness. The average of the clearanceometer readings during cold motoring is used to establish the cold clearance. The cold motoring clearance shape is used to establish the initial engine out-of-roundness. This initial out-of-roundness can then be utilized to modify the out-of-roundness data to reflect the round engine assumed as the analytical starting point.

The Stage 1 blade-to-shroud clearance, as obtained by post test inspection, is shown in Figure 33. Again, this roundness shape is plotted as deviation from average. If a slight rotor eccentricity is assumed and assembly caused out-of-roundness is considered, the similarity between the two shapes (Figures 32 and 33) is close. This is verified by the average of the clearanceometer data and the inspection data being within 0.025 mm (0.001 in) of one another.

7.5 HIGH PRESSURE TURBINE STATOR ROUNDNESS

The objective of this portion of the program was to measure those parameters believed to influence high pressure turbine roundness, analytically determine their effect on roundness, and compare the calculated roundness to the measured roundness obtained from the clearanceometer results.

The measured roundness was obtained by averaging the data from the clearance probes, subtracting out the cold motoring measured assembly out-of-roundness, and then plotting the deviations from the average clearance value. This relates the roundness data to the clearance response data and to a theoretical round engine starting point. Therefore, the variation of readings from the eight clearance probes provides a measure of the roundness of the high pressure turbine Stage 1 shroud system.

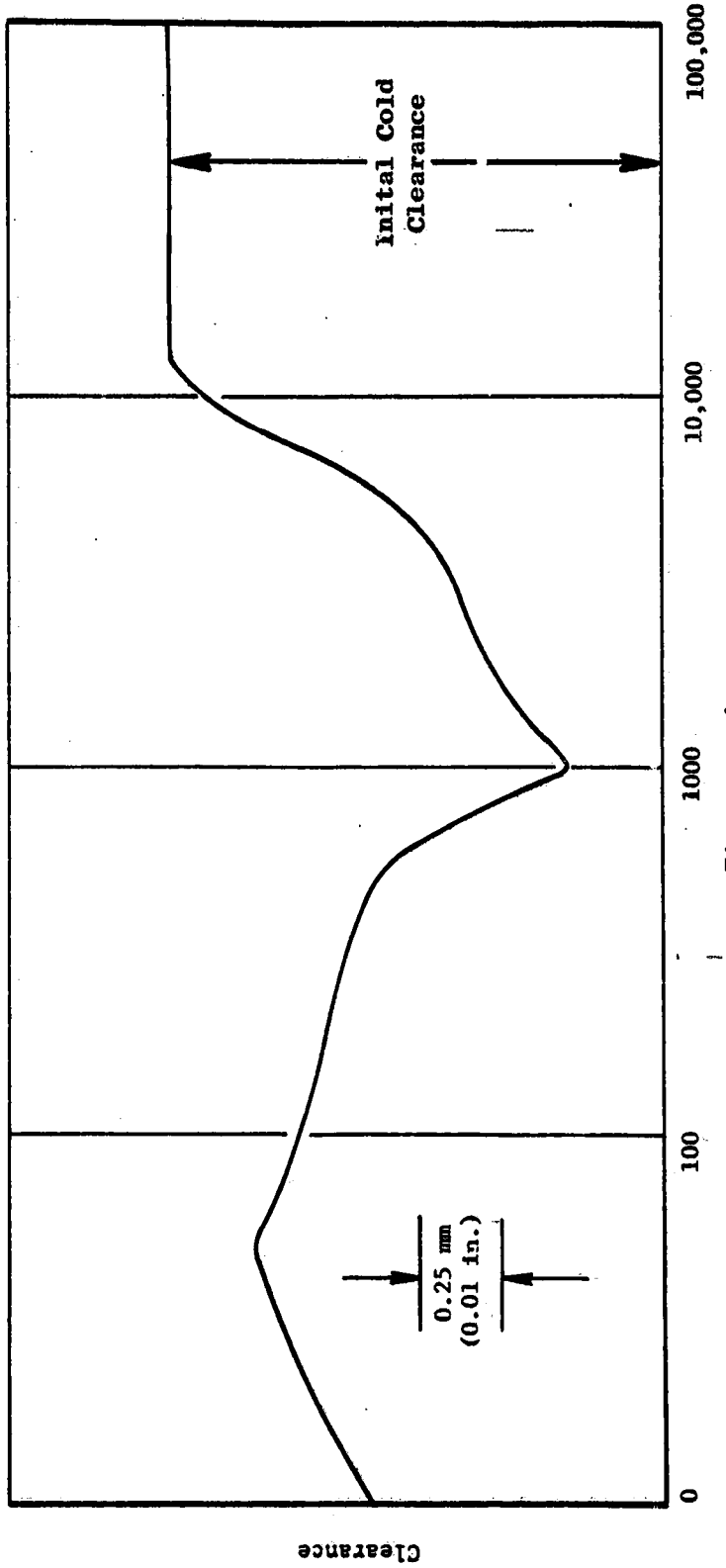

Figure 31. Theoretical Approximation of Stage 1 Blade Tip Clearance Following a Stopcock from Takeoff Power.

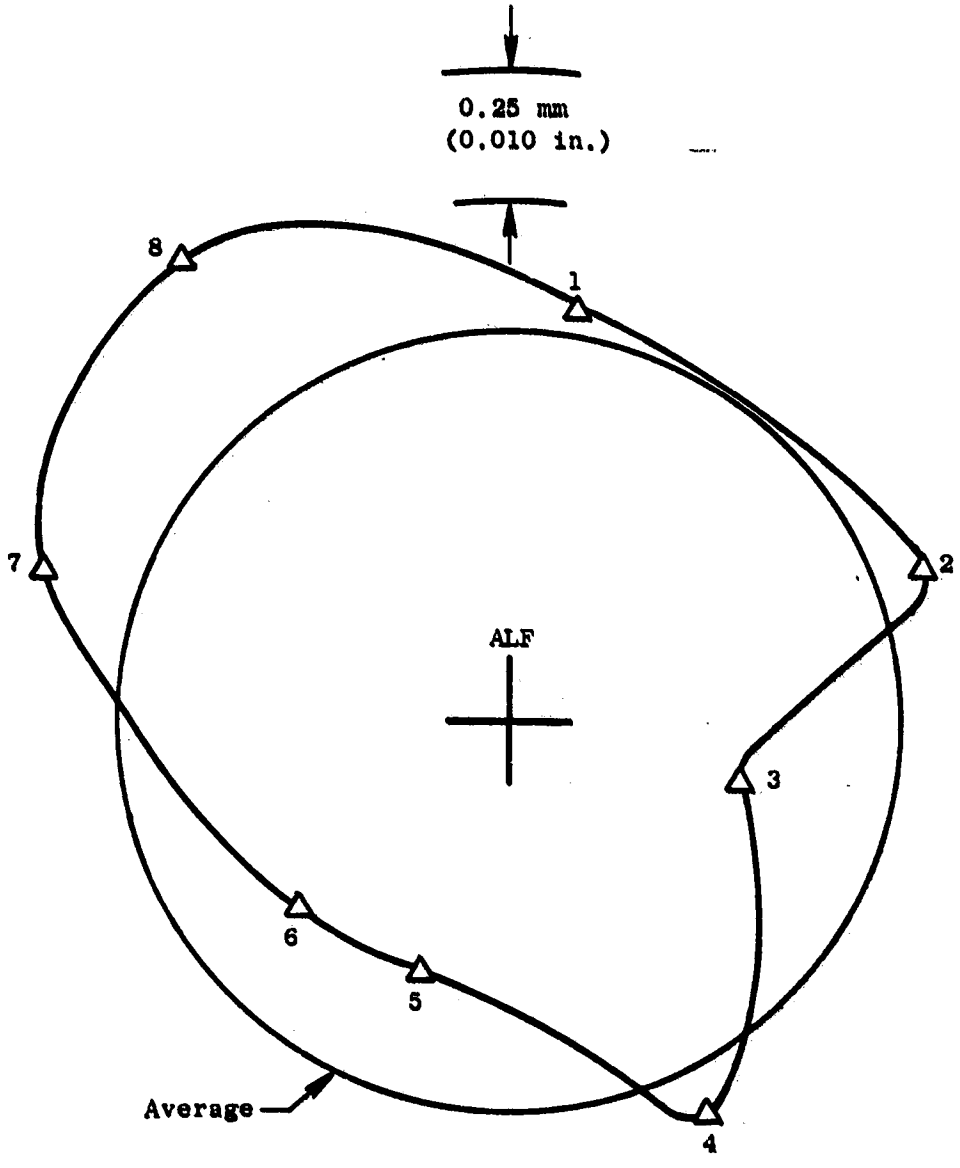

Figure 32. Cold Motor Roundness, Deviation of Individual Probe Reading from the Average of all Readings.

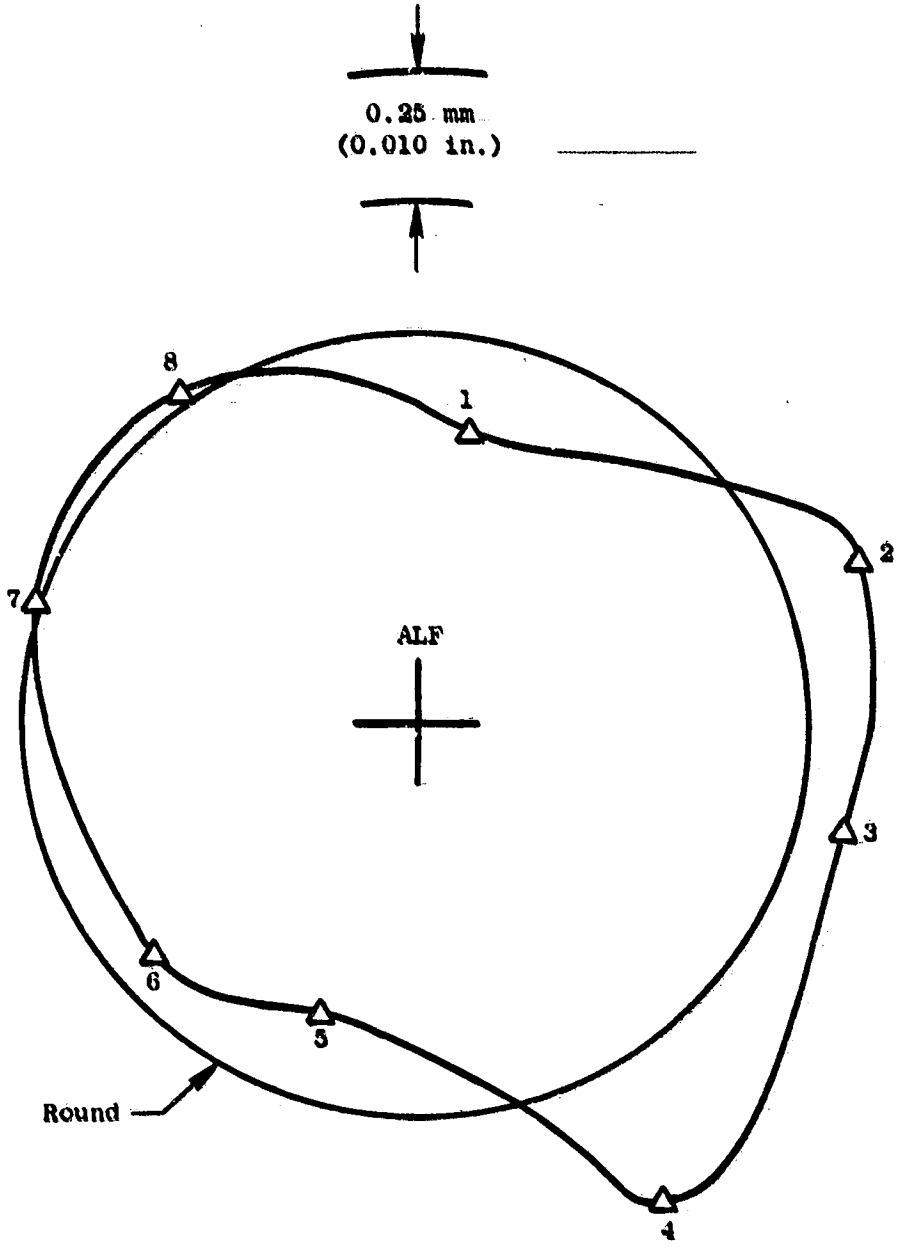

Figure 33. Posttest Stage 1 Shroud Surface Roundness Inspection.

7.5.1 Low Pressure Turbine Temperatures

The LPT stator case was instrumented with 48 skin thermocouples (See Figure 34) in order to obtain data required to analytically determine LPT contributions to HPT out-of-roundness. The two mechanisms believed to contribute significantly to HPT out-of-roundness were temperature differentials between the LPT stator case horizontal flanges and sheet metal skin and circumferential temperature gradients in the LPT stator case skin.

7.5.1.1 Horizontal Flange/Skin Temperature Gradients

The temperature differences between the LPT stator case horizontal flanges and skin were obtained from the test engine skin thermocouple data at various steady-state points including takeoff and ground idle. The maximum temperature difference between the LPT stator case horizontal flanges and skin, for any of the axial stations measured, was 108°C (194°F) at takeoff and the maximum difference between the average temperature of the flanges and skin was 31°C (55°F). Figures 35 and 36 compare the axial test temperature distributions of the LPT stator case horizontal flanges and skin (as well as the overall average of all T/C's) for ground idle and takeoff conditions.

7.5.1.2 Circumferential Temperature Gradients

LPT stator case skin circumferential temperature distributions were obtained for ground idle and takeoff conditions using the test data. These distributions were then represented by Fourier Series in order to determine the principal harmonics contribution to the distorted LPT stator case mode shapes. Figures 37 through 41 illustrate the circumferential test temperature distributions of each of the four axial stations of the LPT stator case and of the average of all axial stations for an engine ground idle condition (refer to Figure 34 for axial station designation). Figures 42 through 46 illustrate circumferential test temperature distributions at the same locations for an engine takeoff condition.

7.5.2 Turbine Midframe Temperatures

Temperatures of the structural elements in the turbine midframe were measured at steady-state ground idle and takeoff power at the same time that clearances in the high pressure turbine were being recorded. The significant engine parameters recorded at these conditions, which are used for determining the mechanical loading on the TMF, are as follows:

	Ground Idle	Takeoff
Fan Speed, RPM	864	3785
Core Speed, RPM	6446	10,235
Engine Thrust, N (Lb)	8496 (1910)	210,978 (47430)
HPT exit temp., °C	400	895
HPT exit pressure, N/cm^2 (PSIA)	11.5 (16.7)	58.7 (85)

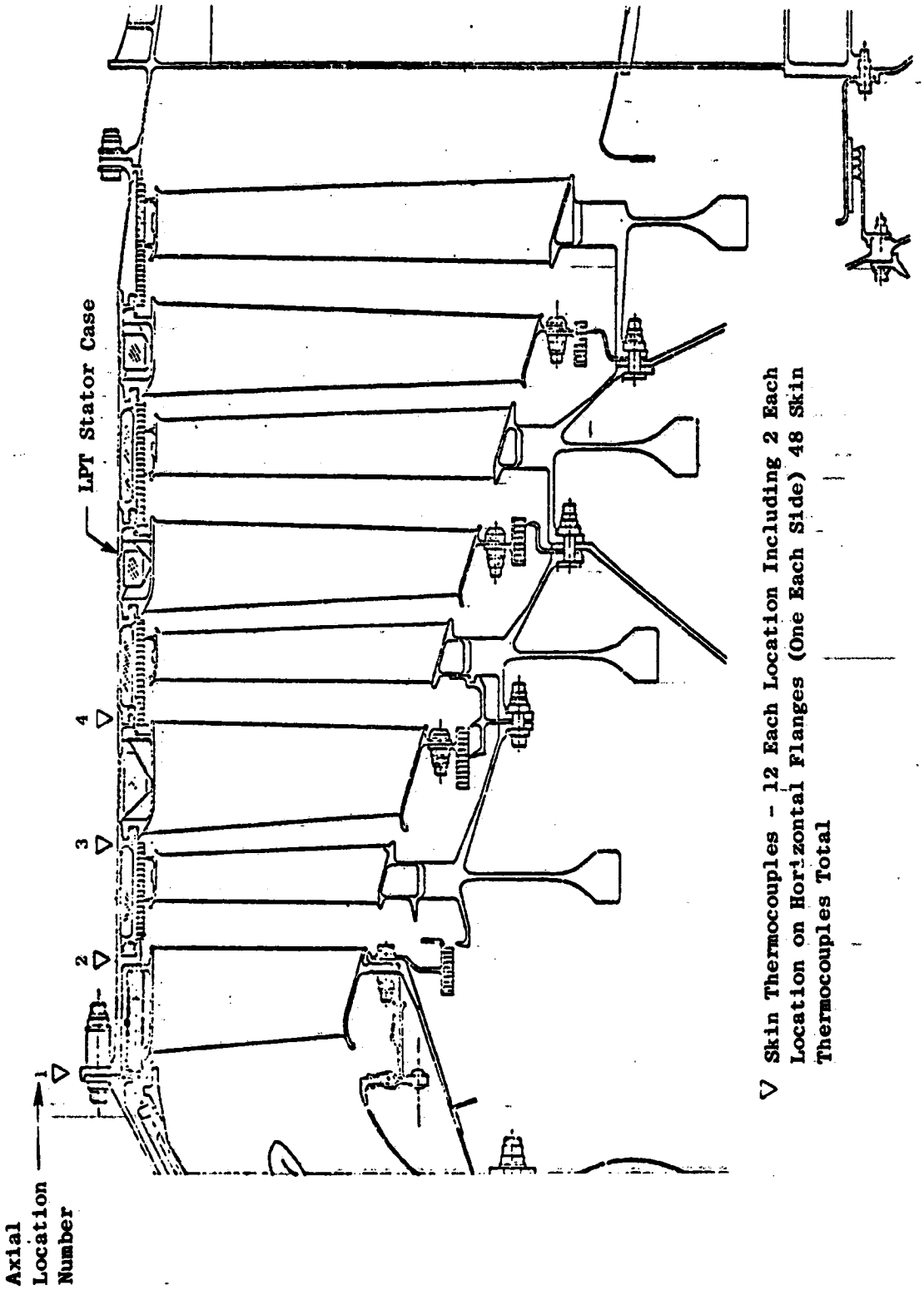

Figure 34. LP Turbine Stator Case Instrumentation.

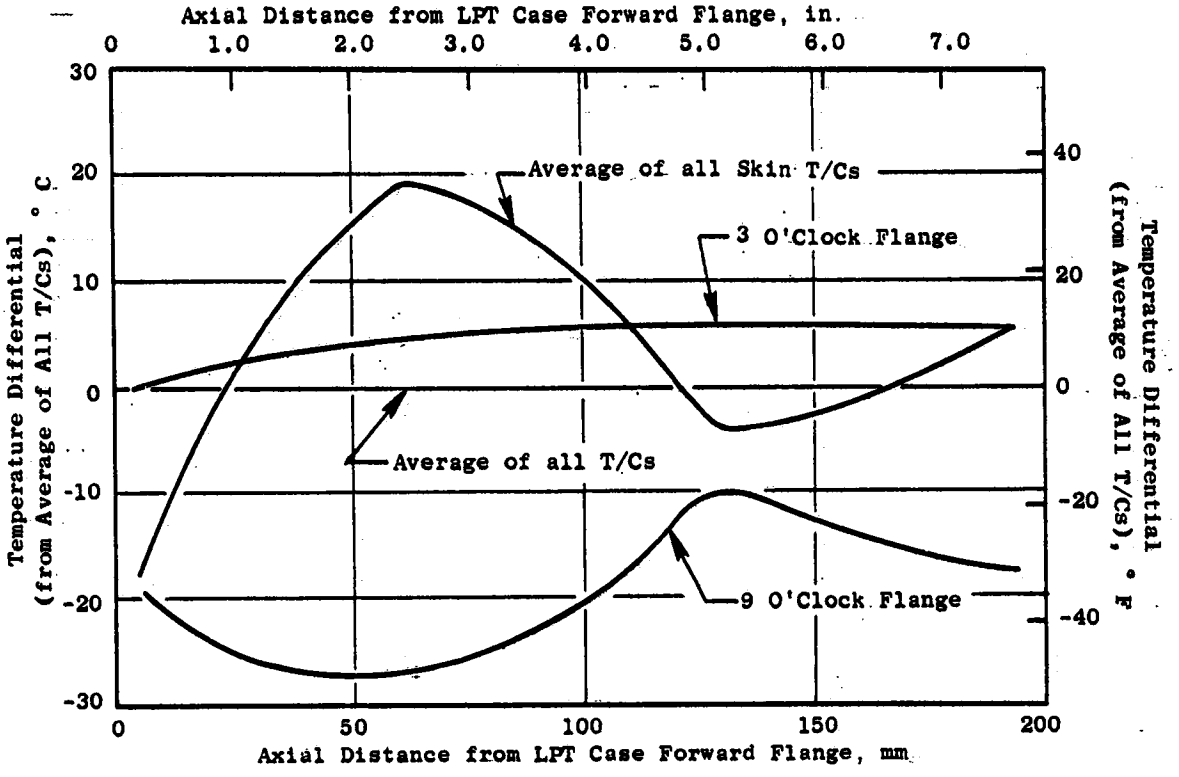

Figure 35. LP Turbine Stator Case Axial Temperature Distribution, Ground Idle.

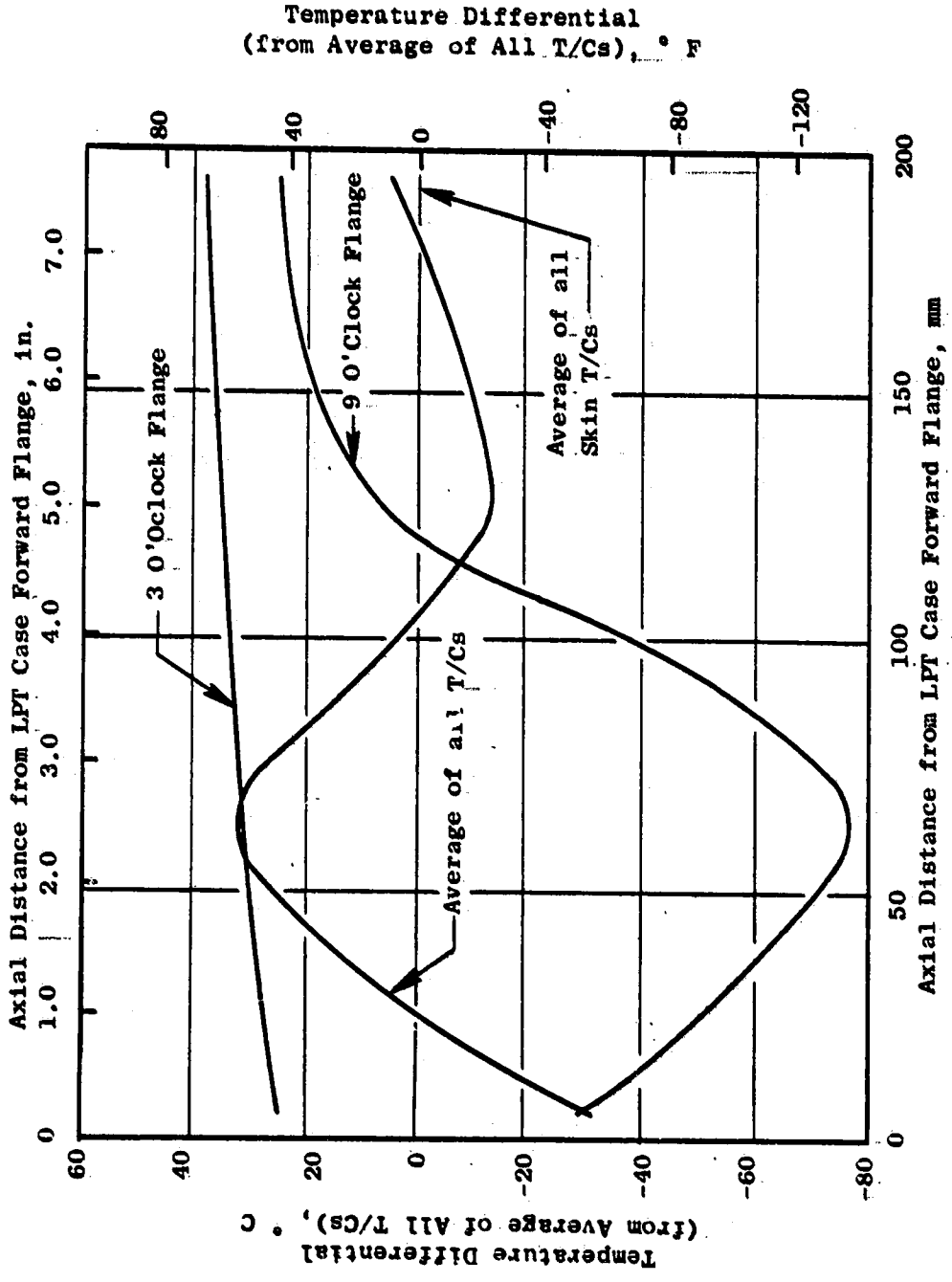

Figure 36. LP Turbine Stator Case Axial Temperature Distribution, Takeoff.

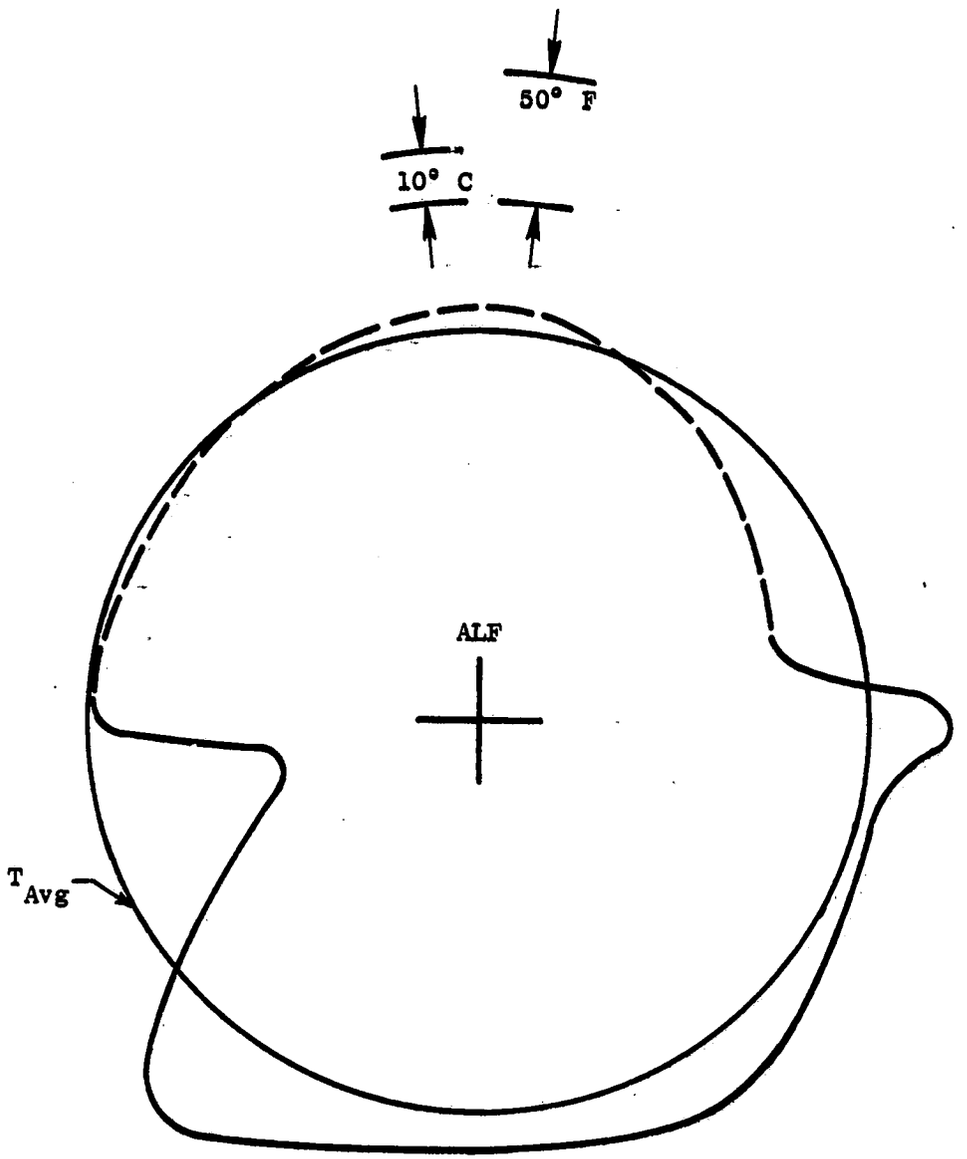

Figure 37. LP Turbine Stator Case Circumferential Temperature Distribution, Axial Location Number 1, Ground Idle.

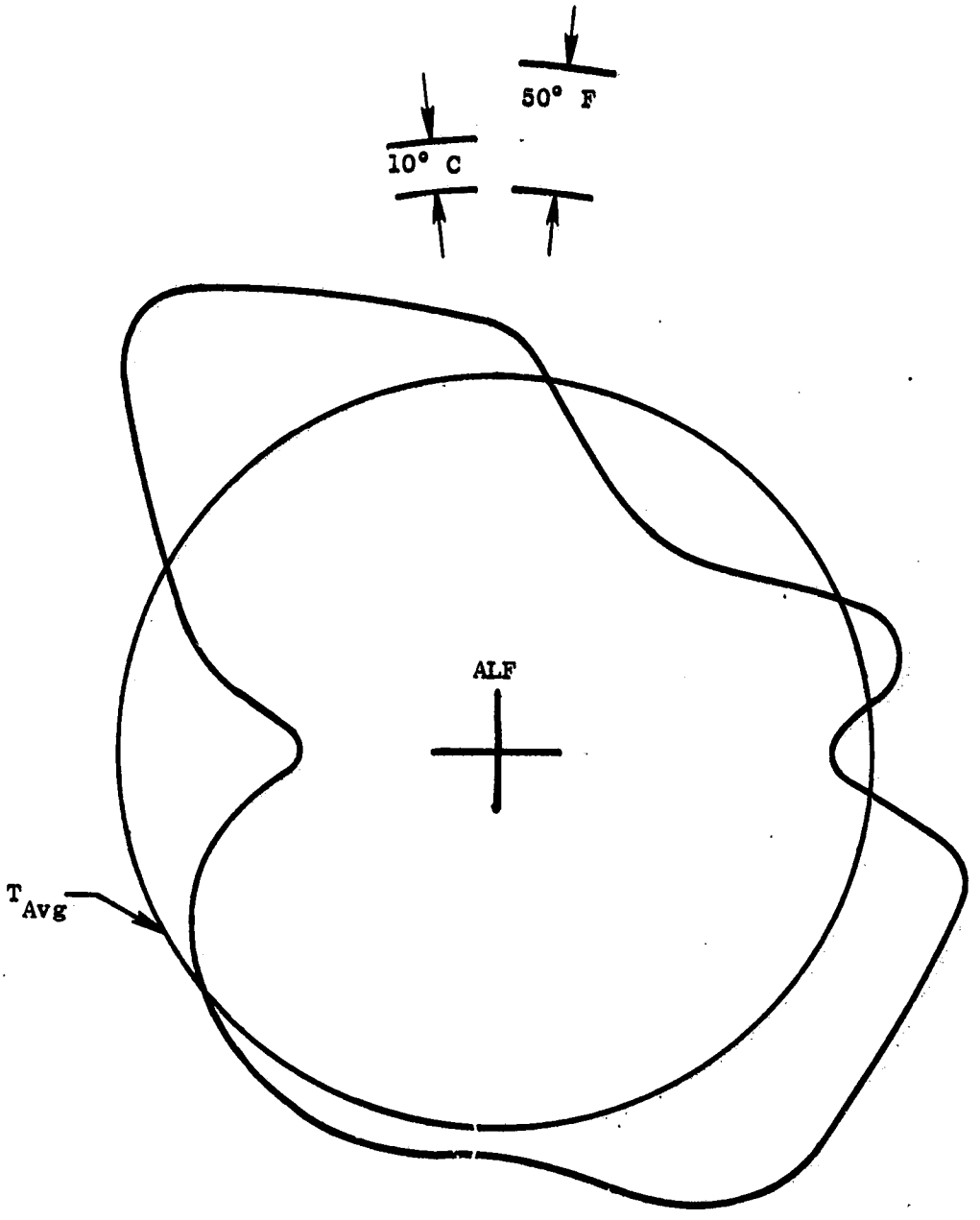

Figure 38. LP Turbine Stator Case Circumferential Temperature Distribution, Axial Location Number 2, Ground Idle.

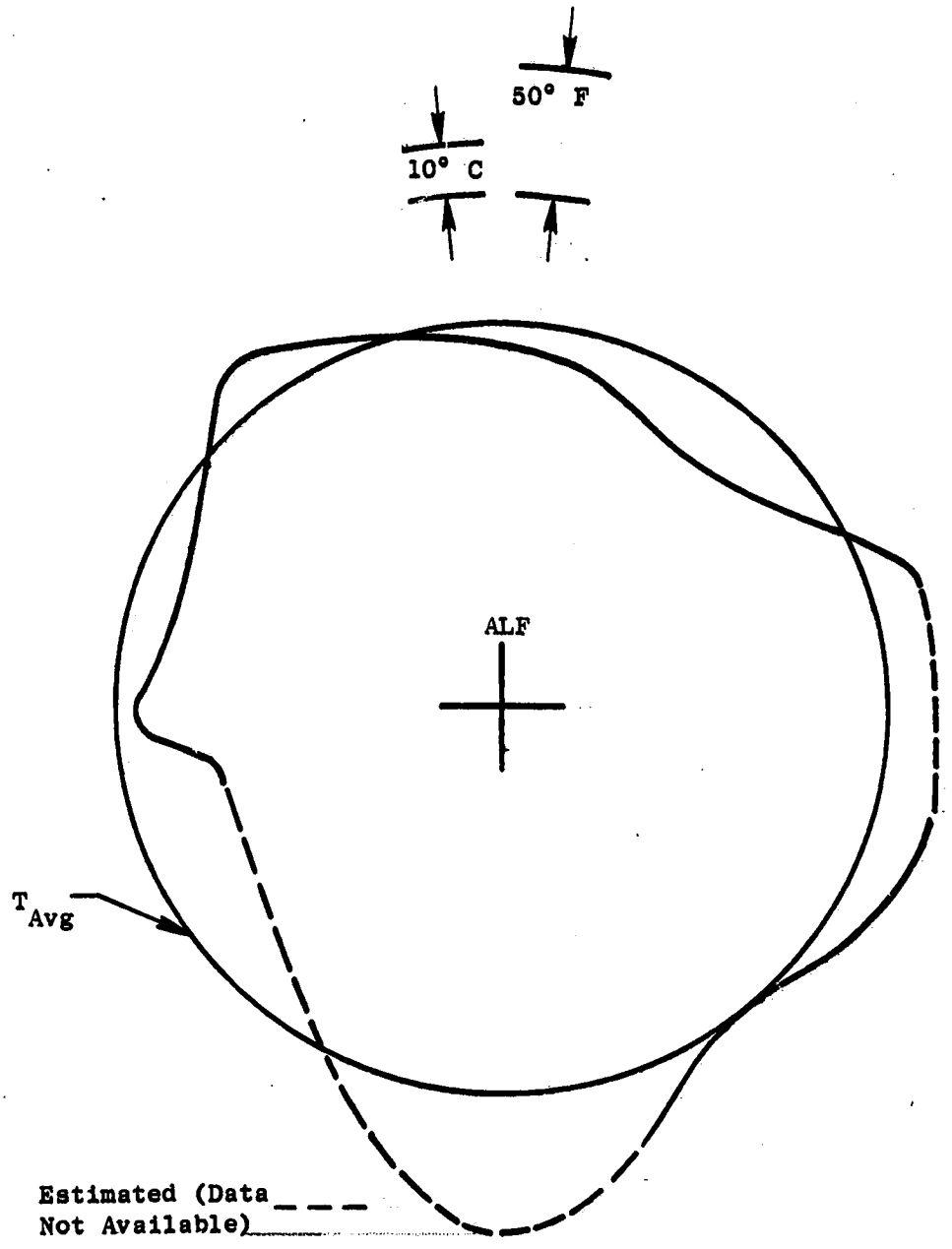

Figure 39. LP Turbine Stator Case Circumferential Temperature Distribution, Axial Location Number 3, Ground Idle.

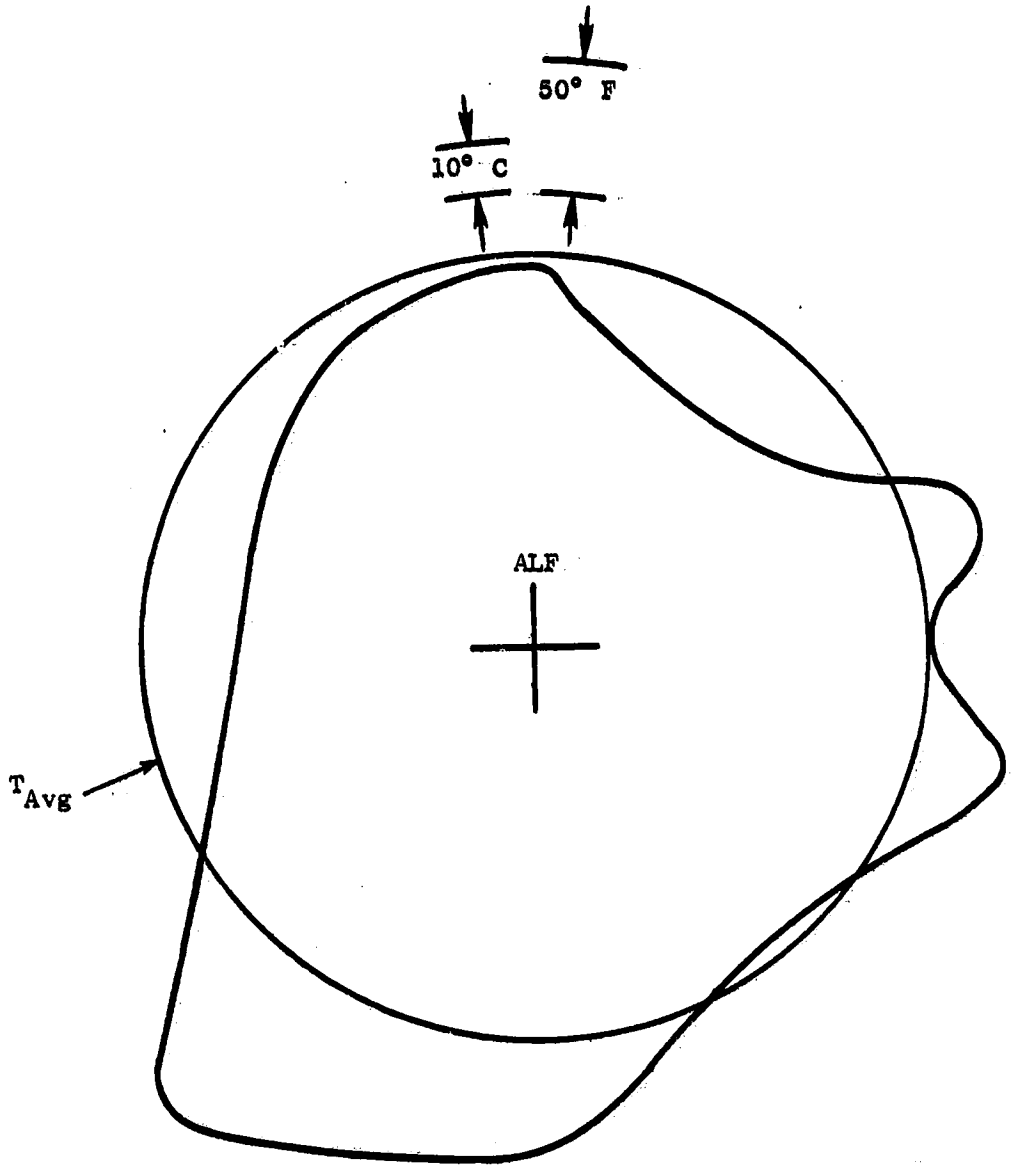

Figure 40. LP Turbine Stator Case Circumferential Temperature Distribution, Axial Location Number 4, Ground Idle.

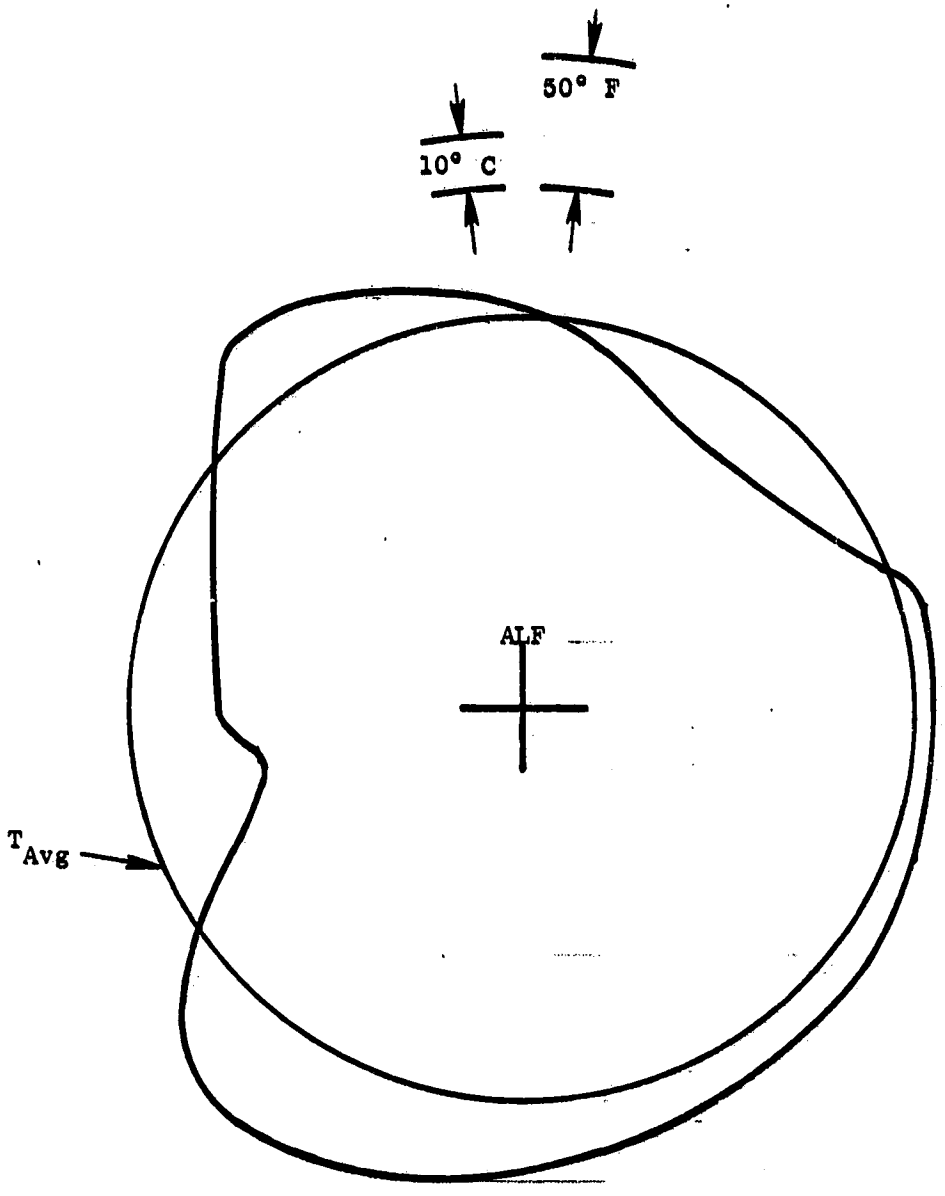

Figure 41. LP Turbine Stator Case Circumferential Temperature Distribution, Axial Average, Ground Idle.

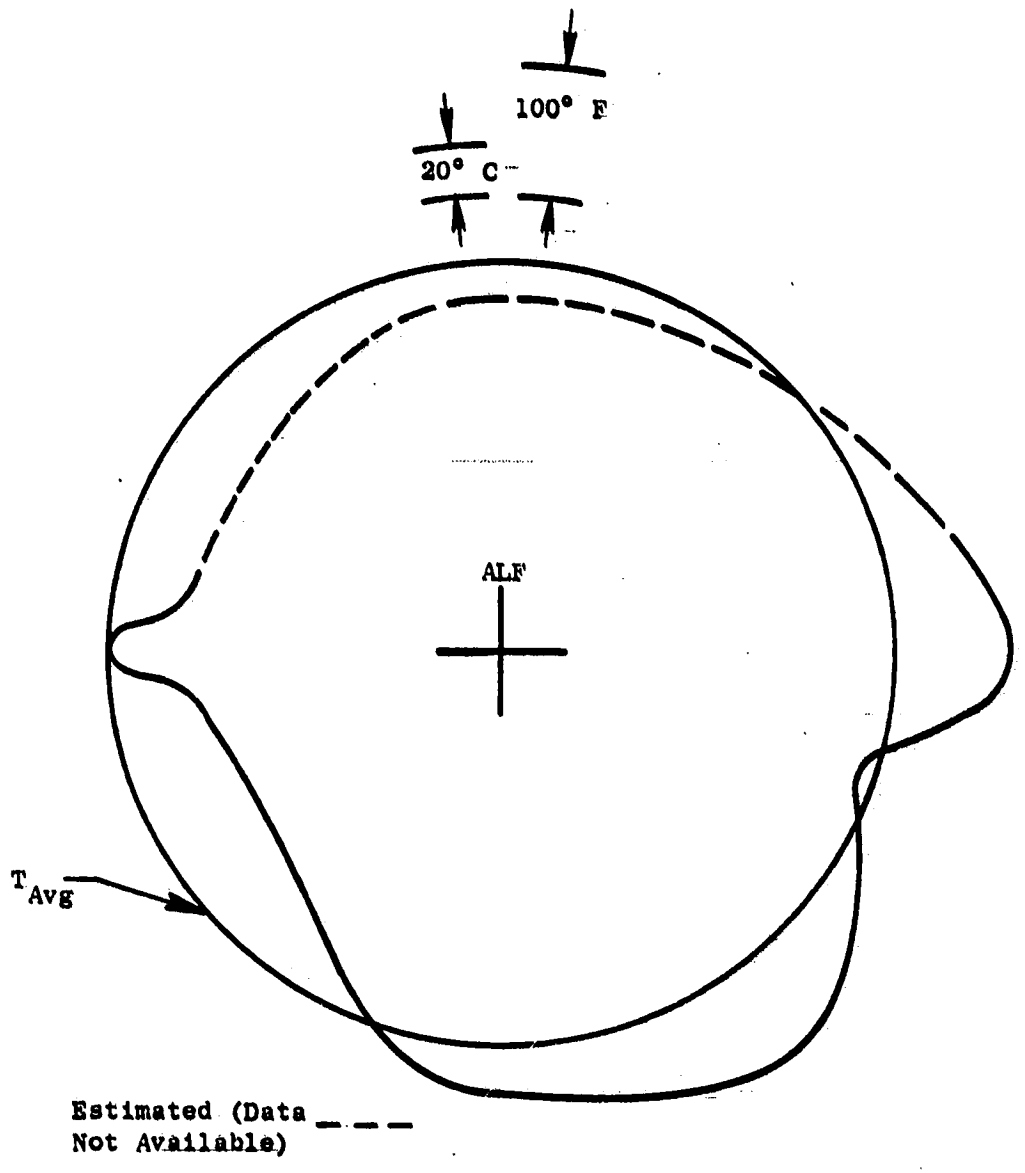

Figure 42. LP Turbine Stator Case Circumferential Temperature Distribution, Axial Location Number 1, Takeoff.

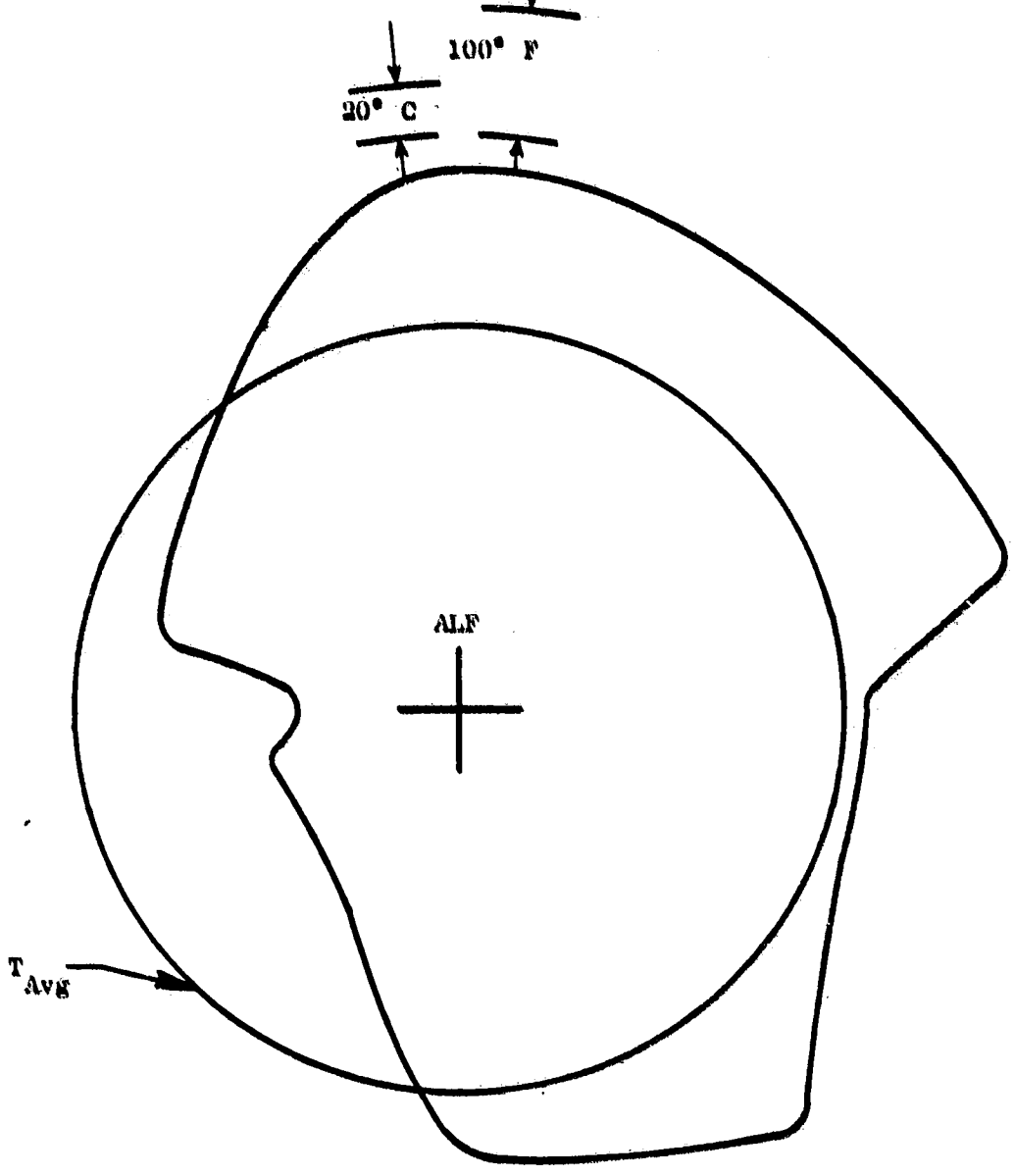

Figure 43. LP Turbine Stator Case Circumferential Temperature Distribution, Axial Location Number 2, Takeoff.

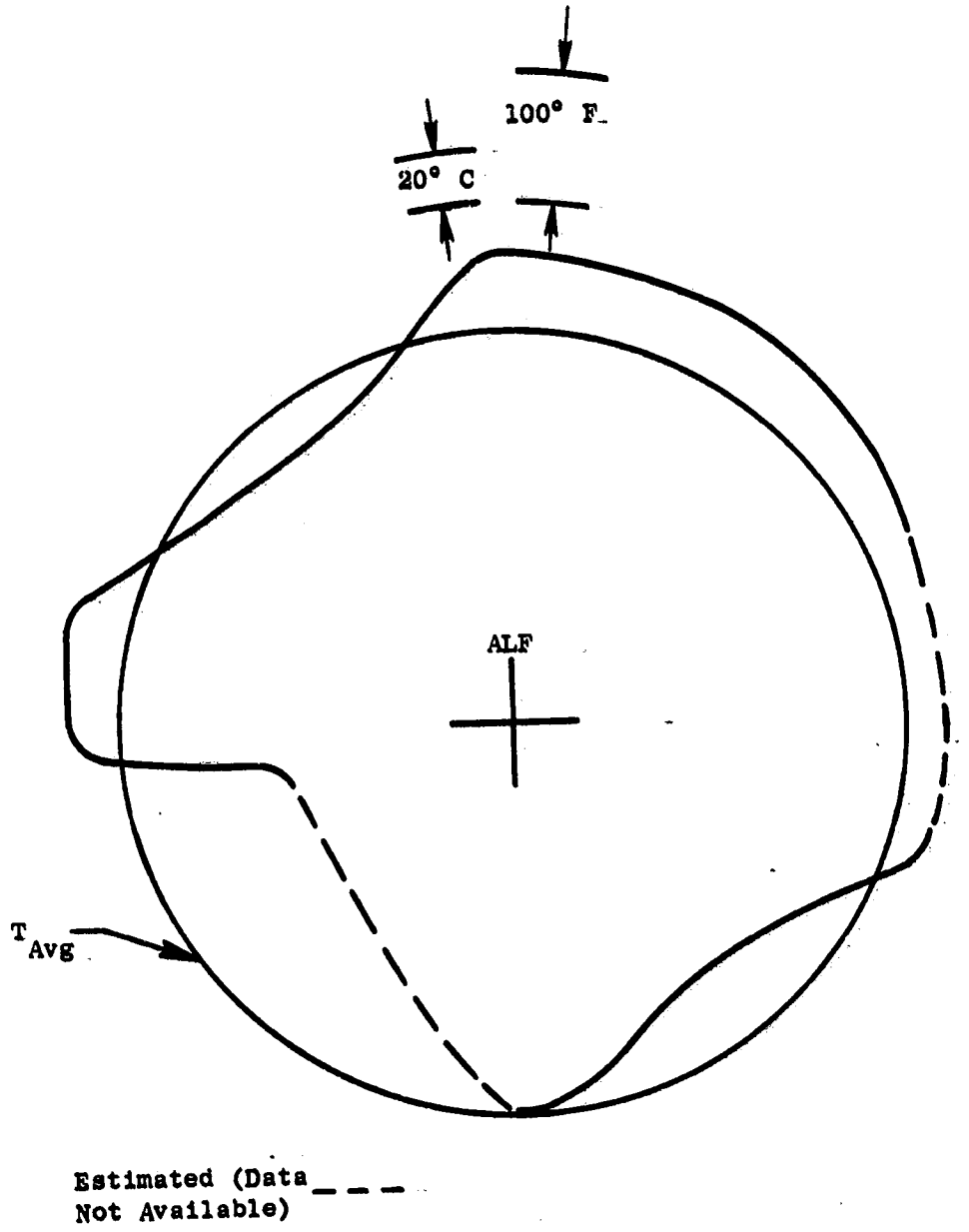

Figure 44. LP Turbine Stator Case Circumferential Temperature Distribution, Axial Location Number 3, Takeoff.

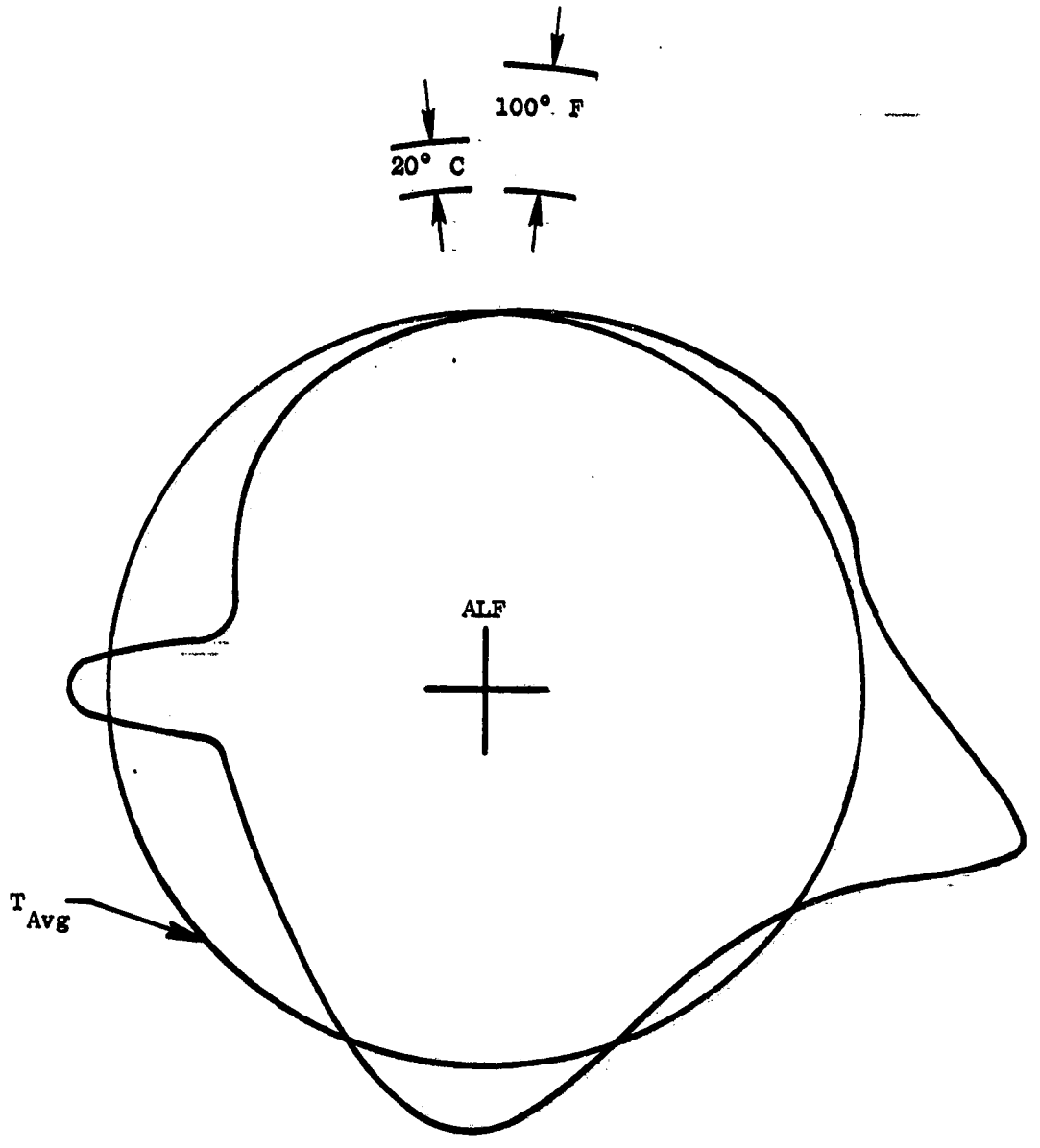

Figure 45. LP Turbine Stator Case Circumferential Temperature Distribution, Axial Location Number 4, Takeoff.

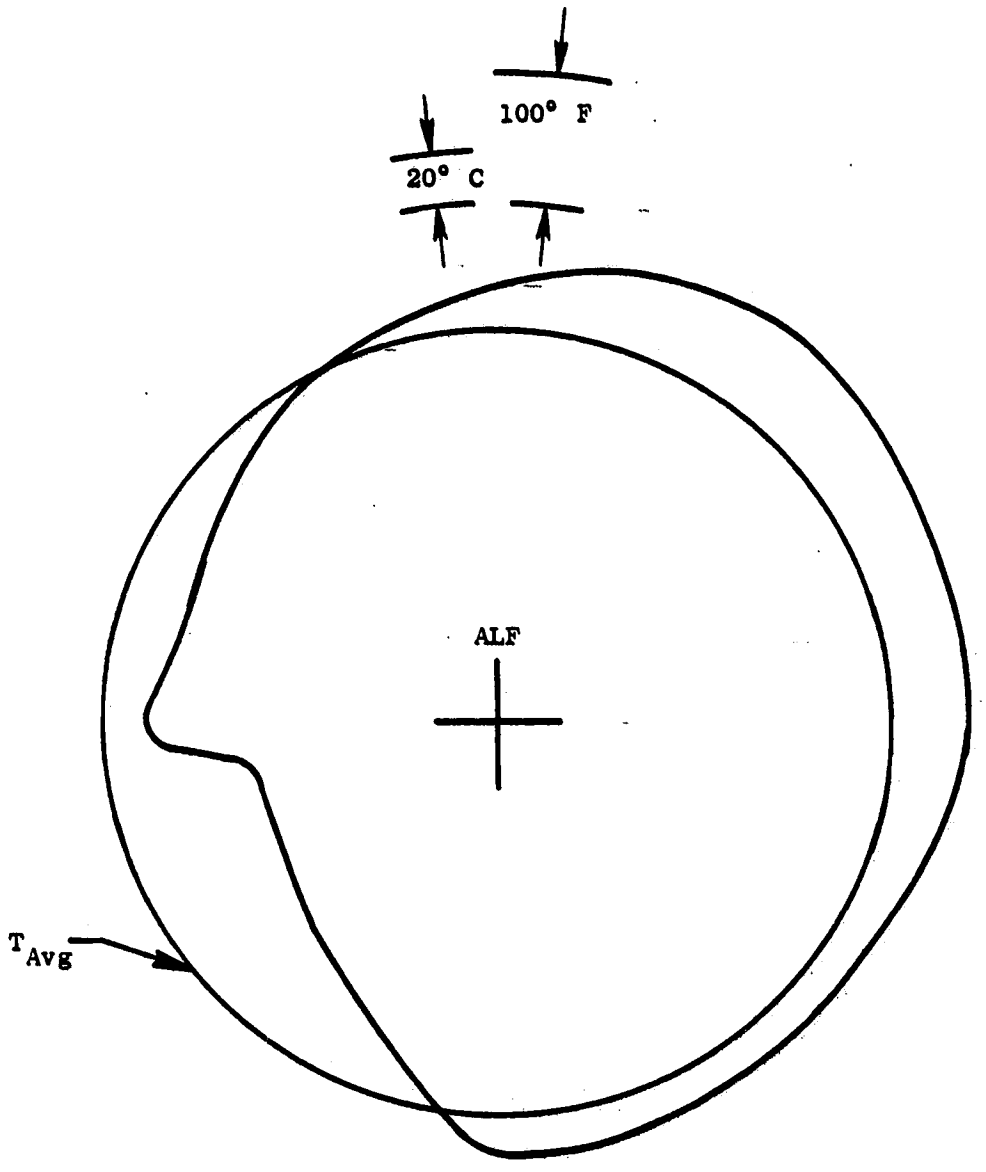

Figure 46. LP Turbine Stator Case Circumferential Temperature Distribution, Axial Average, Takeoff.

The measured temperatures in the TMF structural elements are shown in Figures 47 through 49 for ground idle and Figures 50 through 52 for takeoff.

The temperatures of each of the eight struts was measured to obtain the strut to strut variation shown on Figures 49 and 50. The hub temperature was measured at several circumferential locations. No significant temperature variation was noted; therefore, only the average temperature is shown on Figures 47 and 50.

The temperatures on the TMF casing hat sections were measured at the base and apex of the hat section at a number of circumferential locations. These measurements were then used to calculate the area weighted average temperature and radial gradient at each location. This was done in order to obtain the data in a form which would be usable in the analytical model. These are the data presented on Figures 48, 49, 51 and 52. Also shown on Figures 51 and 52 are the estimates of these temperatures made prior to this testing. These estimates were based on a very limited amount of test data obtained from other engine testing. As the thermal mass and heating/cooling mechanism for the hat section varies around the circumference of the TMF casing, temperature measurements were made at twelve circumferential locations to obtain an accurate representation of the temperature variations in this area.

Temperatures on the TMF/CRF flange were measured at the radial mid point of both the CRF and the TMF flanges as a measure of the average flange temperature and are shown on Figures 53 and 54.

7.5.3 High Pressure Turbine Stator Temperatures

Temperatures were also measured at three locations on the HPT stator at the same engine operating points. The results are shown on Figures 56 through 57 for ground idle and Figures 58 through 60 for takeoff.

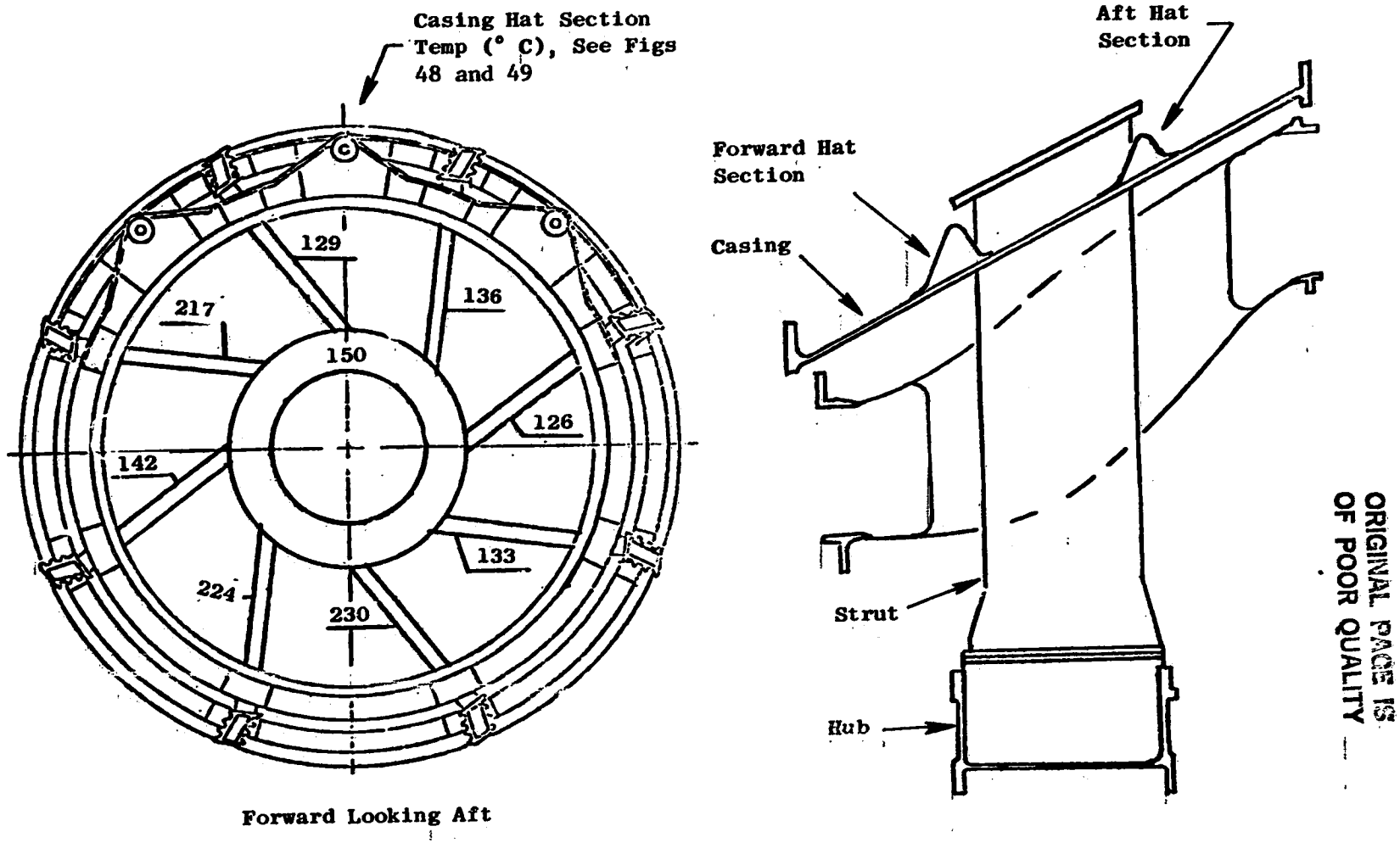

Figure 47. Turbine Midframe Temperature, Ground Idle.

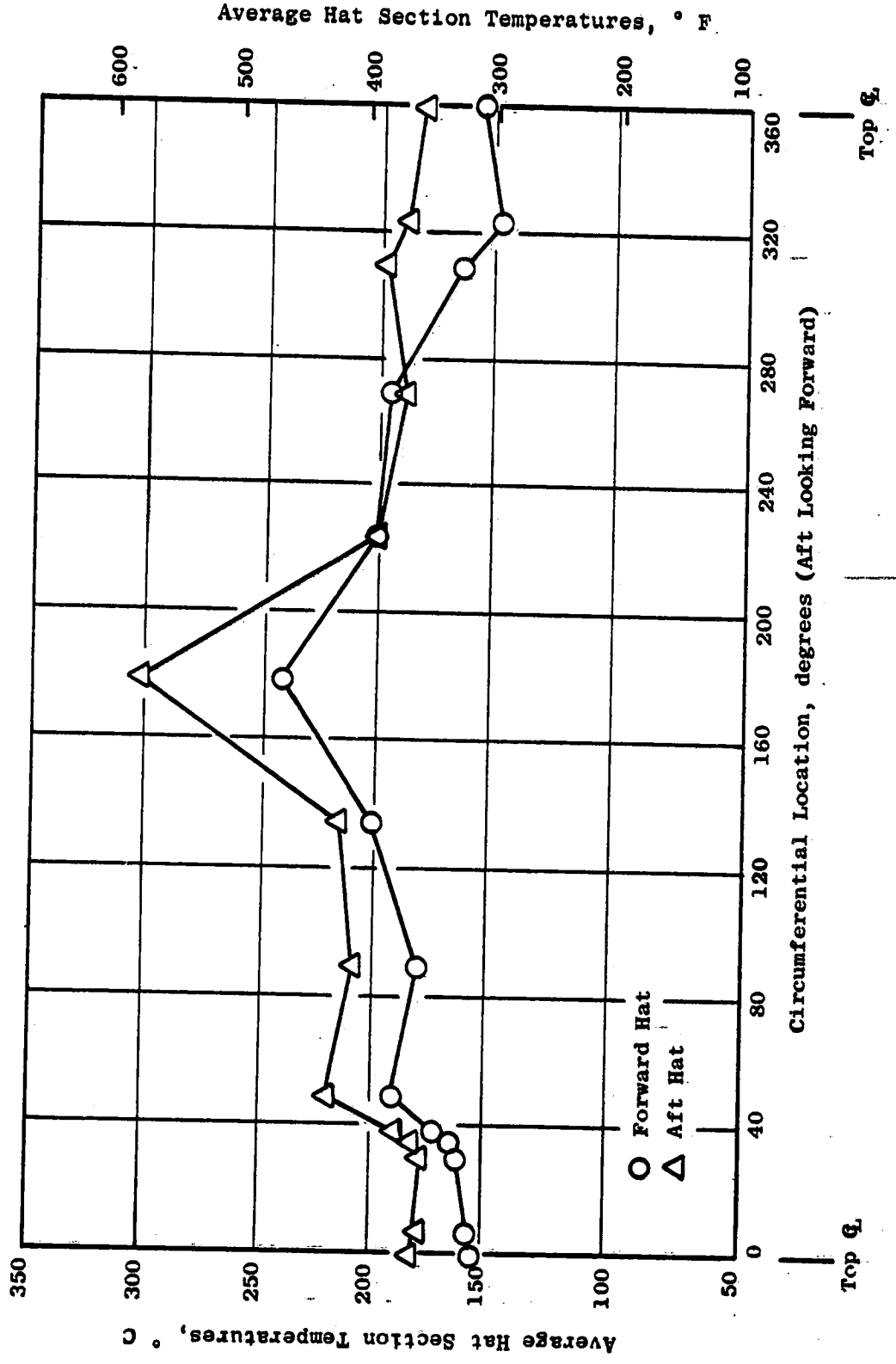

Figure 48. Turbine Midframe Casing Hat Section Average Temperature, Ground Idle.

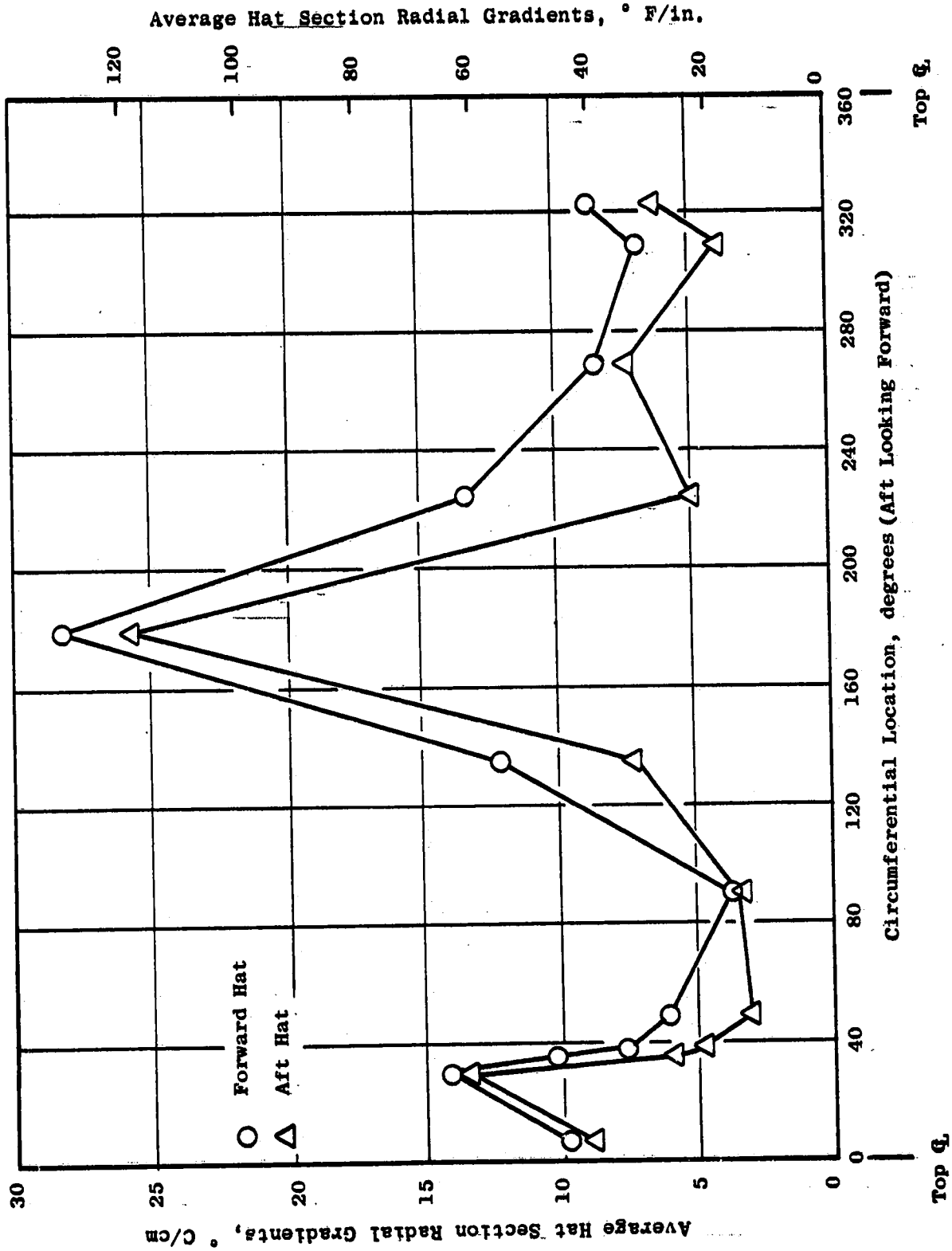

Figure 49. Turbine Midframe Casing Hat Section Radial Temperature Gradient, Ground Idle.

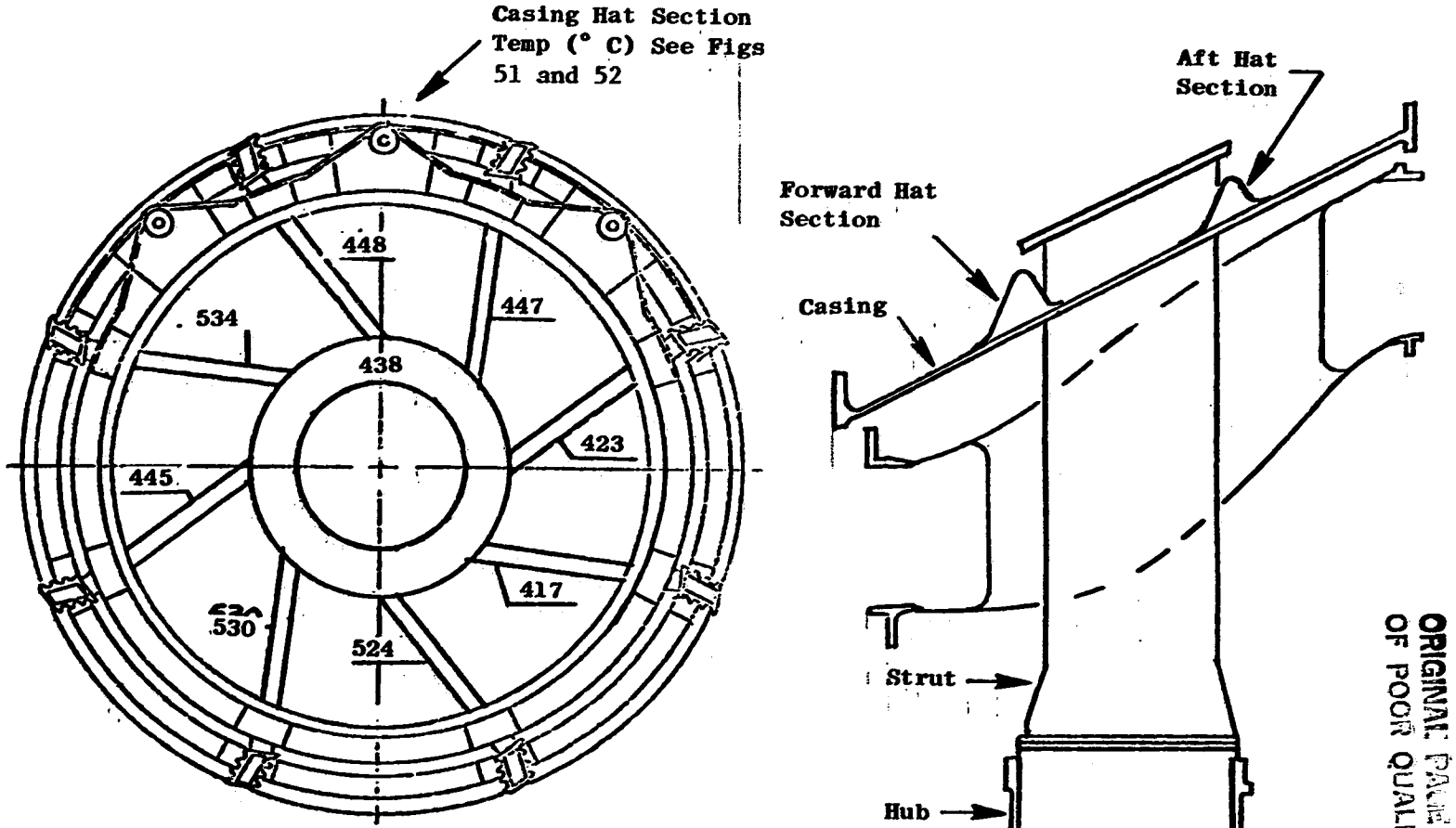

Figure 50. Turbine Midframe Temperature, Takeoff.

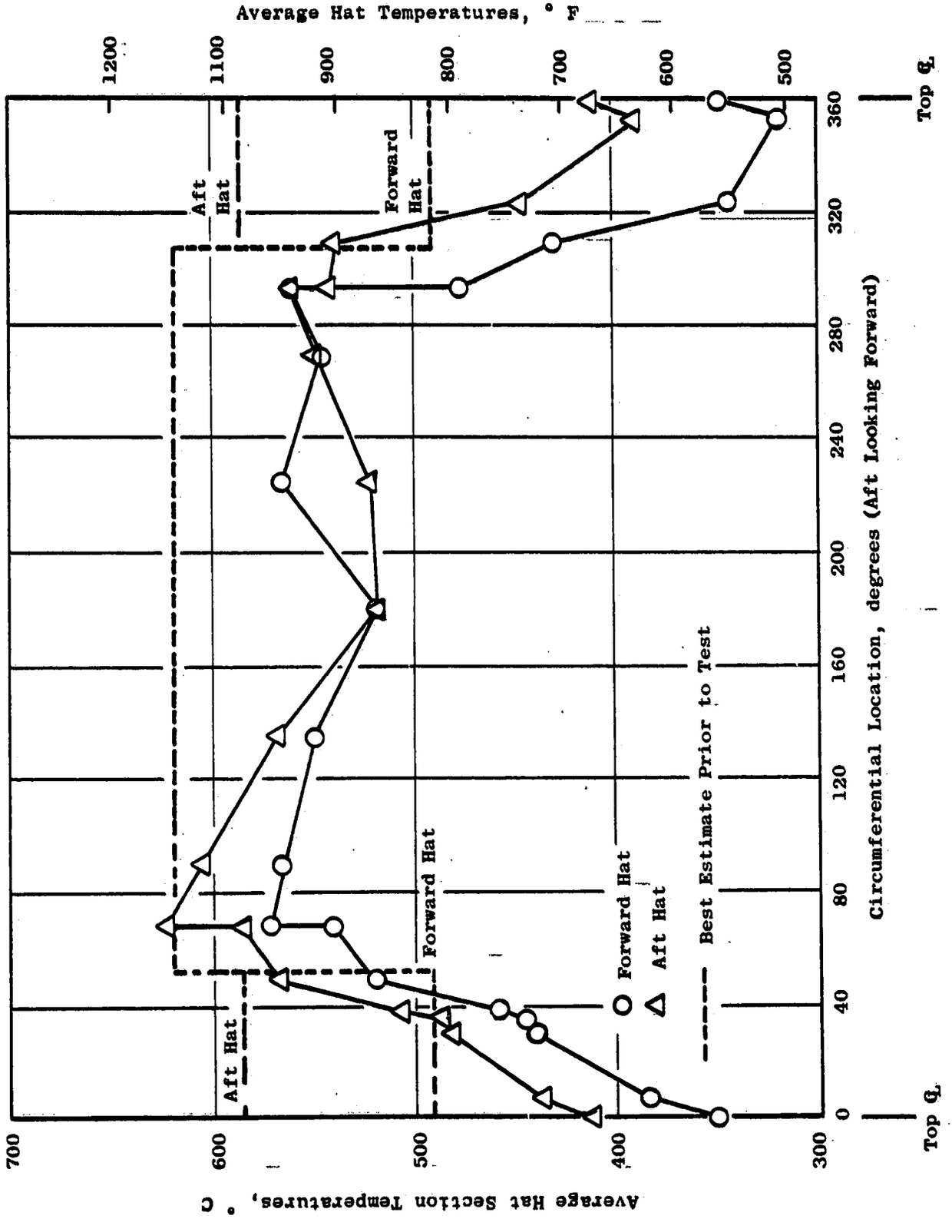

Figure 51. Turbine Midframe Casing Hat Section Average Temperature, Takeoff.

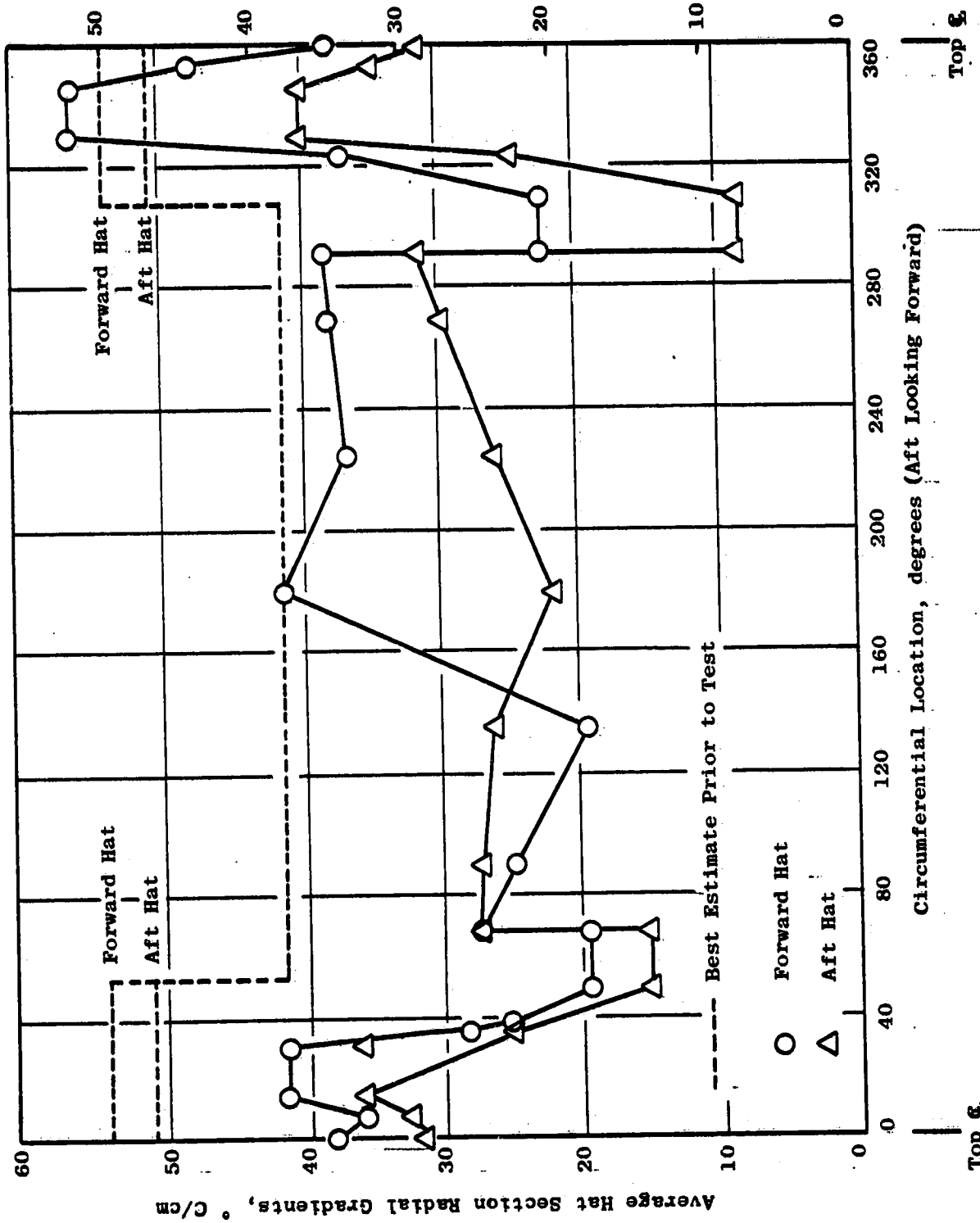

Figure 52. Turbine Midframe Casing Hat Section Radial Temperature Gradient, Takeoff.

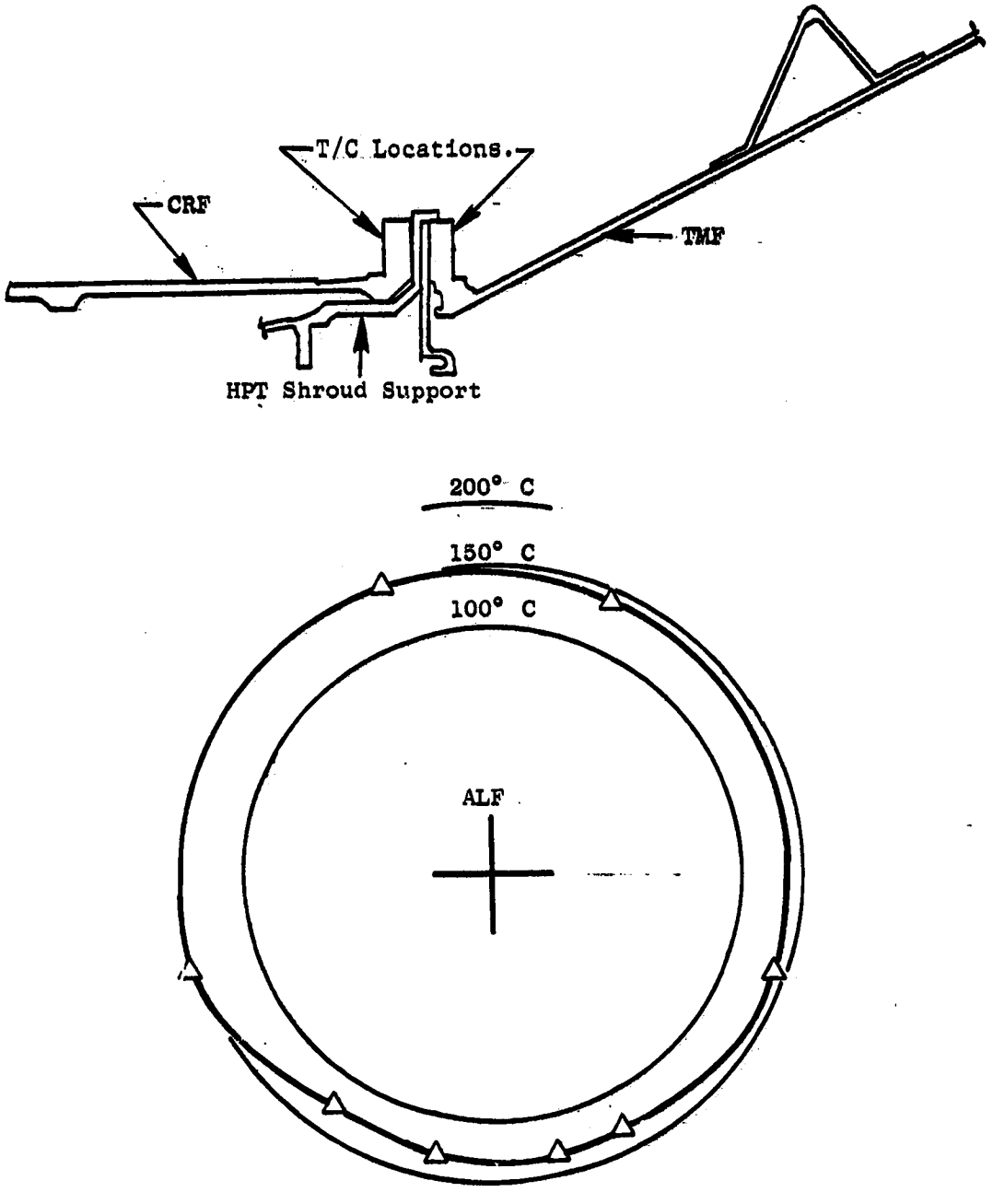

Figure 53. Turbine Midframe/Compressor Rear Frame Flange Average Temperature, Ground Idle.

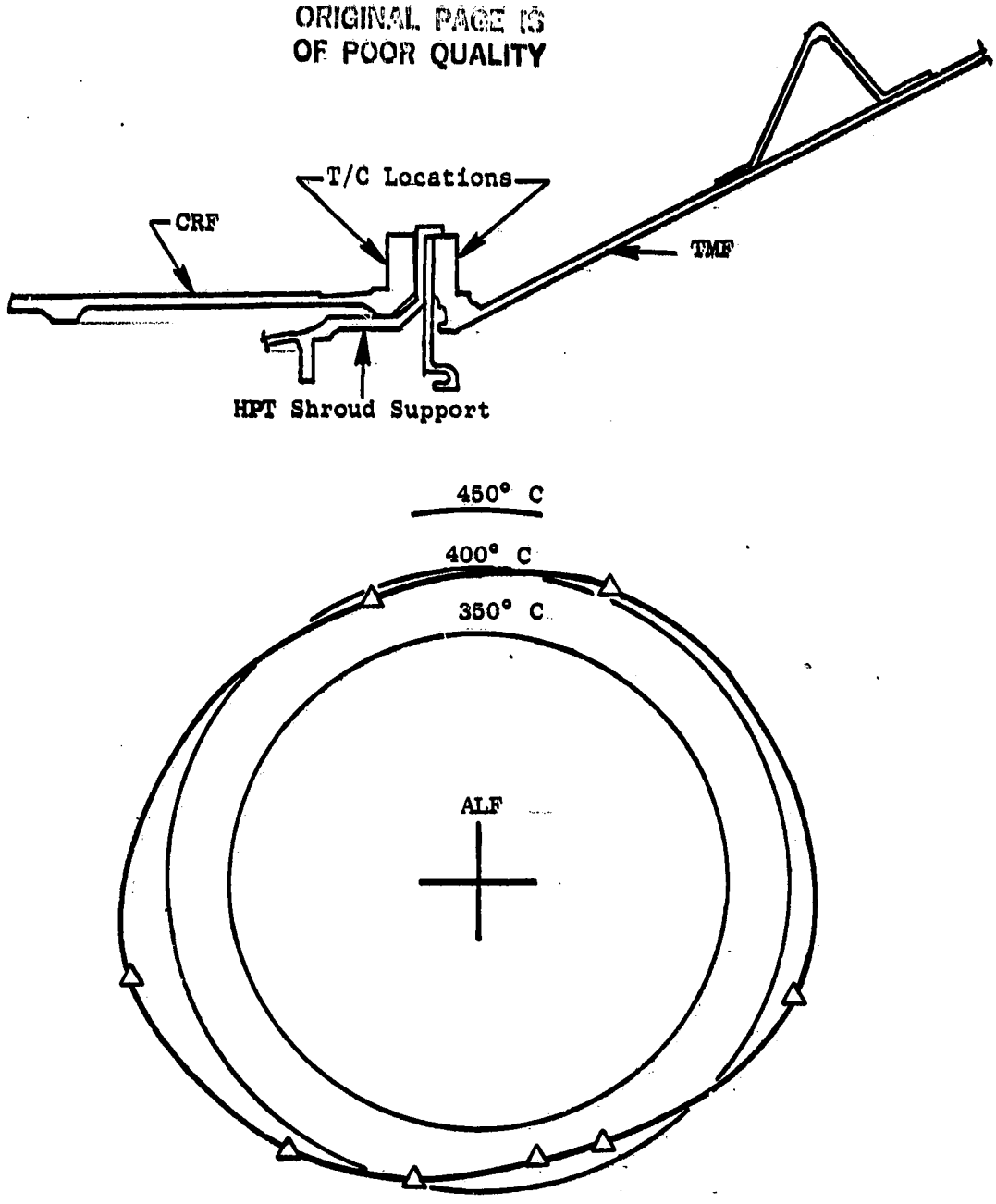

Figure 54. Turbine Midframe/Compressor Rear Frame Flange Average Temperature, Takeoff.

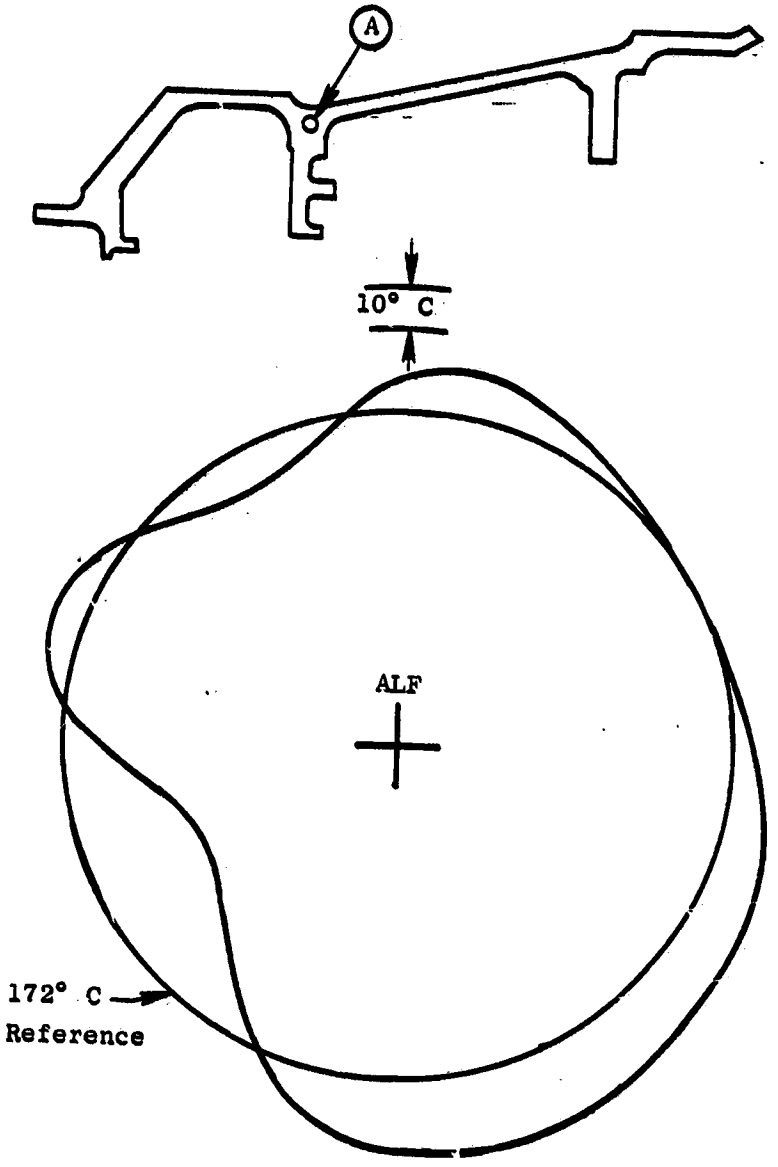

Figure 55. HP Turbine Stator Temperature, Ground Idle (Location A).

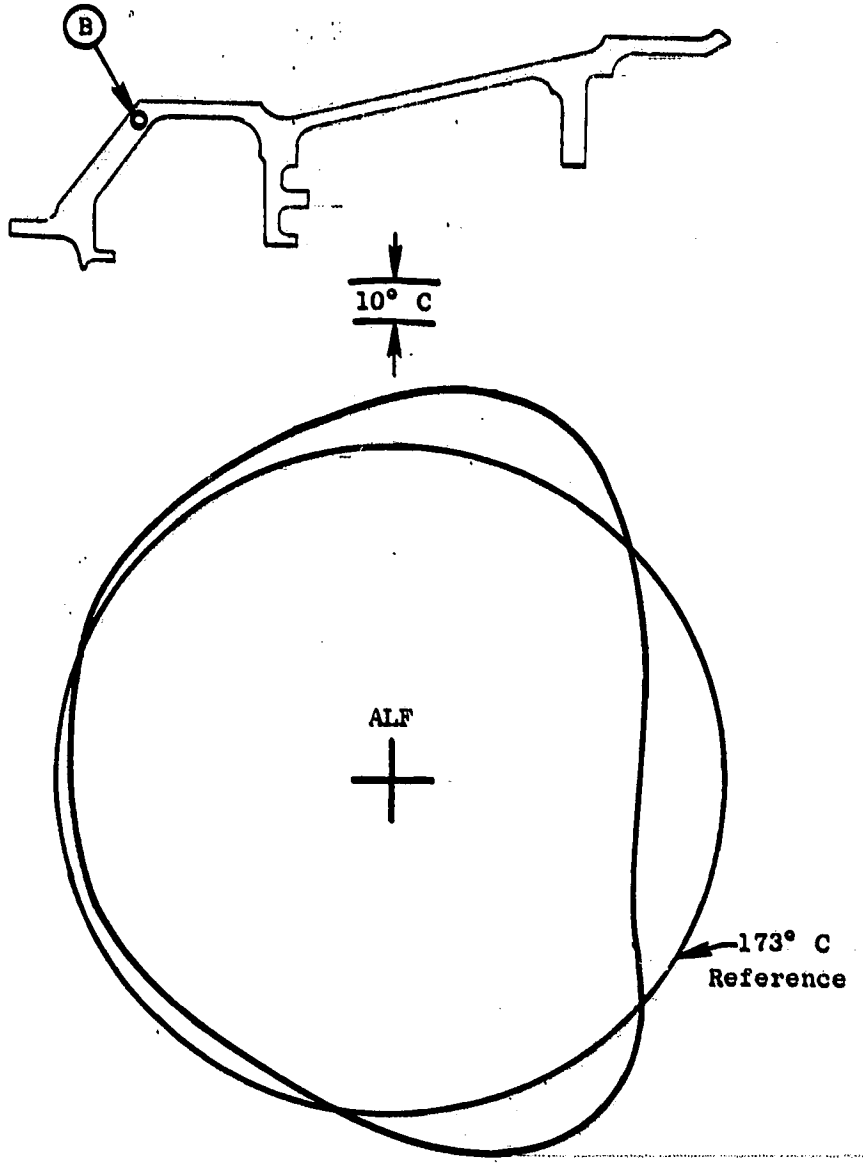

Figure 56. HP Turbine Stator Temperature, Ground Idle (Location B).

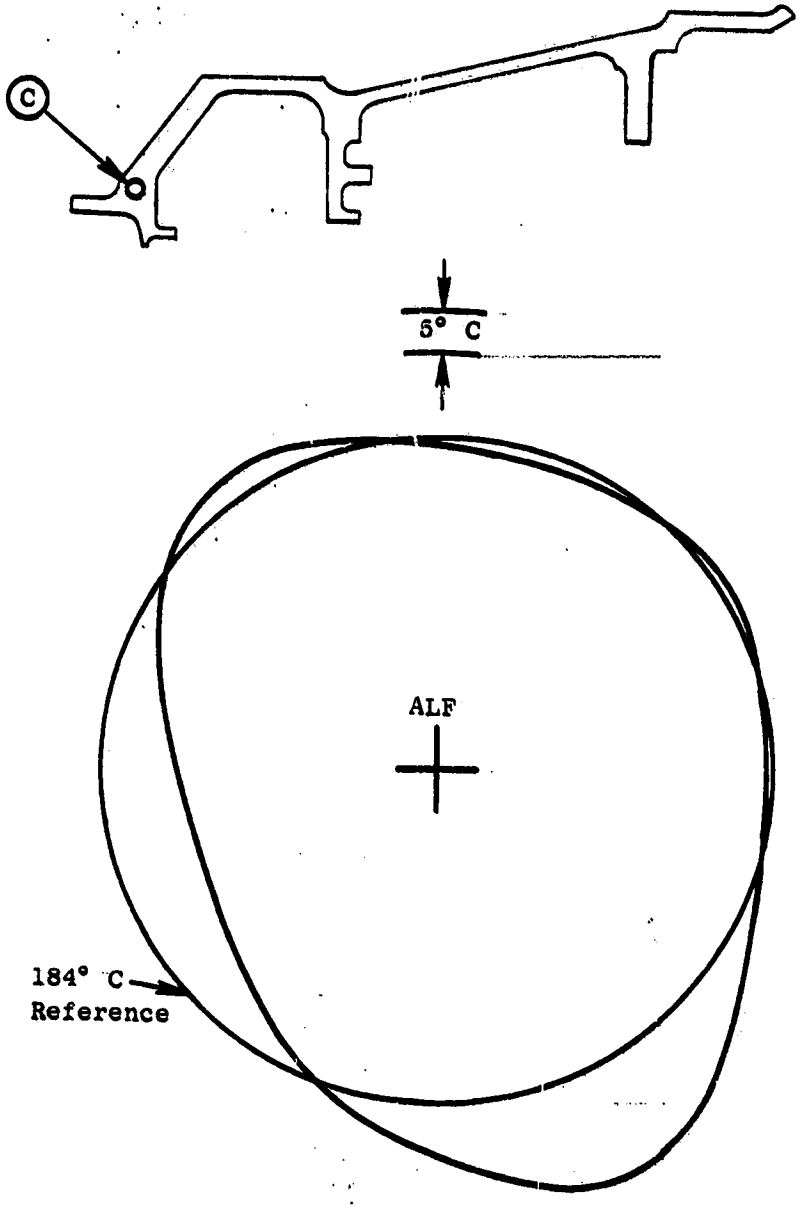

Figure 57. HP Turbine Stator Temperature, Ground Idle (Location C).

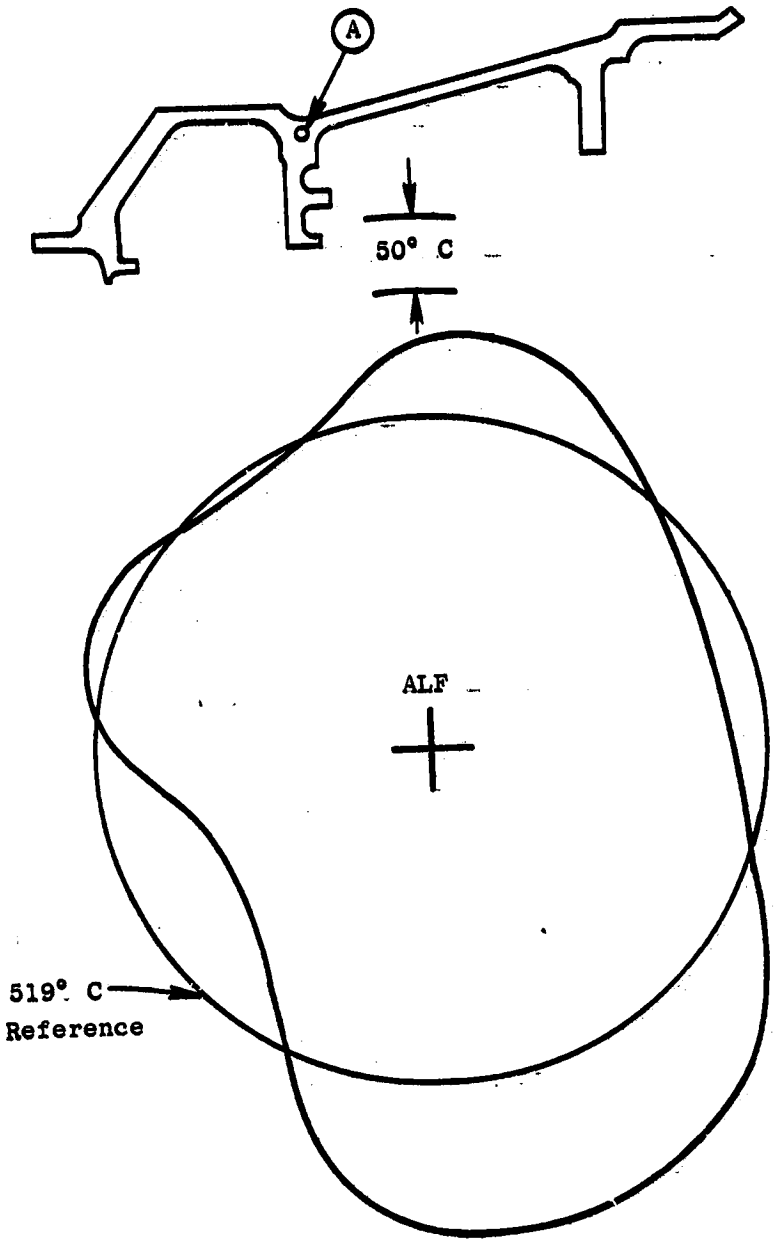

Figure 58. HP Turbine Stator Temperature, Takeoff (Location A).

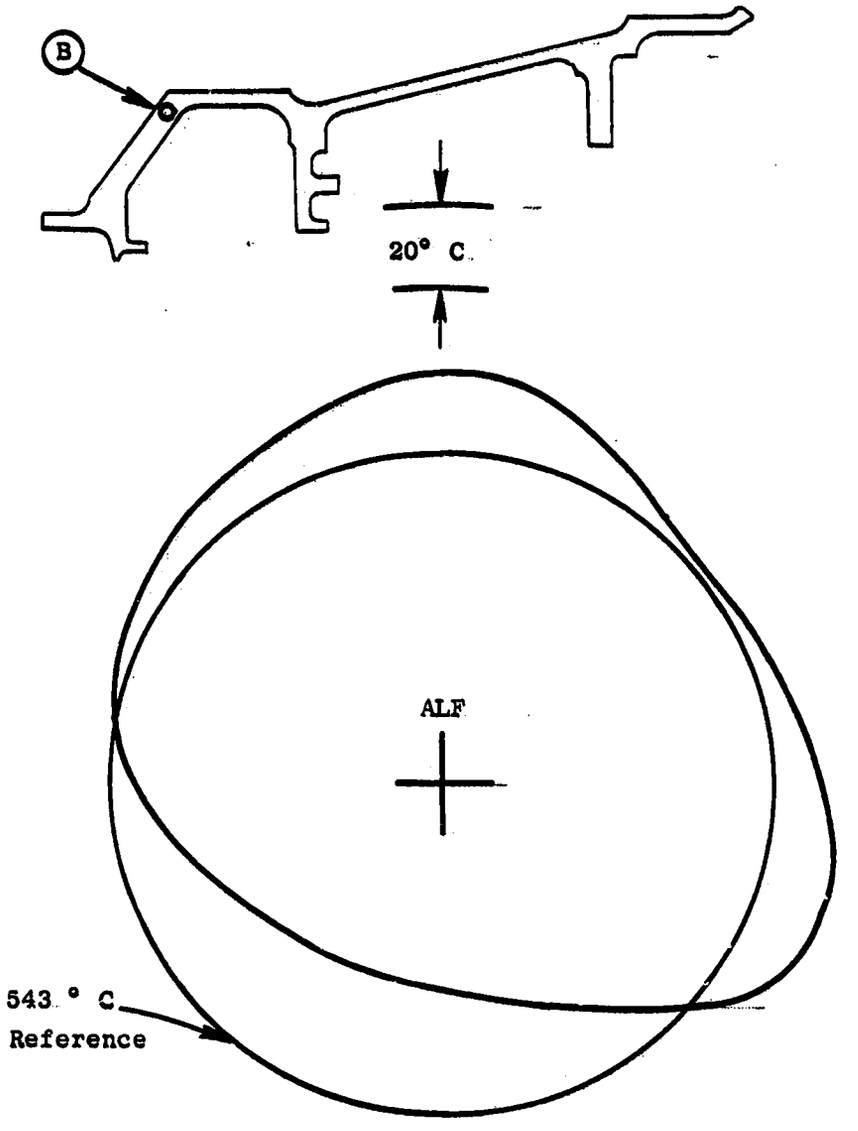

Figure 59. HP Turbine Stator Temperature, Takeoff (Location B).

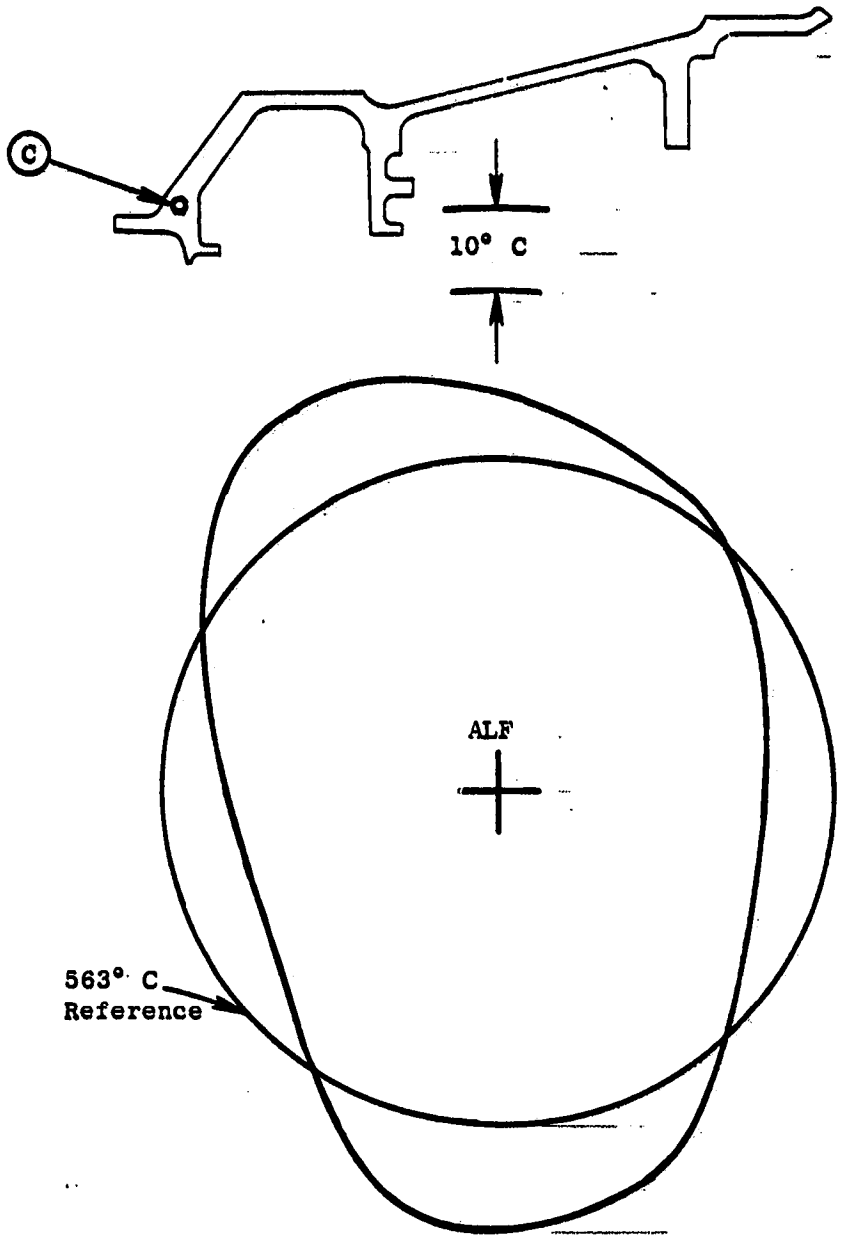

Figure 60. HP Turbine Stator Temperature, Takeoff (Location C).

7.5.4 Low Pressure Turbine Effects

Horizontal Flange/Skin Temperature Gradient Effects

Based on the CF6-50 structural system model, the gradient of the averages of the LPT horizontal flange/skin temperatures (see Figures 35 and 36) translates into an HPT stator out-of-roundness of less than 0.025 mm (0.001 in).

Circumferential Temperature Gradients

Each of the circumferential temperature distributions depicted in Figures 37 through 46 was represented by a Fourier Series. These representations demonstrated that no single harmonic dominated the mode shapes at the ground idle condition but that for the takeoff condition, the first harmonic clearly dominated. The Fourier Series representations of the circumferential average mode shapes for both ground idle and takeoff were used in conjunction with the "CLASS/MASS" influence coefficients to determine that the LPT induced HPT out-of-roundness is approximately 0.025 mm (0.001 in.) for both ground idle and takeoff conditions.

Discussion Of LPT Caused HPT Out-Of-Roundness

The LPT-caused HPT out-of-roundness of approximately .025 mm (0.001 in.) from the thermal gradient of the flange/skin system and of approximately 0.025 mm (0.001 in.) from the skin circumferential gradient are very small compared to the out-of-roundness caused by the turbine midframe. Considering the complexity of the model and the many approximations made throughout the analysis technique, these small out-of-roundnesses were neglected.

7.5.5 Turbine Midframe Effects

Using the measured temperatures on the turbine midframe structural elements and TMF/CRF flange, and the engine operating parameters to establish mechanical loading on the TMF, the out-of-roundness in the HPT stator was calculated for ground idle and takeoff. This calculated out-of-roundness is shown in Figures 61 and 62.

High Pressure Turbine Stator Temperature Gradient Effects

The calculated stator out-of-roundness due to the measured temperature variation in the stator is shown in Figures 63 and 64.

Total Calculated Out-Of-Roundness

The total calculated HPT stator out-of-roundness, due to turbine midframe effects and high pressure turbine stator temperature gradients is shown in

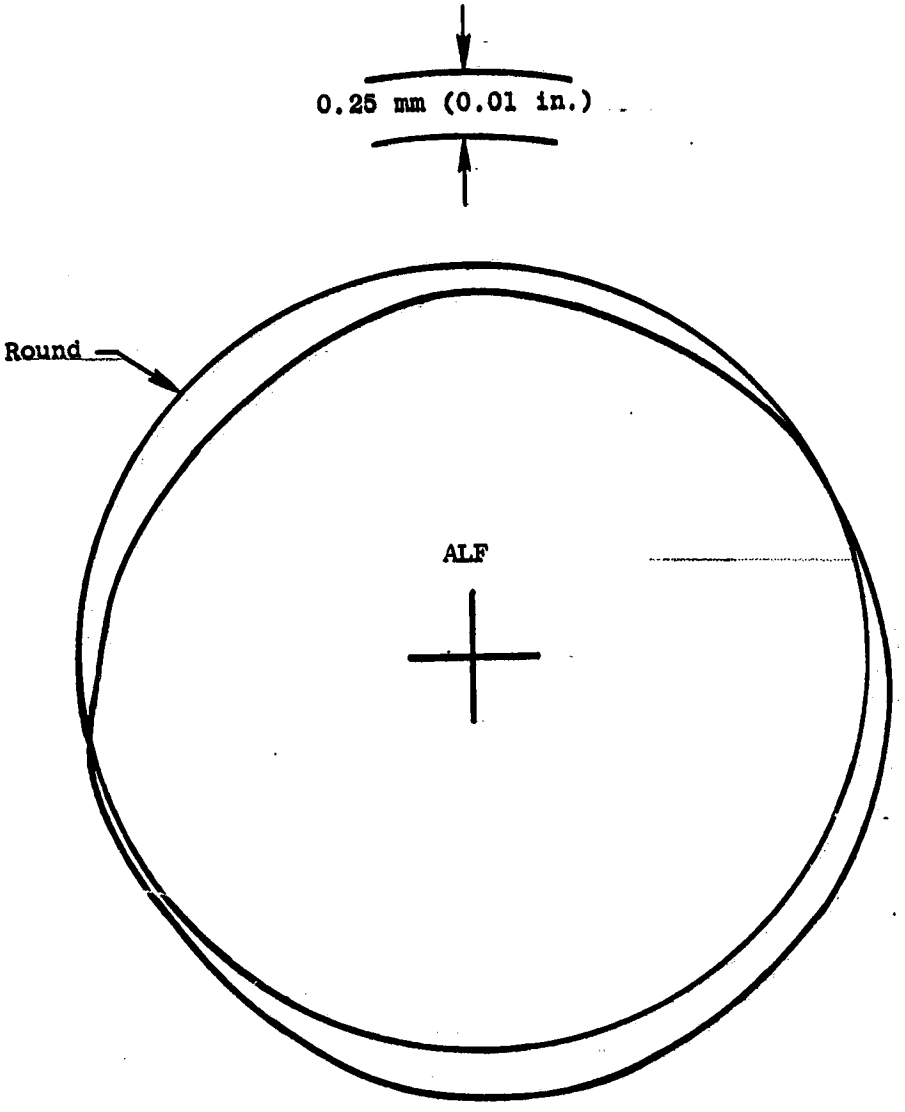

Figure 61. Calculated HPT Stator Out-of-Roundness Due to TMF, Ground Idle.

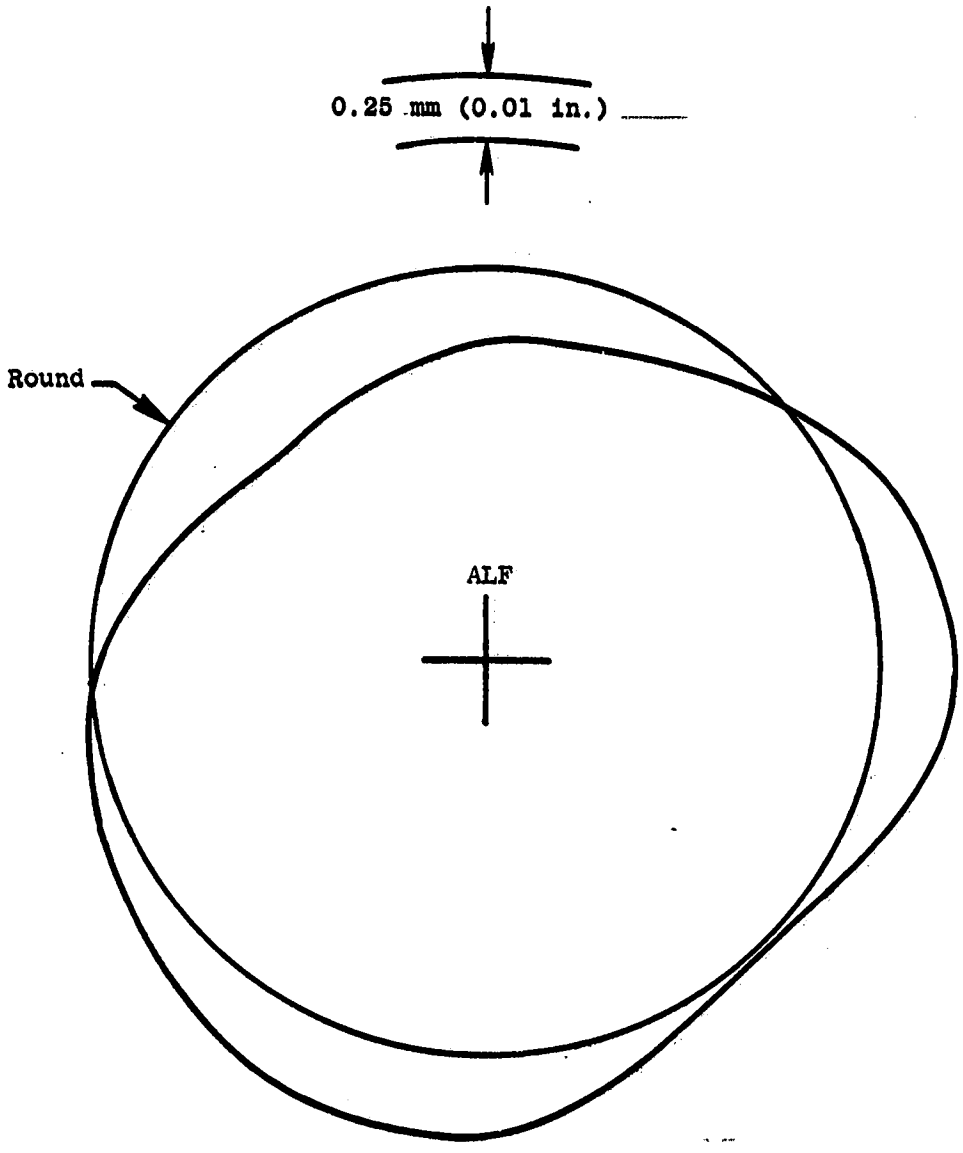

Figure 62. Calculated HPT Stator Out-of-Roundness Due to TMF, Takeoff.

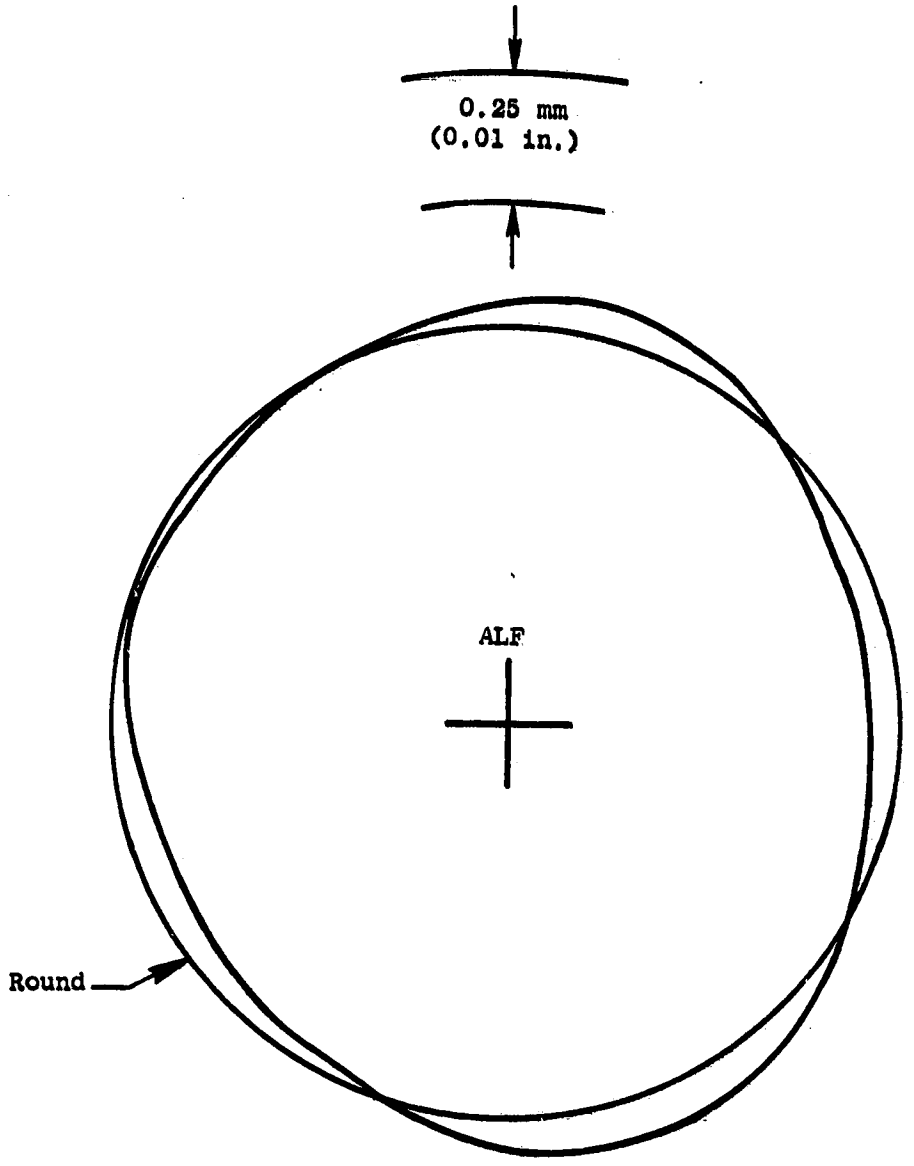

Figure 63. Calculated HPT Stator Out-of-Roundness Due to Stator Temperature Variation, Ground Idle.

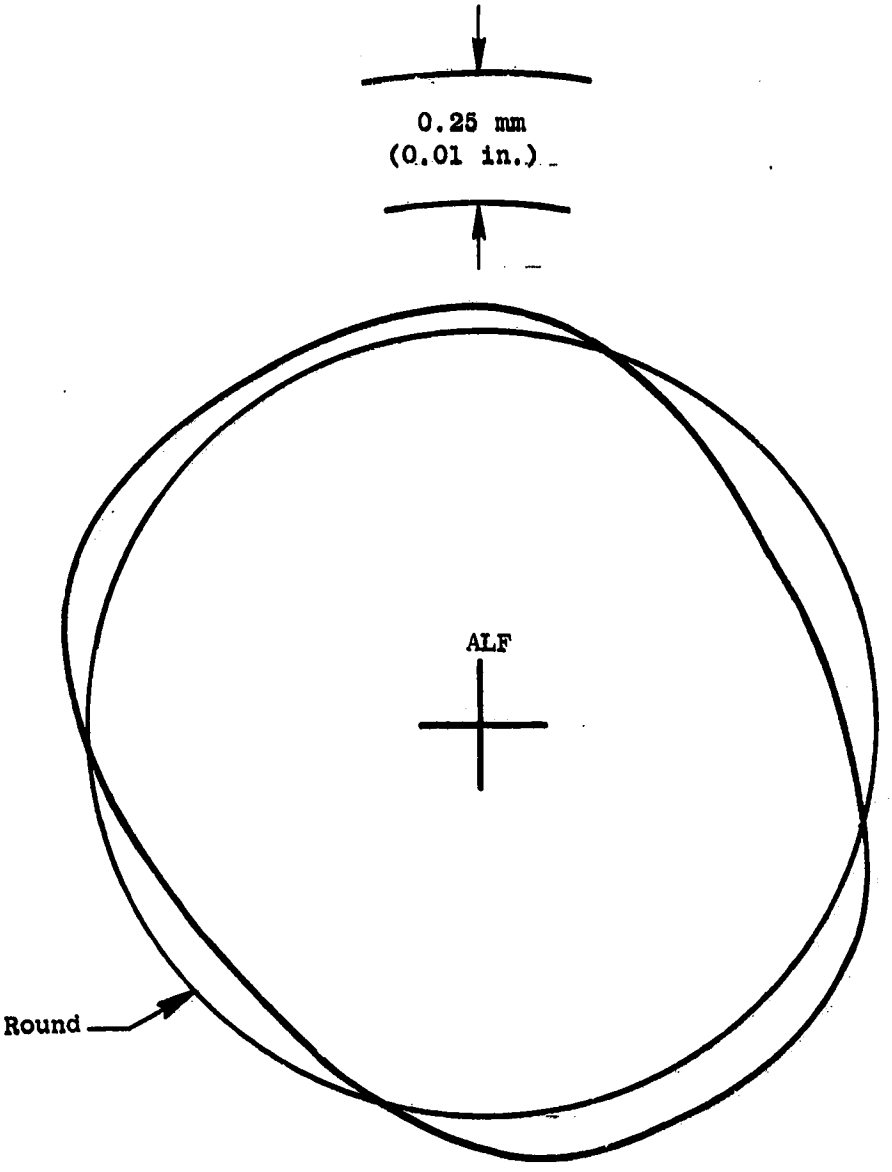

Figure 64. Calculated HPT Stator Out-of-Roundness Due to Stator Temperature Variation, Takeoff.

Figures 65 and 66 and compared to the measured data at these points from the engine test.

7.5.6 Measured Transient HPT Stator Roundness

The high pressure turbine stator out-of-roundness for a throttle burst is presented in Figures 67 through 72 and the out-of-roundness during a throttle chop is shown in Figures 73 through 80. These figures show the slowly changing roundness relationship with respect to time during these throttle movements.

7.5.7 Discussion of Roundness Data

The measured versus calculated out-of-roundness is used to correlate the analytical models, techniques, and assumptions used in HPT out-of-roundness predictions. Comparison of calculated to measured out-of-roundness under operating conditions has not been possible prior to the testing conducted in this program. Comparison of the HPT out-of-roundness measured during this test to that calculated from the operating conditions and adjacent structure temperatures obtained at the same time provides the data required to show where improvements need to be made in the analytical prediction methods. These data can also be used in the future to verify the effectiveness of any such improvements.

The correlation between measured and calculated out-of-roundness is not good, especially at the takeoff condition. A review of the measured transient out-of-roundness data following a rapid accel from ground idle to takeoff and also following a rapid decel from takeoff to ground idle, Figures 81 and 82, shows that the change in distorted HPT stator shape occurs gradually over a period of several minutes. From this, it is concluded that the major driving element for out-of-roundness is the differential thermal response in the engine structures which is known to occur slowly. Mechanical loads will result in a near step change in out-of-roundness as the parameters which cause these loads (thrust and internal pressures) change only during the initial 10-20 seconds and then remain relatively constant. Prior component static load testing has shown good correlation of measured to calculated out-of-roundness for mechanical and thermal loading with the TMF structural elements. From the above discussion, it is concluded that improvements in out-of-roundness prediction methods are required in the area of thermally induced distortion in the engine casings and HPT stator structure.

7.6 CLEARANCE AND ROUNDNESS QUANTITATIVE BASELINE

A quantitative baseline has been defined from the clearance curves and the out-of-roundness plots obtained from this test. Although the relationship between performance and clearance has not been experimentally evaluated, the data obtained from tests conducted do provide a basis for more accurate theoretical predictions.

Although there is a minor mismatch between the measured and analytically predicted clearance as a function of time relationships, the curve shapes of the analytical model correlate well (Ref. Figures 21 and 22). This will enable accurate assessments of response rates, total times, slope changes, etc. of proposed design changes.

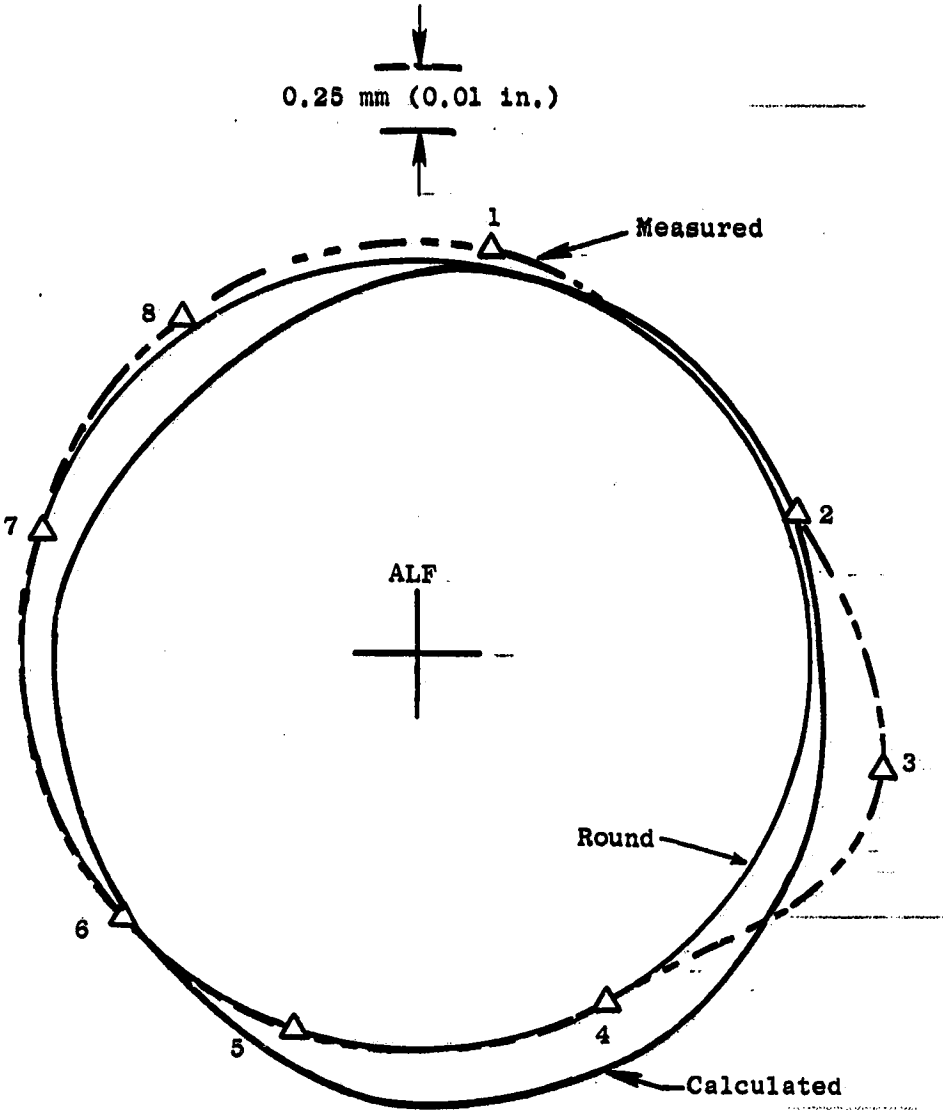

Figure 65. Total HP Turbine Stator Out-of-Roundness, Ground Idle.

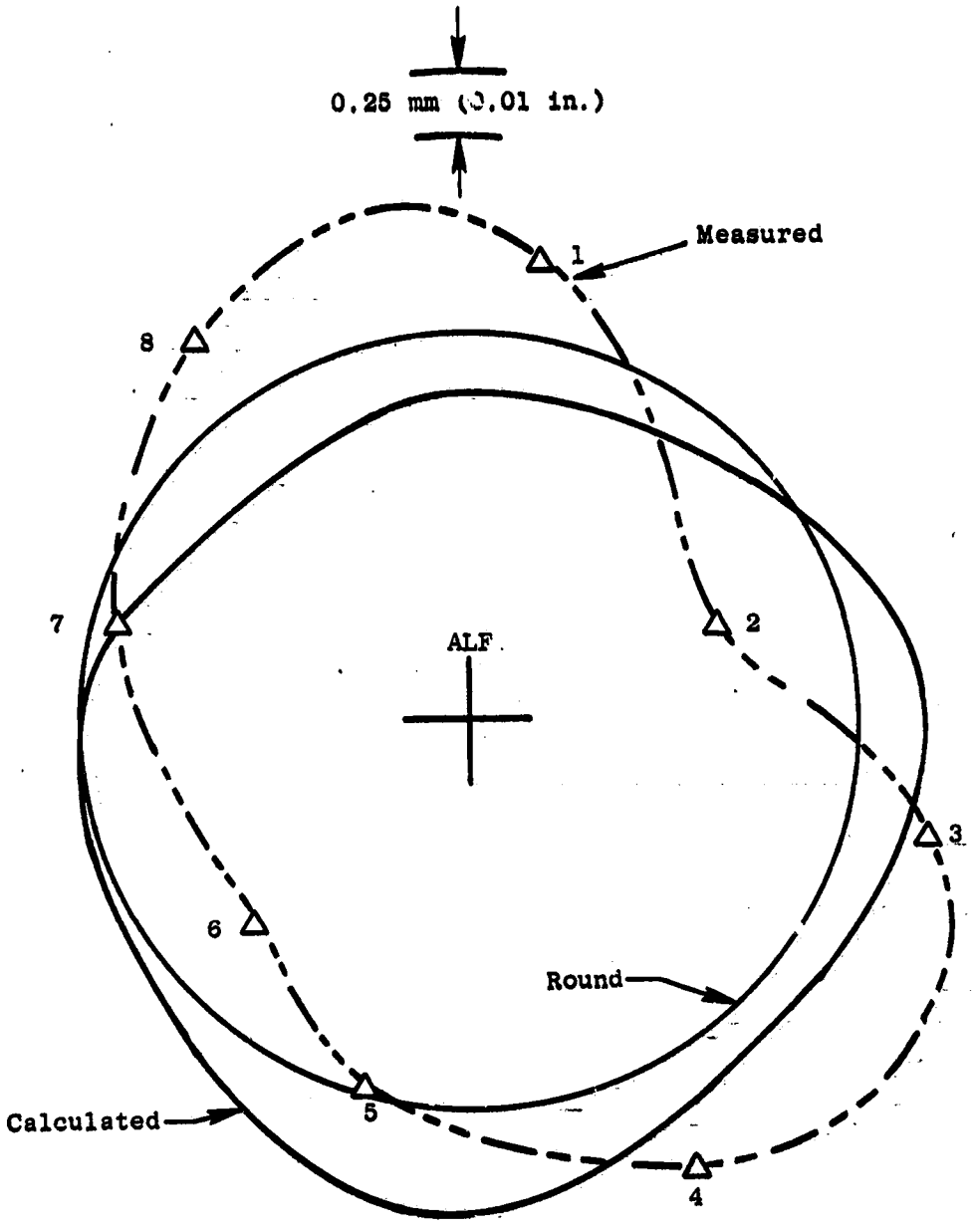

Figure 66. Total HP Turbine Stator Out-of-Roundness, Takeoff.

C - 2

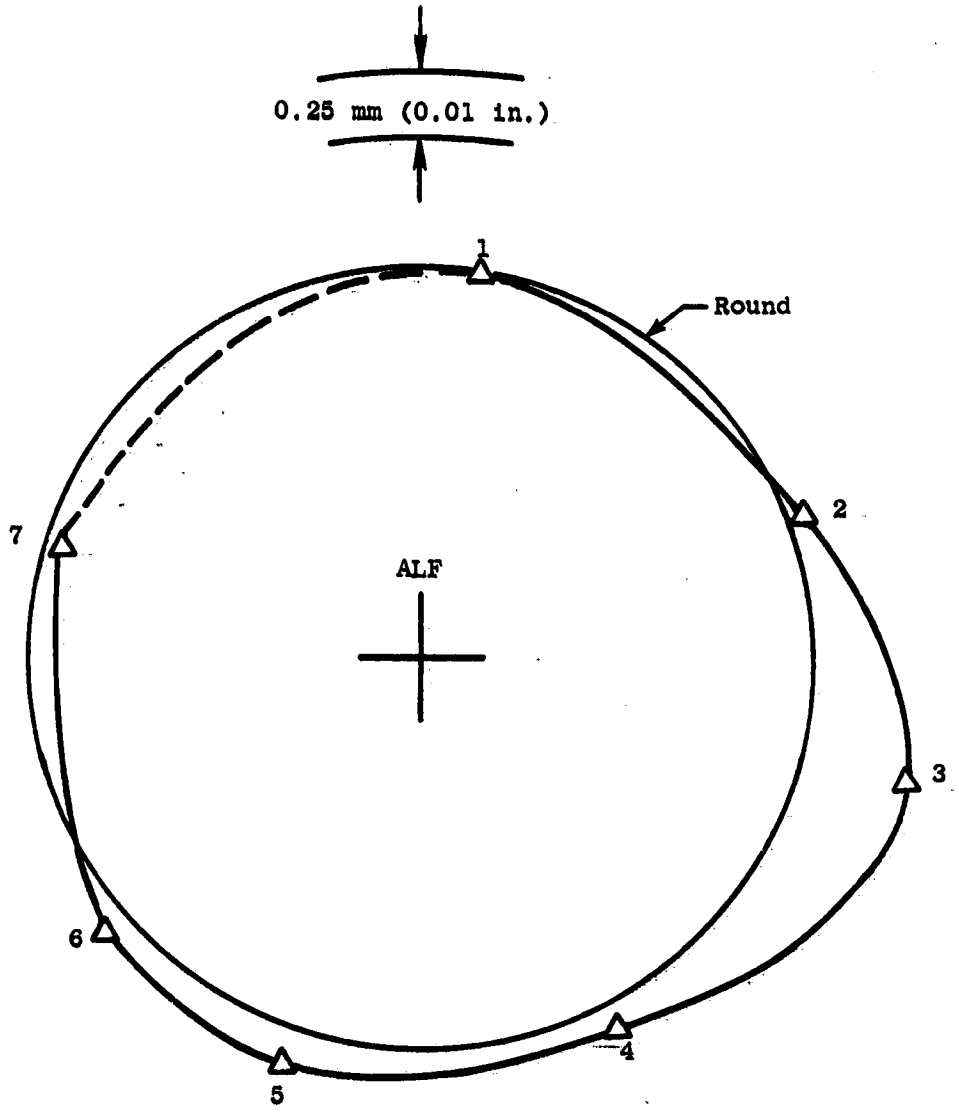

Figure 67. HP Turbine Stator Out-of-Roundness, Burst + 0 Seconds.

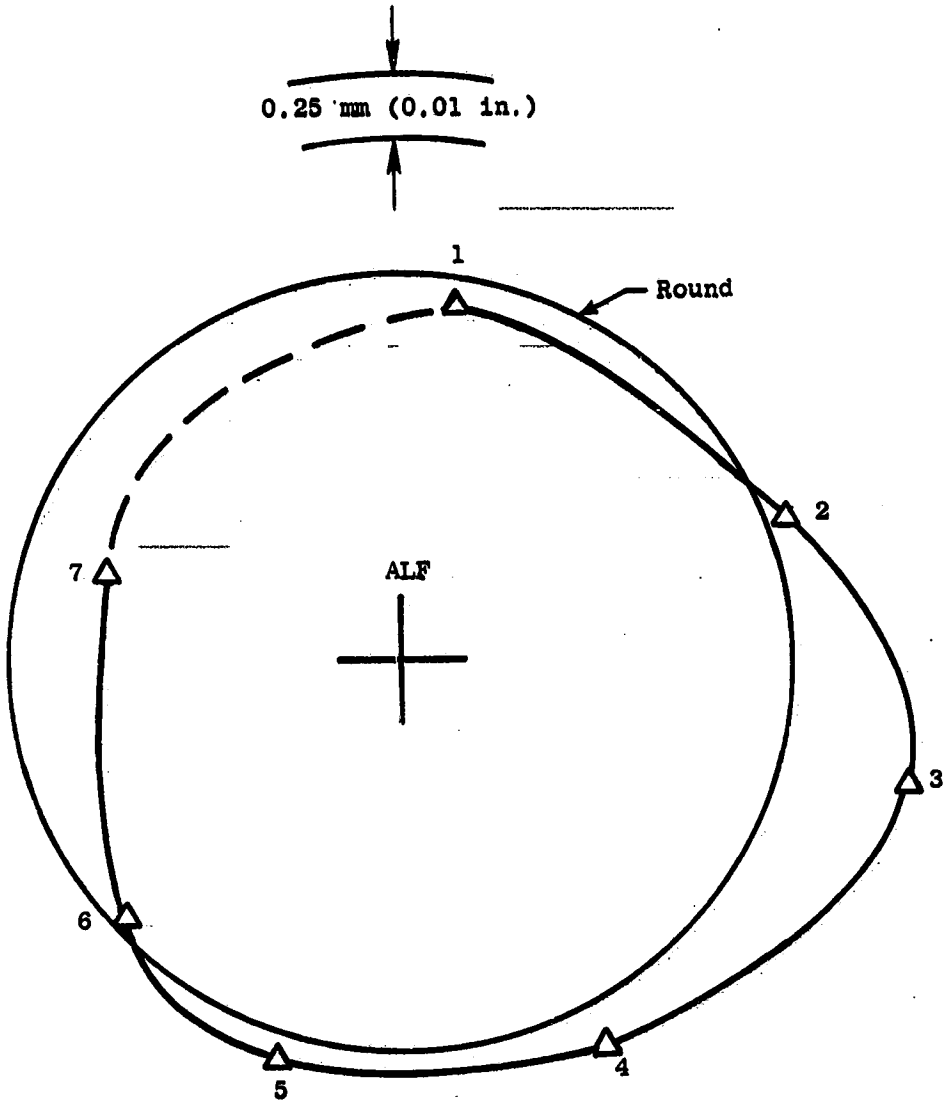

Figure 68. HP Turbine Stator Out-of-Roundness, Burst + 9 Seconds.

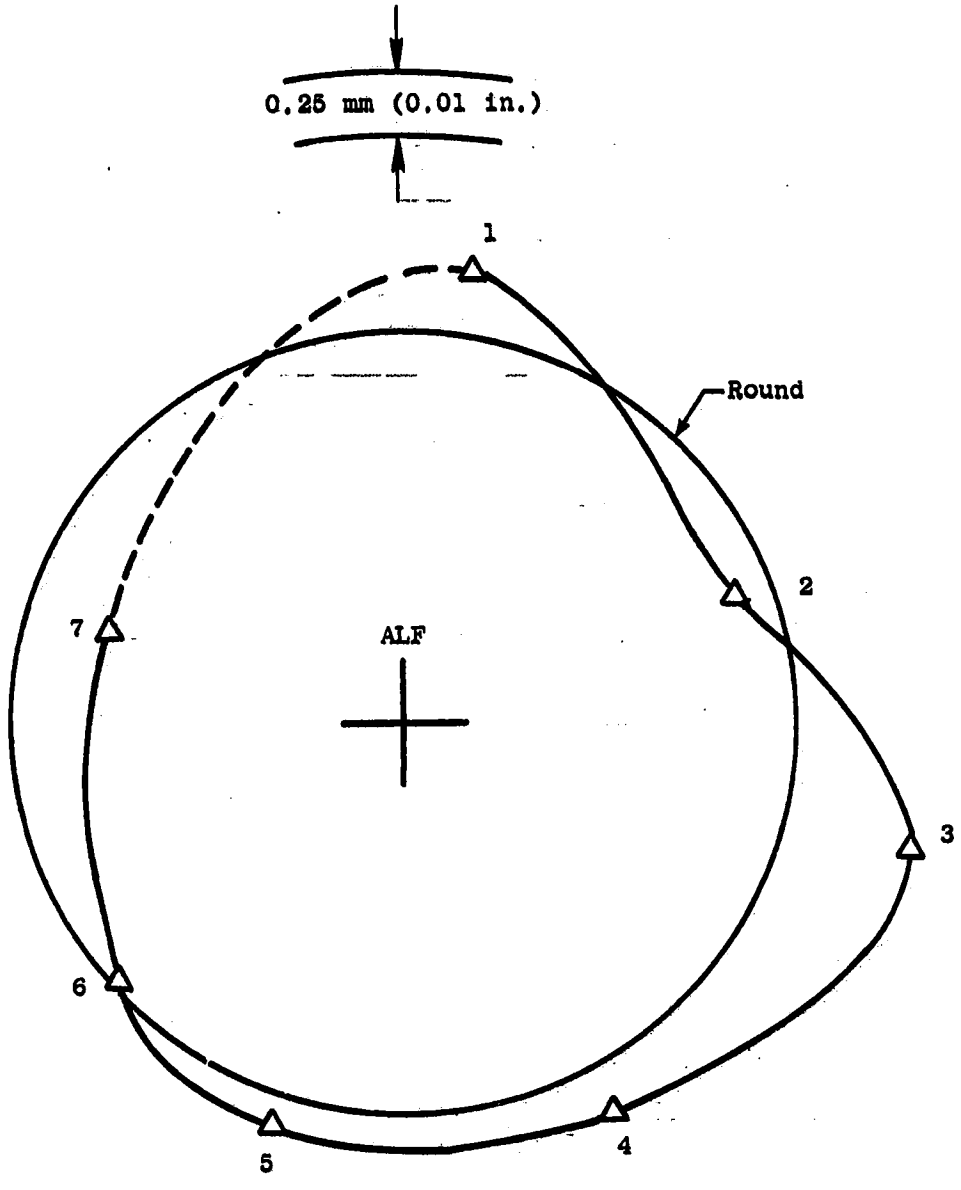

Figure 69. HP Turbine Stator Out-of-Roundness, Burst + 20 Seconds.

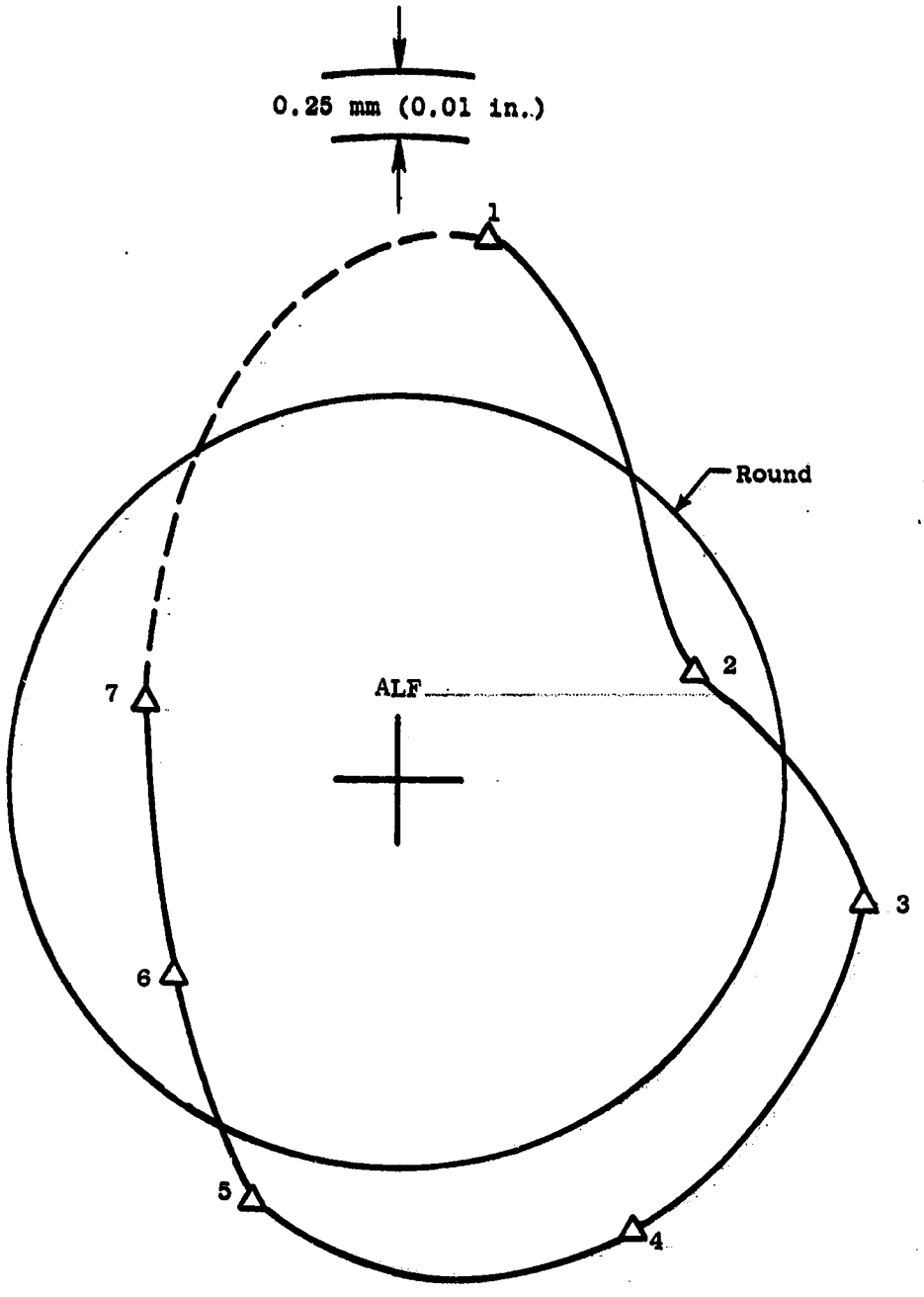

Figure 70. HP Turbine Stator Out-of-Roundness, Burst + 123 Seconds.

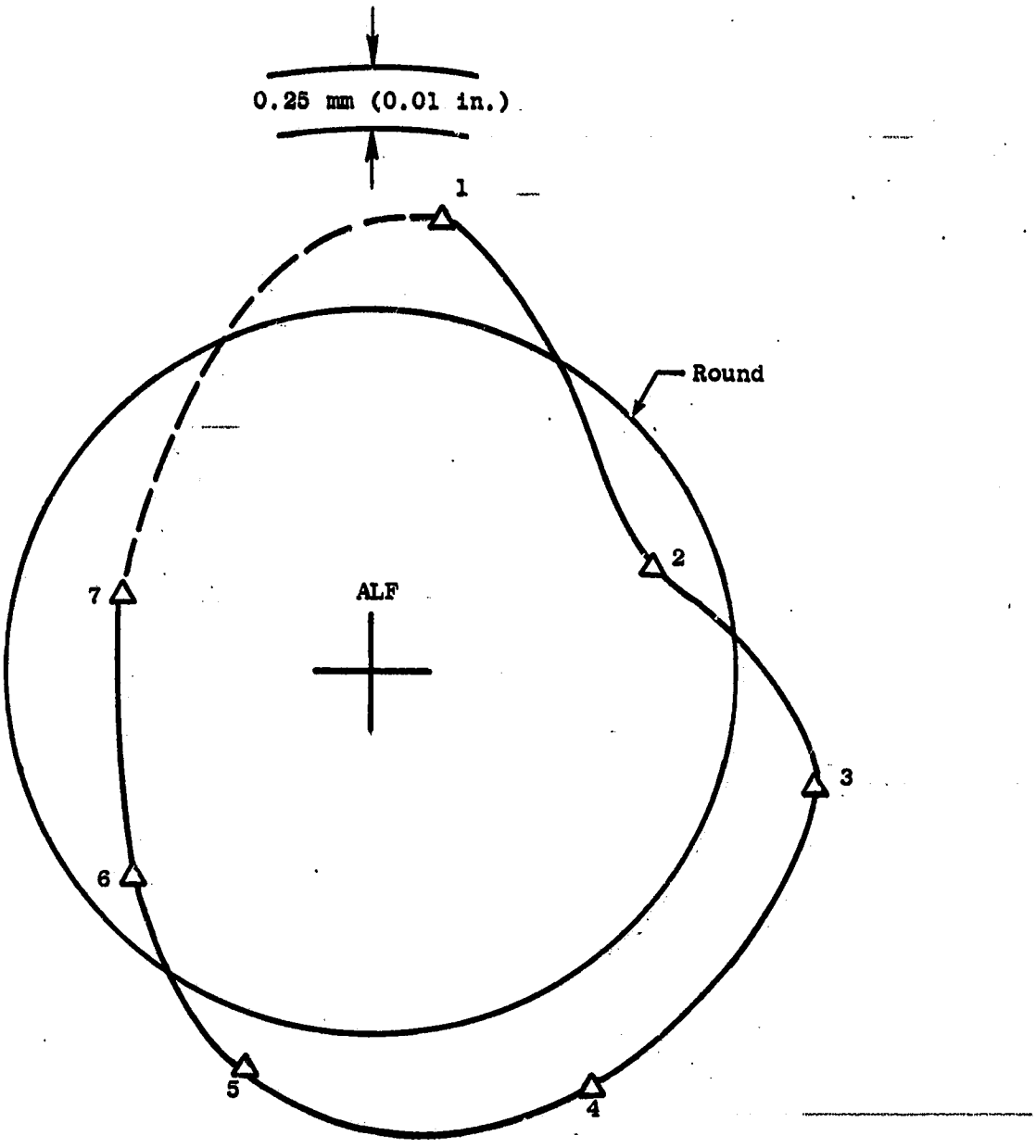

Figure 71. HP Turbine Stator Out-of-Roundness, Burst + 305 Seconds.

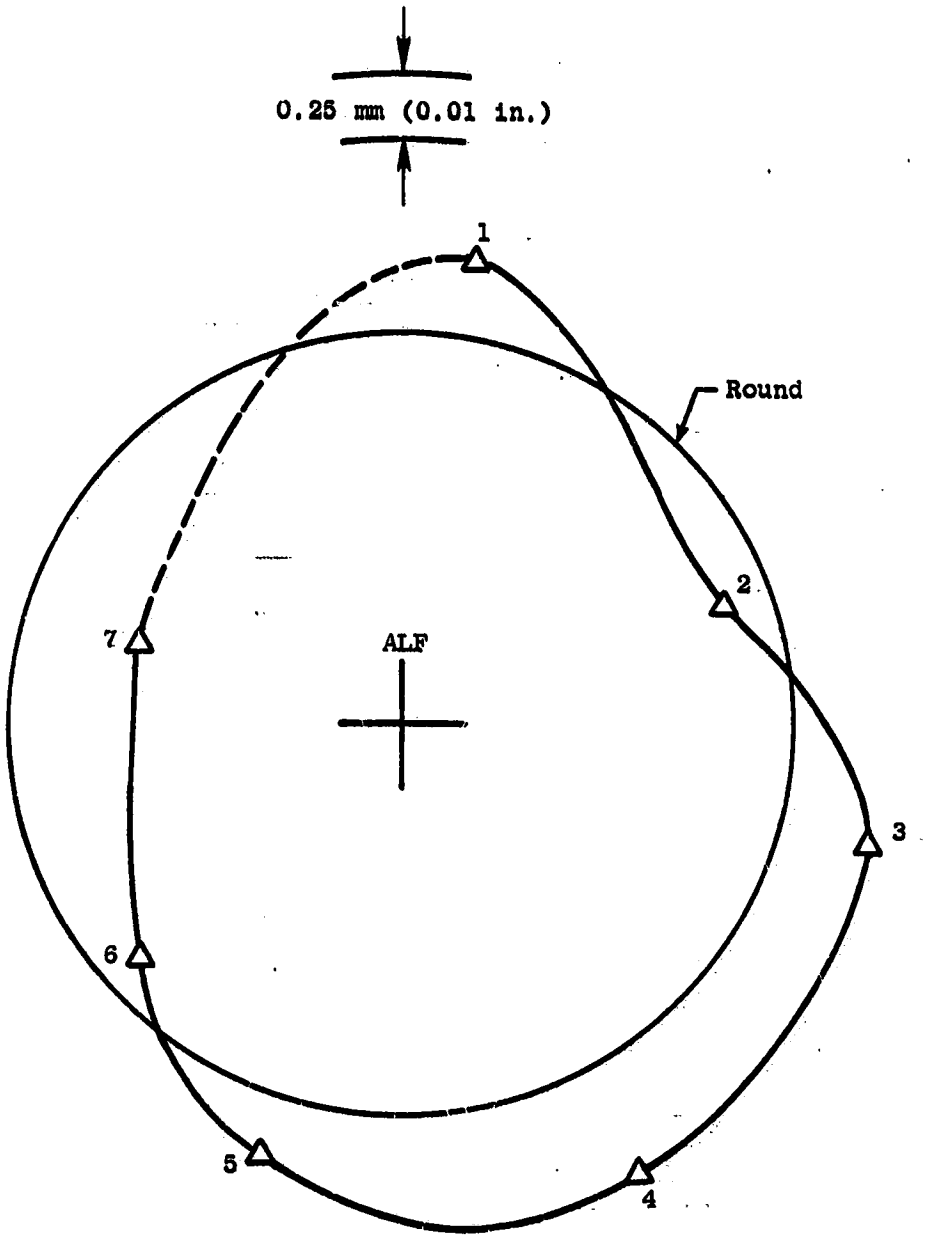

Figure 72. HP Turbine Stator Out-of-Roundness, Burst + 747 Seconds.

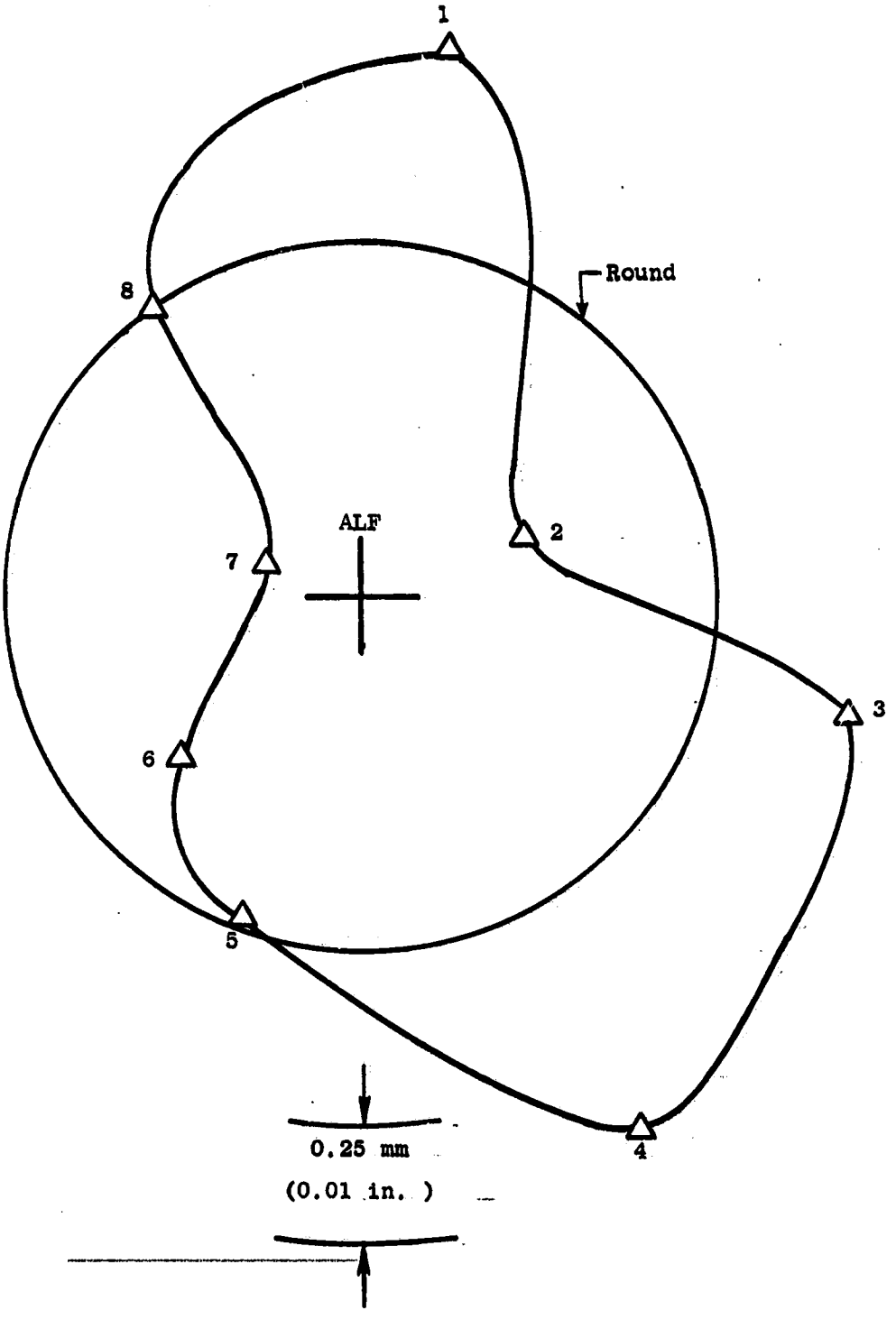

Figure 73. HP Turbine Stator Out-of-Roundness, Chop + 0 Seconds.

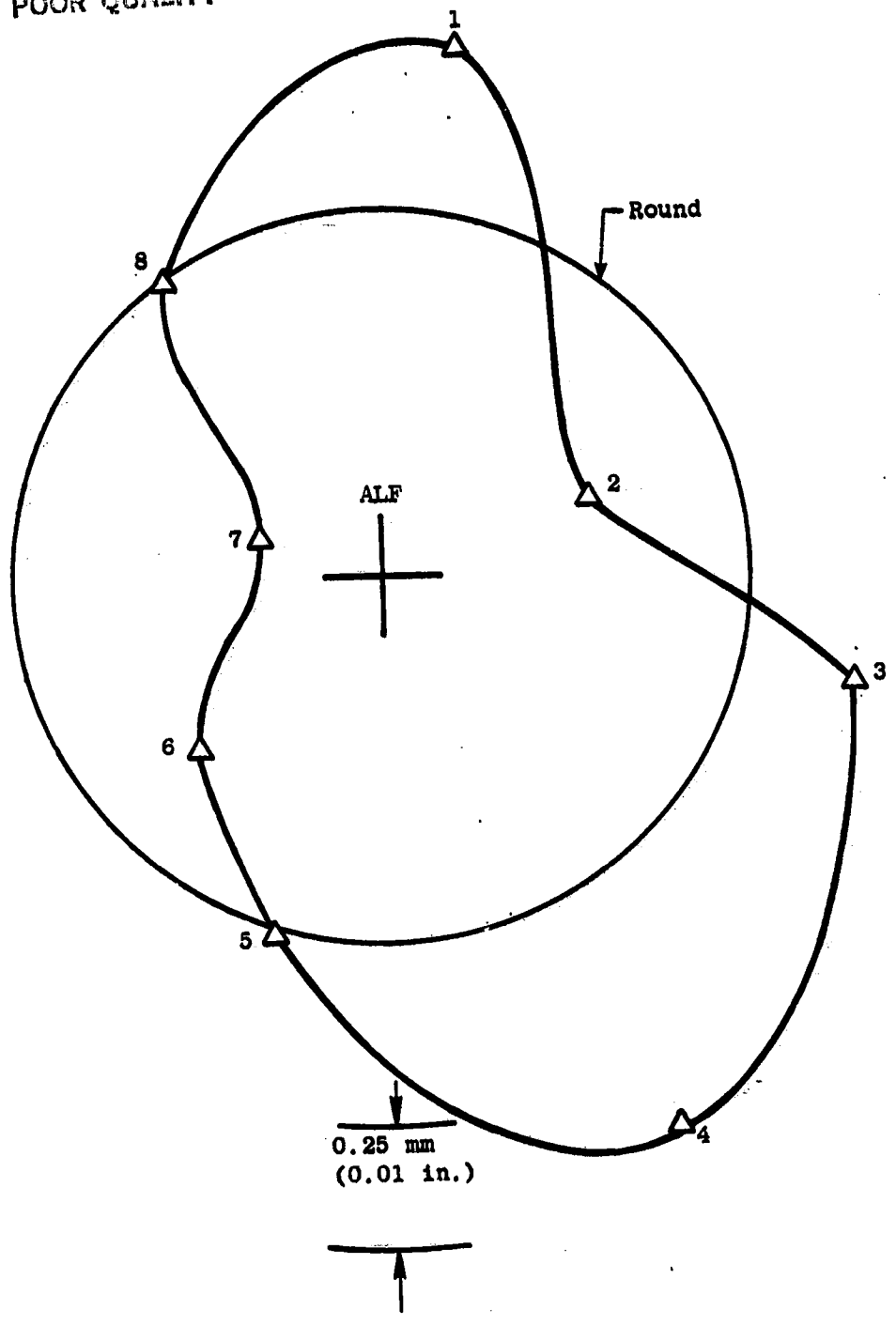

Figure 74. HP Turbine Stator Out-of-Roundness, Chop + 10 Seconds.

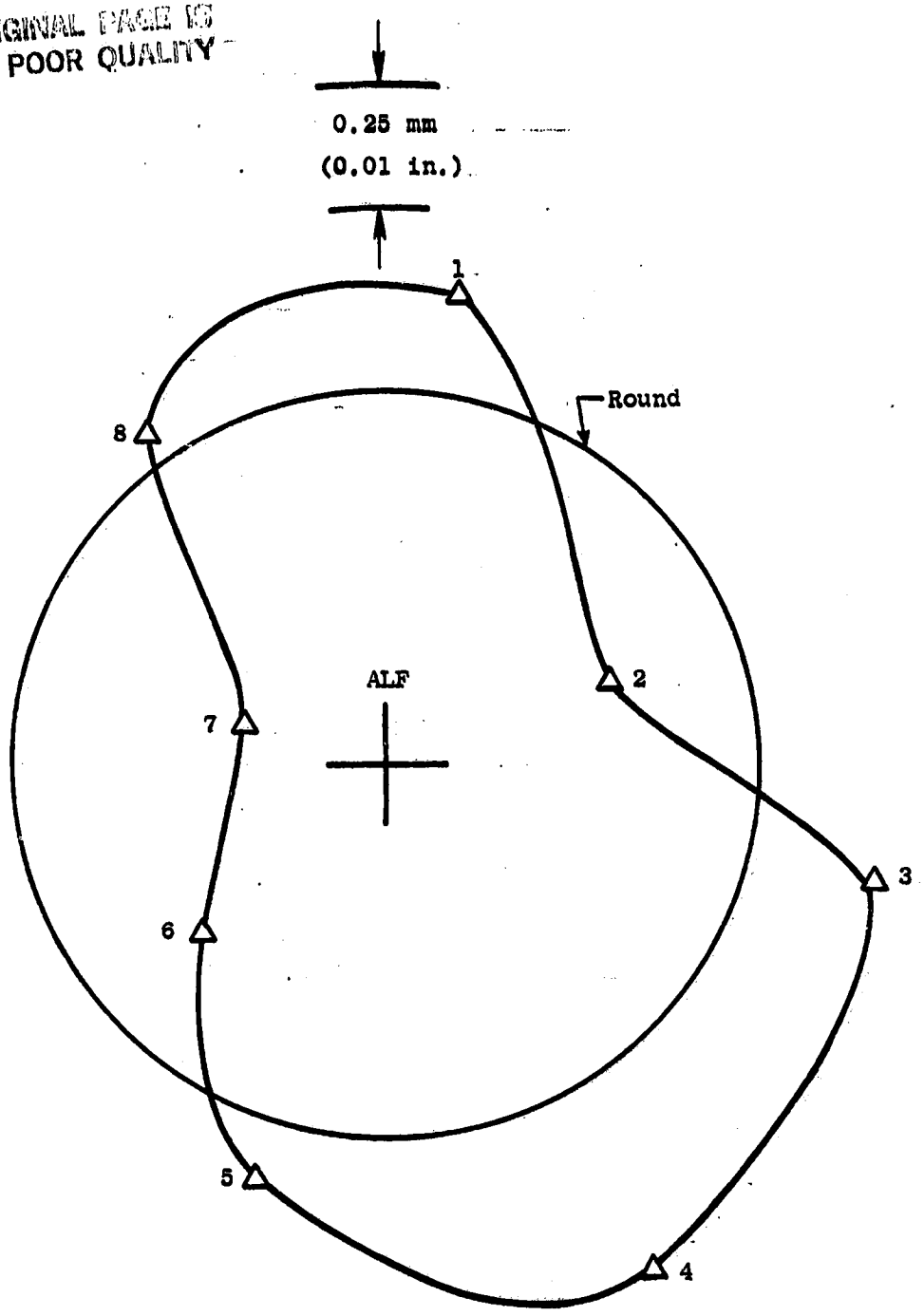

Figure 75. HP Turbine Stator Out-of Roundness, Chop + 20 Seconds.

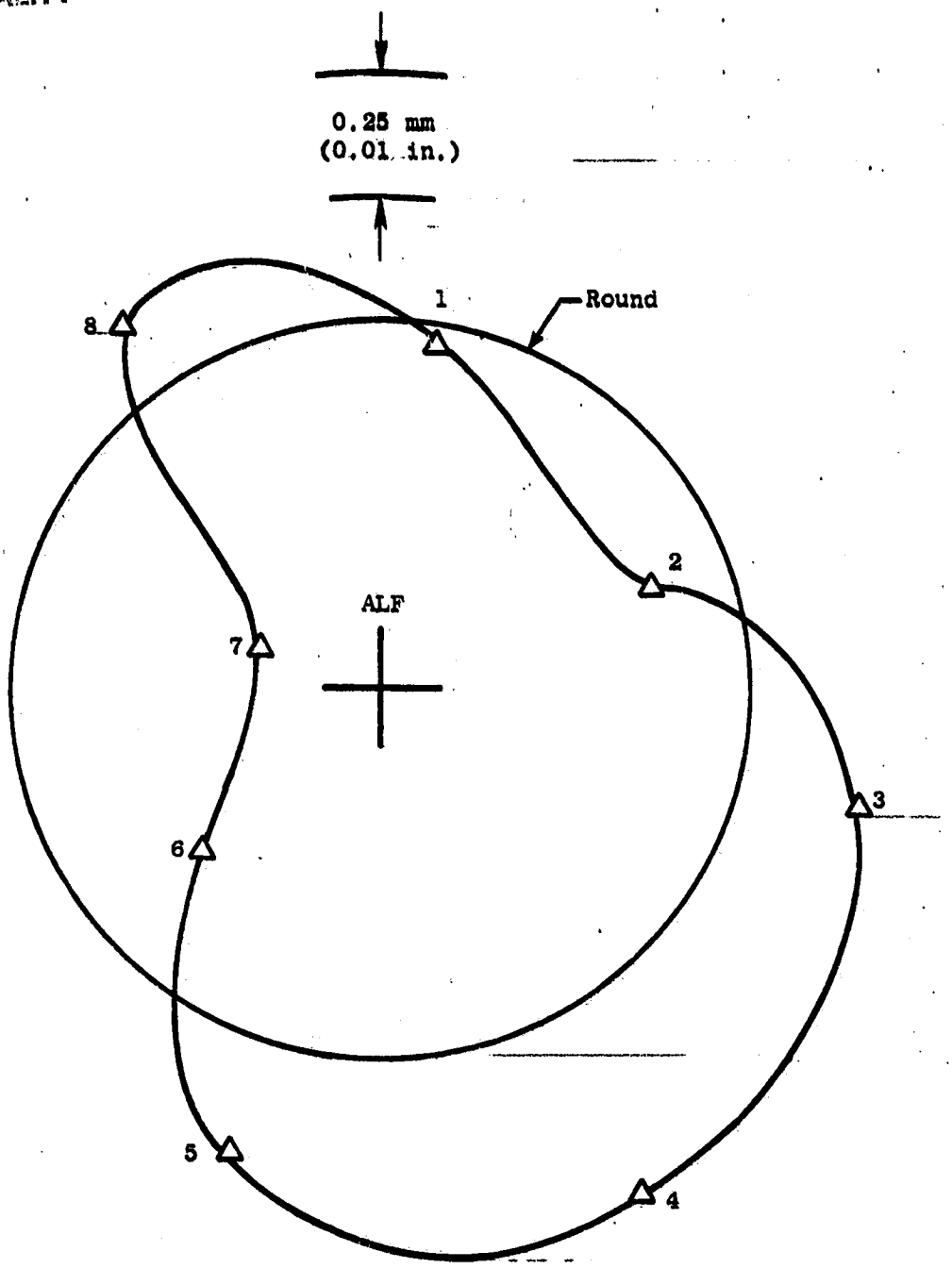

Figure 76. HP Turbine Stator Out-of-Roundness, Chop + 40 Seconds.

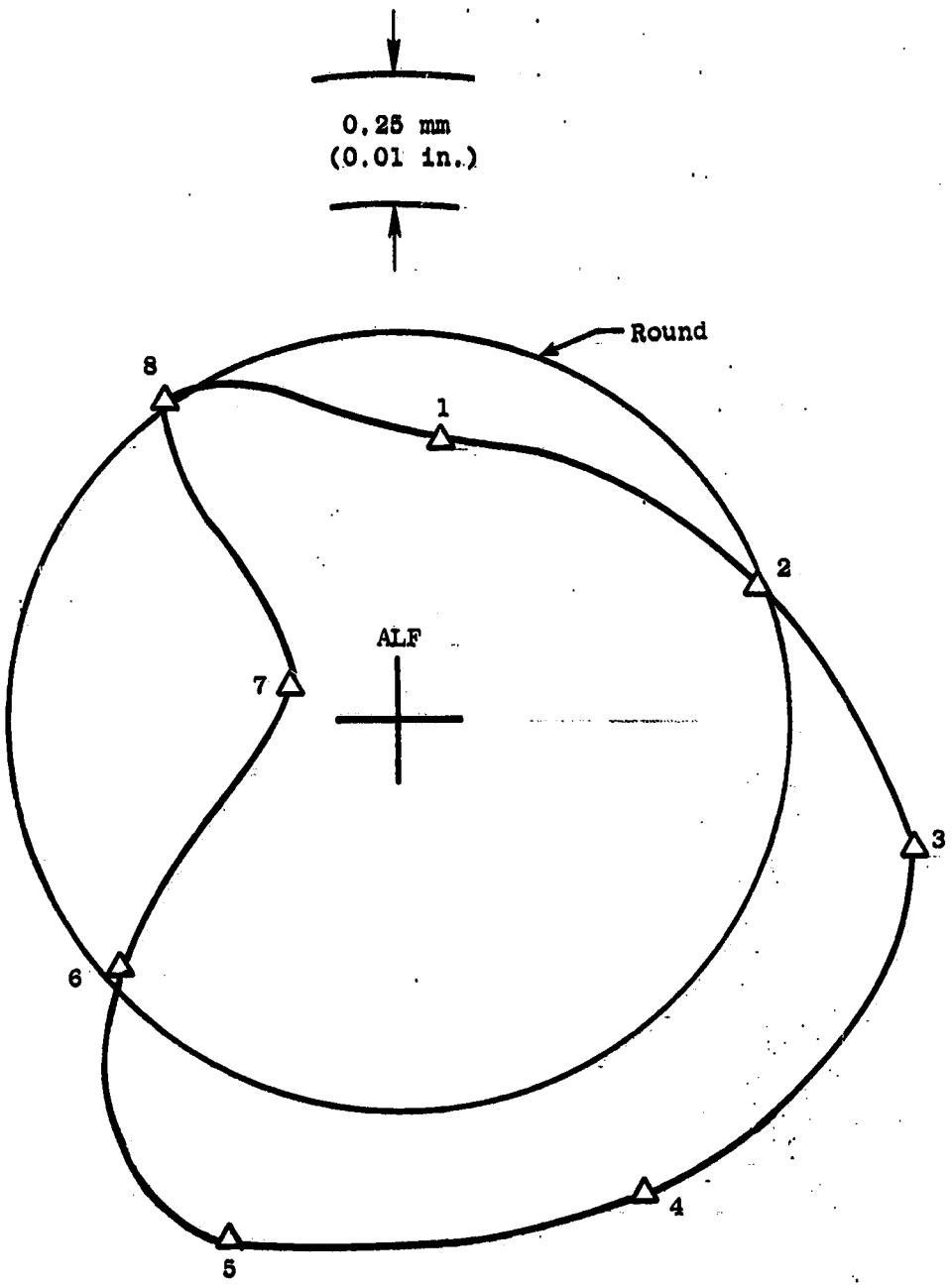

Figure 77. HP Turbine Stator Out-of-Roundness, Chop + 100 Seconds.

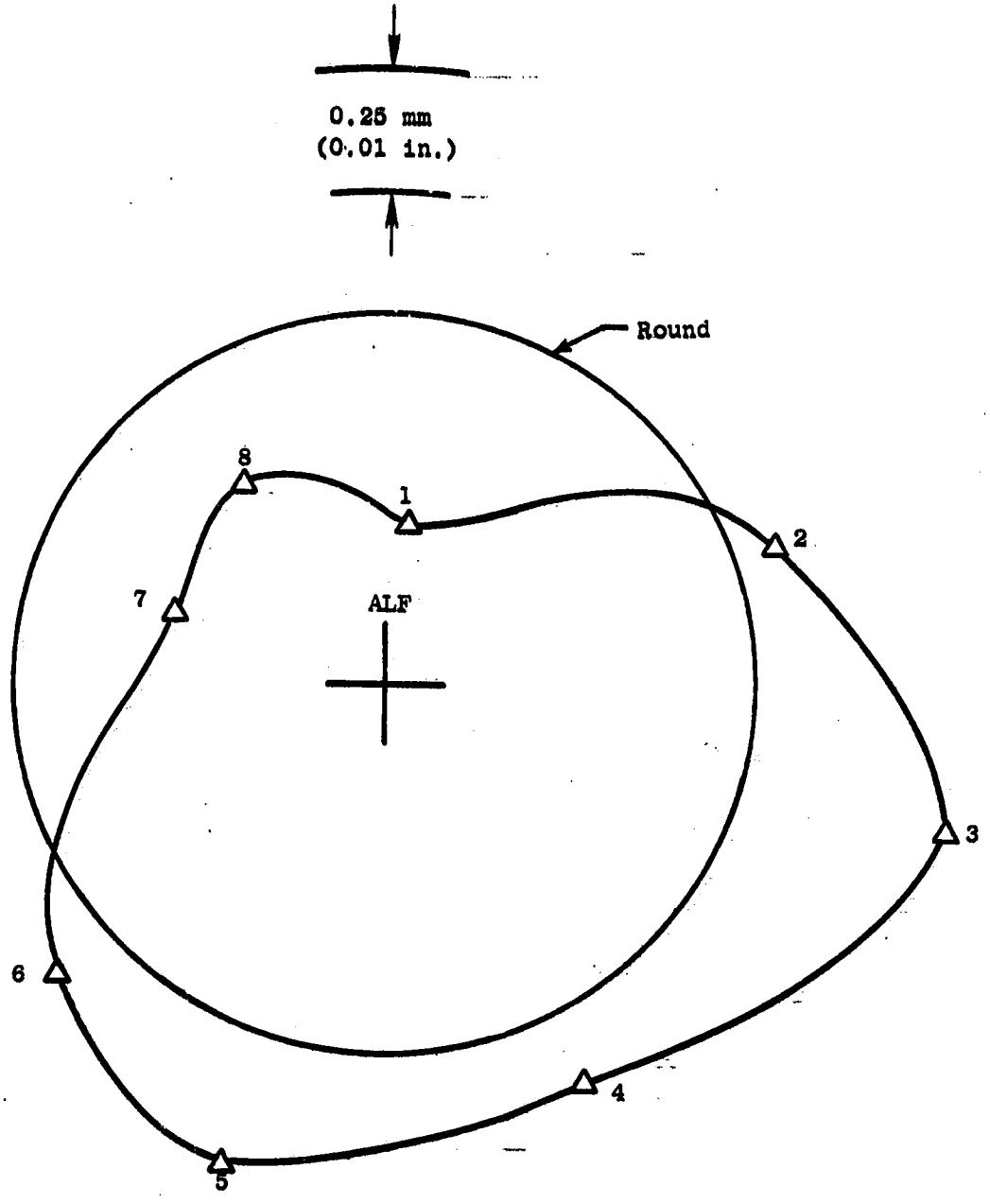

Figure 78. HP Turbine Stator Out-of-Roundness, Chop + 300 Seconds.

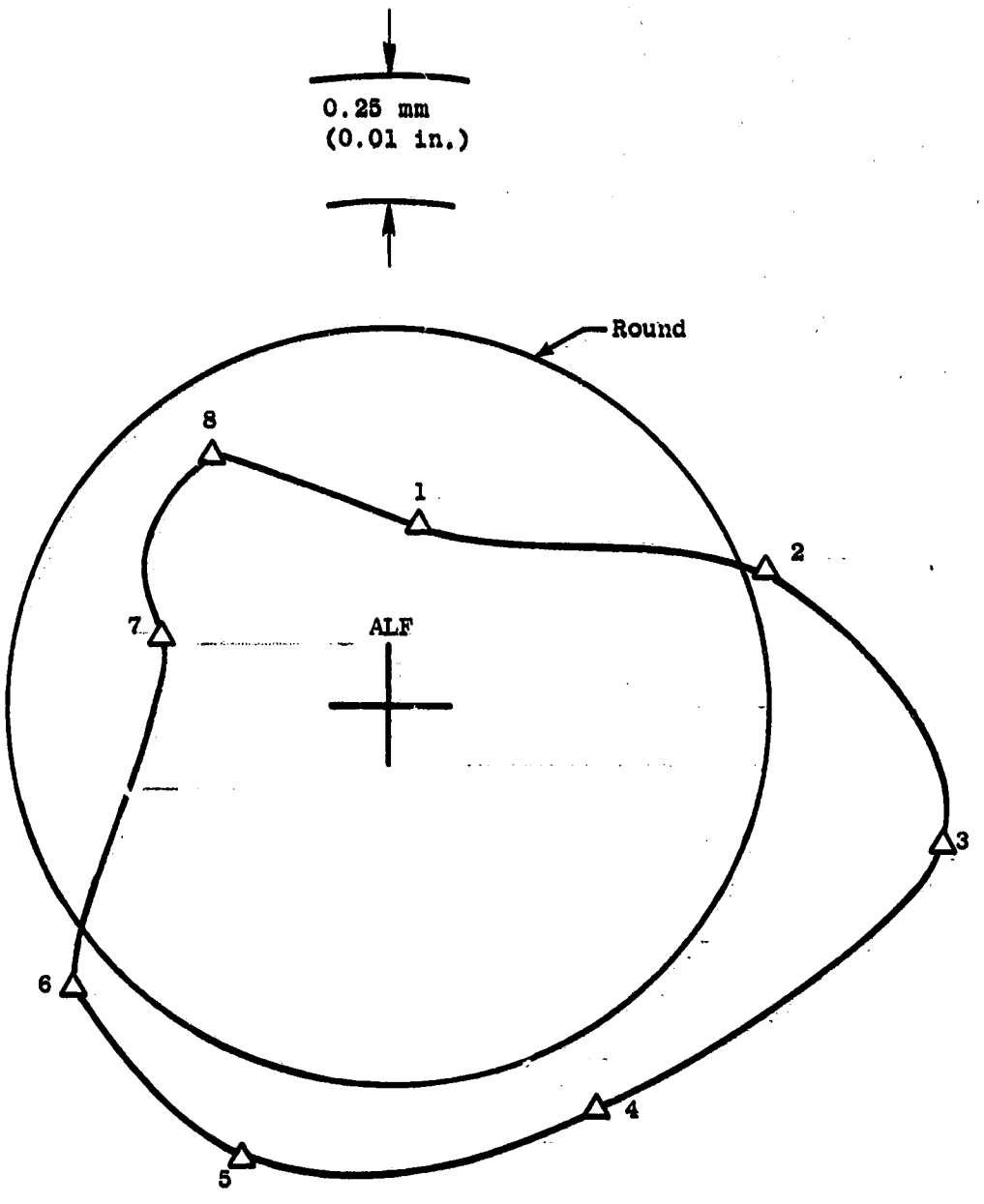

Figure 79. HP Turbine Stator Out-of-Roundness, Chop + 425 Seconds.

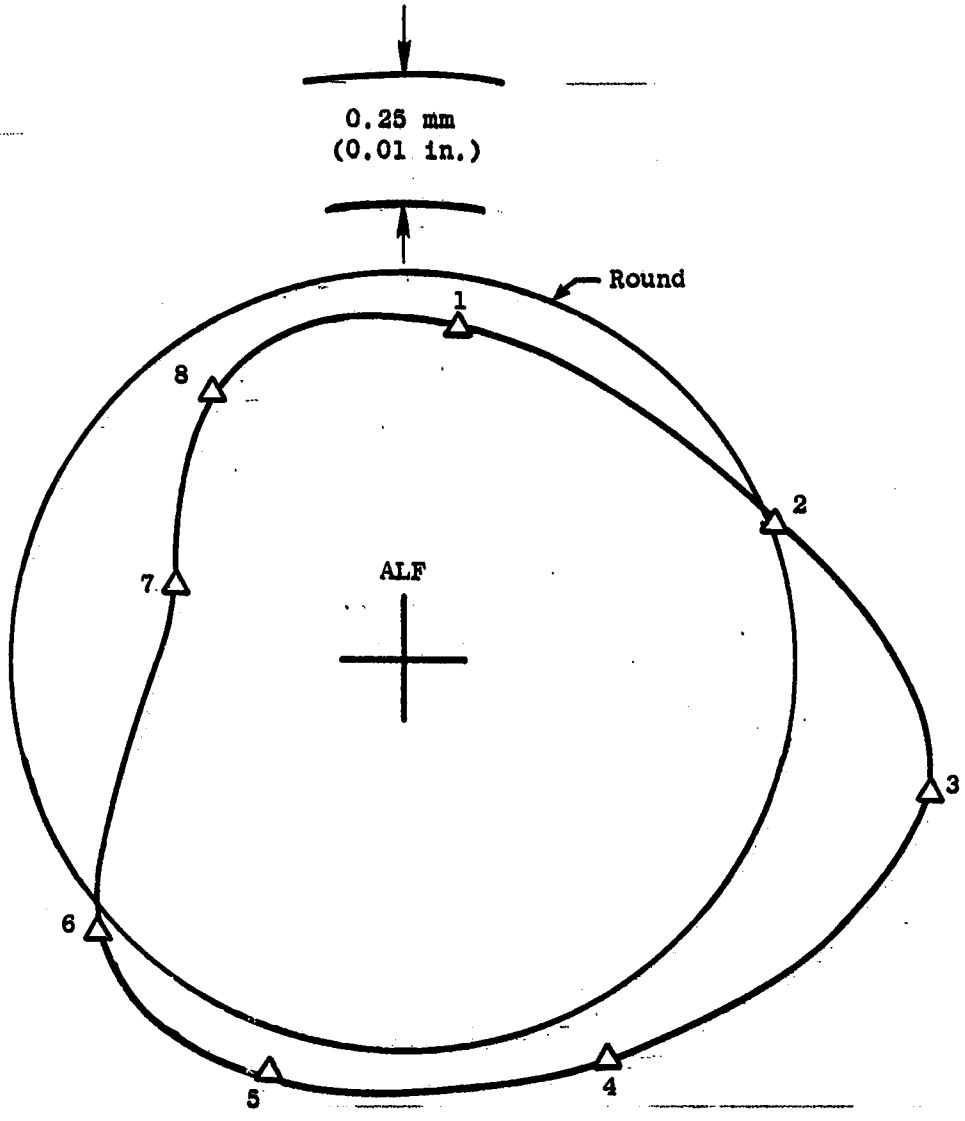

Figure 80. HP Turbine Stator Out-of-Roundness, Chop + 1020 Seconds.

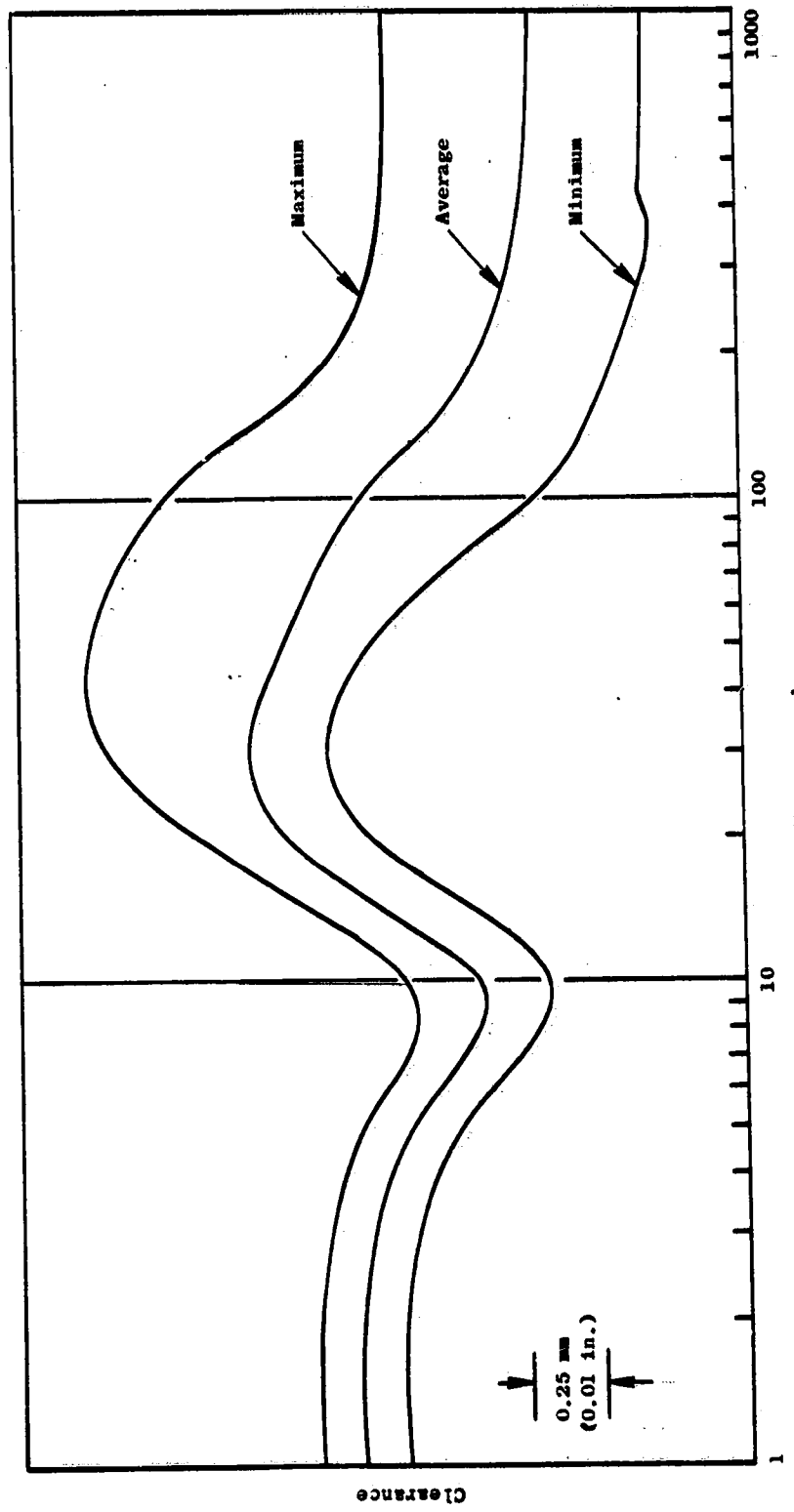

Figure 81. Maximum and Minimum Probe Readings During An Accel.

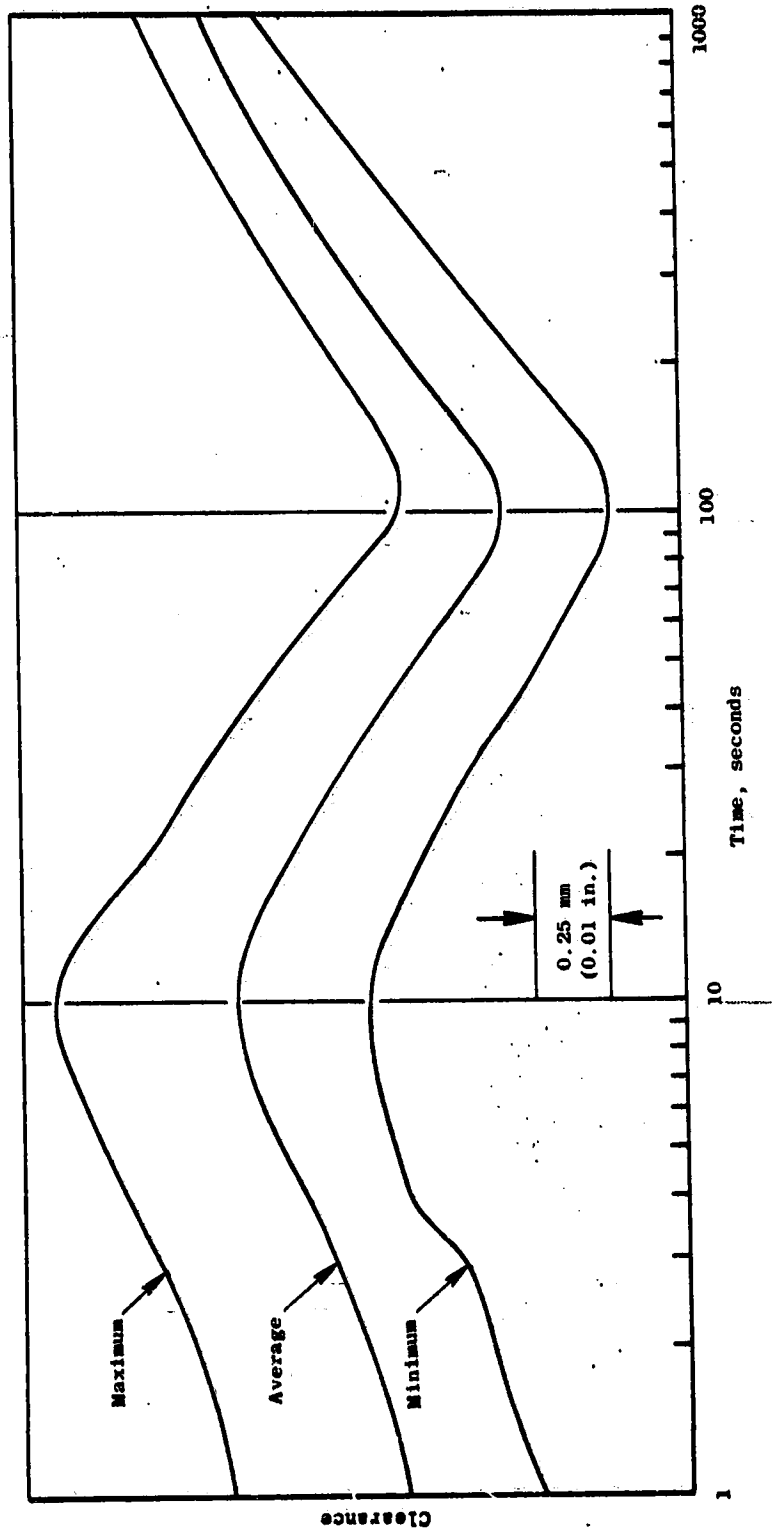

Figure 82. Maximum and Minimum Probe Readings During a Decel.

8.0 DISCUSSION OF RESULTS

This engine diagnostics investigation was undertaken fundamentally to provide insight into the causes and magnitudes of Stage 1 blade tip clearance-related engine performance deterioration of the CF6-50 turbofan engine. In so doing, it was judged that the principal gain to be realized would be the identification of improvements which could be made to the engine in order to reduce its fuel consumption.

Analyses conducted prior to this contract indicated that a meaningful investigation would have to include the following elements:

a) A survey of normal transient and steady state clearance behavior such as:

   1) Accels from low to high power
   2) Decels from high to low power
   3) Establishing clearances as functions of N2, P3, T3

b) A survey of non-routine transients including:

   1) Throttle reburst with varying ground idle dwell times
   2) Engine shutdown (stopcock) from high power

c) A survey of shroud surface out-of-roundness during transient and steady state operation and an assessment of the causes of this out-of-roundness

d) A direct measurement on a full-scale operating engine of the effect that a change in Stage 1 blade tip clearance has on engine fuel consumption.

The results of this investigation have been meaningful in all of these areas:

a) Normal Transient and Steady State Clearance Behavior

The results of this investigation show that a good understanding exists of the behavior of the engine when it is assumed to remain round and the rotor and stator concentric. A relatively constant error exists between the measured and predicted clearances for an accel from ground idle to takeoff power (Figure 21). The disagreement is about 0.25 mm (0.01 in). The location of maximum and minimum clearance values in time are in excellent agreement. These results indicate that the analytical tools being employed and the assumptions made with respect to transient thermal and mechanical response will result in reliable predictions of round engine clearances.

The above statement is further supported by the transient decel response from takeoff to idle, (Figure 29), which also exhibits good correlation both in level of clearance and in timewise location of maximum and minimum values.

With respect to the establishment of clearance as a function of power level (N_2, P_3, T_3), that information will be of value in the determination of the impact on fuel consumption of part-power and off-design point engine operation. It is necessary to know these relationships when conducting integrated fuel burn calculations, for example; conducting such studies was not a task or goal of this investigation.

b) Non-Routine Transient Behavior

This investigation provided a survey of an important class of transient engine operations called reburst. A reburst is defined as a decel from a high, stabilized power point to idle followed by an accel back to a high power point. The variable which characterizes the severity (nearness-to-rub) of a reburst is the length of time the engine is operated at idle prior to the acceleration to high power. This interval is termed the dwell time. Figure 23 shows the clearance behavior during the reburst acceleration for various dwell times.

This information is of value for two major reasons. One reason is that by knowing the dwell intervals over which rubs are most likely to occure, factory acceptance tests and aircraft acceptance and commercial operation procedures may be adjusted, wher possible, to avoid both short term and longer term deterioration caused by increased blade tip clearances. The other is that it provides a baseline with which improved designs, intended to make the engine less sensitive to rebursts, may be compared (Reference 2makes use of these data to show the improvement achieved in a modified design).

The other non-routine transient investigated was an engine shutdown. There are two types of engine shutdowns of interest, a shutdown from high power at or near sea level ambient condition (stopcock) and a shutdown at altitude followed by a dwell time during which the fan continues to rotate (windmill) by virtue of the aircraft's forward momentum and finally an engine restart and accel back to the power level from which the engine had been shut down. The latter case is a form of a reburst called a windmilling air start. Investigation of windmilling air starts was beyound the scope of this investigation. Nevertheless, the are an important source of deterioration and data from the engine shutdown actually performed in the investigation was used to predict clearance behavior for windmilling air starts.

The engine shutdown actually performed was a stopcock. The clearance and core speed transients are shown in Figures 29 and 30 respectively. The stopcock was interrupted, for reasons discussed earlier, at 200 sec. The engine was refired and returned to idle. Figure 31 is an extension of the stopcock data,assuming that the stopcocked engine was not restarted and adjusted to initiate from takeoff power rather than from cruise power as actually conducted. It shows that a rub would not be expected to occur.

Two things stand out. One is that a pure (uninterrupted) stopcock will not result in a rub. Secondly, a stopcock which is interrupted may very well result in a rub even though the engine is being returned to only idle power. This is significant. It demonstrates that more attention needs to be paid to what one previously would have considered to be of little significance: the transient

movements from shutdown to motoring and motoring to idle. Depending on what preceded these transients and on the length of shutdown time, rubs (deterioration) are predictable.

One final note on windmilling air starts. The data from this investigation were adjusted to analytically predict the clearance behavior during a windmilling air start performed during the flight test program of a different model of the CF6 engine. Because of geometry differences between engines, probable imprecision in the extrapolation to different ambient conditions and other adjustment inaccuracies, this analysis must be considered an approximation; however, rubs were predicted of a magnitude in reasonable agreement with those actually observed by borescope inspection.

Since windmilling air starts are performed during aircraft acceptance testing, they represent a potentially significant source of short term deterioration which may be recoverable either by adjusting acceptance test procedures or by incorporating designs which are less sensitive to these throttle movements.

c) Shroud Roundness Survey

This investigation was the first survey of transient and steady-state roundness performed on an actual full scale operating CF6-50 engine. Previous, and unrelated, component testing had established relationships between the out-of-roundness of various engine structures and the resulting induced shroud out-of-roundness. These relationships were used in stress and deflection models to establish shroud shapes. This present investigation has demonstrated that previously established estimates of shapes do not mirror the actual shapes well. Figure 66 illustrates the point and demonstrates the value of having run this investigation. From empirical investigations, it is known that the measured shape is an accurate reflection of the net out-of-roundness of the Stage 1 shroud surface. Engines which run with a Stage 1 shroud surface ground to a round condition have the highest likelihood of sustaining rubs between 2:30 - 3:30 and 7:30 - 9:00 o'clock, aft looking forward. The measured results of this investigation are in agreement with this empirically determined out-of-roundness shape.

Both the shape and magnitude of shroud out-of-roundness can be determined empirically as has been the practice. The significant aspect for potential fuel efficiency improvements is the magnitude, not the shape, of out-of-roundness. This investigation has established that the potential for improvements in roundness is on the order of 0.38 mm (0.015 in.) equivalent to 0.86 percent in turbine efficiency which translates to a cruise SFC improvement potential of approximately 0.36 percent.

d) Tip Clearance Performance Derivative

The results of this investigation have assigned an importance to Stage 1 blade tip clearance which is in reasonable agreement with unrelated previous testing and with the investigation of Reference 1. This present investigation indicates that the Stage 1 blade tip clearance has a somewhat stronger effect on fuel efficiency than has been the accepted case.

9.0 CONCLUSIONS

This test program has provided many outstanding results. Real-time Stage 1 blade-to-shroud clearance measurements have been obtained for a CF6-50C engine. Since eight clearanceometer probes were located around the circumference of the Stage 1 shroud area, the circumferential variation was used to obtain the roundness of the Stage 1 shroud area. Using the clearanceometer probes while sustaining a Stage 1 blade-on-shroud rub established the magnitude of the clearance increase during the rub. By monitoring engine performance before and after the rub, the effect of clearance upon performance was experimentally determined.

The test engine was very heavily instrumented. This instrumentation provided temperatures, pressures, flows, etc. for many significant engine parameters and areas of interest. These data points allowed a correlation with these engine parameters and high pressure turbine Stage 1 clearances.

The pressure and temperature measurements provided data that were used to predict the effect of both the turbine midframe and the low pressure turbine upon Stage 1 high pressure turbine roundness. The comparison of this prediction and the measured roundness was used to verify that the current analysis technique for mechanically caused loads and distortions was correct and that the method used to evaluate the effects of certain circumferential thermal gradients required modification.

The average clearance data showed that, although a small steady state error exists, the analytical model of round engine clearance response is quite good.

Areas of improvement in the fuel consumption characteristics of the CF6-50 engine explored in the discussion of results are:

1. Design changes to make the engine less reburst sensitive.

2. Design and/or aircraft acceptance test changes to make the engine less sensitive to windmilling air starts.

3. Incorporation of designs which will improve shroud surface roundness.

Reference 2 explores aspects of these improvements.

APPENDIX A - SYMBOLS

ALF	Aft Looking Forward
CDP	Compressor Discharge Pressure, N/cm^2 (lb/in^2)
CRF	Compressor Rear Frame
HEX	High Energy X-Ray
HPT	High Pressure Turbine
LPT	Low Pressure Turbine
N_1	Fan Speed, rpm
N_2	Core Speed, rpm
P_3	Compressor Exit Pressure, N/cm^2 (lb/in^2)
SFC	Specific Fuel Consumption, $\frac{kg}{hr\ N}$ ($\frac{lb}{hr\ lb}$)
T_3	Compressor Exit Temperature, °C(°F)
T/C	Thermocouple
TMF	Turbine Midframe
TRF	Turbine Rear Frame
W_{2c}	Core Inlet Flow, kg/sec(lb/sec)
LVDT	Linear Variable Displacement Transducer

APPENDIX B - REFERENCES

1. R.H. Wulf, "Engine Diagnostics Program, CF6-50 Engine Performance Deterioration", NASA CR-159867, November 1980.

2. W.D. Howard and W.A. Fasching, "CF6 Jet Engine Performance Improvement - High Pressure Turbine Roundness", NASA CR-165555 December 1981.

APPENDIX C

QUALITY ASSURANCE

INTRODUCTION

The quality program applied to this contract is a documented system throughout the design, manufacture, repair, overhaul and modification cycle for gas turbine aircraft engines. The quality system has been constructed to comply with military specifications MIL-Q-9858A, MIL-I-45208, and MIL-STD-45662 and Federal Aviation Regulations FAR-145 and applicable portion of FAR-21.

The quality system and its implementation are defined by a complete set of procedures which has been coordinated with the DOD and FAA and has their concurrence. In addition, the quality system as described in the quality program meets the contractor requirements required by the NASA-Lewis Research Center. The following is a brief synopsis of the system.

QUALITY SYSTEM

The quality system is documented by operating procedures which coordinate the quality-related activities in the functional areas of Engineering, Manufacturing, Materials, Purchasing, and Engine Programs. The quality system is a single-standard system wherein all product lines are controlled by the common quality system. The actions and activities associated with determination of quality are recorded, and documentation is available for review.

Inherent in the system is the assurance of conformance to the quality requirements. This includes the performance of required inspections and tests. In addition, the system provides change control requirements which assure that design changes are incorporated into manufacturing, procurement and quality documentation, and into the products. Material used for parts is verified for conformance to applicable engineering specifications, utilizing appropriate physical and chemical testing procedures.

Measuring devices used for product acceptance and instrumentation used to control, record, monitor, or indicate results of readings during inspection and test are initially inspected and calibrated and periodically are reverified or recalibrated at a prescribed frequency. Such calibration is performed by technicians against standards which are traceable to the National Bureau of Standards. The gages are identified by a control number and are on a recall schedule for reverification and calibration. The calibration function maintains a record of the location of each gage and the date it requires recalibration. Instructions implement the provisions of MIL-STD-45662 and the appropriate FAR requirements.

Work sent to outside vendors is subject to quality plans which provide for control and appraisal to assure conformance to the technical requirements. Purchase orders issued to vendors contain a technical description of the work to be performed and instructions relative to quality requirements.

Engine parts are inspected to documentad quality plans which define the characteristics to be inspected, the gages and tools to be used, the conditions under which the inspection is to be performed, the sampling plan, laboratory and special process testing, and the identification and record requirements.

Work instructions are issued for compliance by operators, inspectors, testers, and mechanics. Component part manufacture provides for laboratory overview of all special and critical processes, including qualification and certification of personnel, equipment and processes.

When work is performed in accordance with work instructions, the operator/inspector records that the work has been performed. This is accomplished by the operator/inspector stamping or signing the operation sequence sheet to signify that the operation has been performed.

Various designs of stamps are used to indicate the inspection of status of work in process and finished items. Performance or acceptance of special processes is indicated by distinctive stamps assigned specifically to personnel performing the process or inspection. Administration of the stamp system and the issuance of stamps are functions of the Quality Operation. The stamps are applied to the paperwork identifying or denoting the items requiring control. When stamping of hardware occurs, only laboratory approved ink is used to assure against damage.

The type and location of other part marking are specified by the design engineer on the drawing to assure effects do not compromise design requirements and part quality.

Control of part handling, storage and delivery is maintained through the entire cycle. Engines and assemblies are stored in special dollies and transportation carts. Finished assembled parts are stored so as to preclude damage and contamination, openings are covered, lines capped and protective covers applied as required.

Nonconforming hardware is controlled by a system of material review at the component source. Both a Quality representative and an Engineering representative provide the accept (use-as-is or repair) decisions. Nonconformances

are documented, including the disposition and corrective action if applicable to prevent recurrence.

The system provides for storage, retention for specified periods, and retrieval of nonconformance documentation. Documentation for components is filed in the area where the component is manufactured/inspected.